NASA/TP—2020-220152

Compass Final Report: Venus Bridge Orbiter and Surface Study (V-BOSS)

Gary W. Hunter
Glenn Research Center, Cleveland, Ohio

Noam Izenberg
Johns Hopkins University, Applied Physics Laboratory, Baltimore, Maryland

Steven R. Oleson and J.M. Newman
Glenn Research Center, Cleveland, Ohio

Martha Gilmore
Wesleyan University, Middletown, Connecticut

Kandis Lea Jessup
Southwest Research Institute, Boulder, Colorado

Robert Herrick
University of Alaska, Fairbanks, Alaska

Jeffrey Balcerski
Ohio Aerospace Institute, Brook Park, Ohio

Anthony Colozza
Vantage Partners, LLC, Brook Park, Ohio

Brent Faller and James Fincannon
Glenn Research Center, Cleveland, Ohio

James Fittje and John Gyekenyesi
Vantage Partners, LLC, Brook Park, Ohio

Robert Jones, Brandon Klefman, Geoffrey Landis, Michael Martini, Steven McCarty, and Thomas Packard
Glenn Research Center, Cleveland, Ohio

David Smith
Vantage Partners, LLC, Brook Park, Ohio

Elizabeth Turnbull
Glenn Research Center, Cleveland, Ohio

May 2020

NASA STI Program . . . in Profile

Since its founding, NASA has been dedicated to the advancement of aeronautics and space science. The NASA Scientific and Technical Information (STI) Program plays a key part in helping NASA maintain this important role.

The NASA STI Program operates under the auspices of the Agency Chief Information Officer. It collects, organizes, provides for archiving, and disseminates NASA's STI. The NASA STI Program provides access to the NASA Technical Report Server—Registered (NTRS Reg) and NASA Technical Report Server—Public (NTRS) thus providing one of the largest collections of aeronautical and space science STI in the world. Results are published in both non-NASA channels and by NASA in the NASA STI Report Series, which includes the following report types:

- TECHNICAL PUBLICATION. Reports of completed research or a major significant phase of research that present the results of NASA programs and include extensive data or theoretical analysis. Includes compilations of significant scientific and technical data and information deemed to be of continuing reference value. NASA counter-part of peer-reviewed formal professional papers, but has less stringent limitations on manuscript length and extent of graphic presentations.

- TECHNICAL MEMORANDUM. Scientific and technical findings that are preliminary or of specialized interest, e.g., "quick-release" reports, working papers, and bibliographies that contain minimal annotation. Does not contain extensive analysis.

- CONTRACTOR REPORT. Scientific and technical findings by NASA-sponsored contractors and grantees.

- CONFERENCE PUBLICATION. Collected papers from scientific and technical conferences, symposia, seminars, or other meetings sponsored or co-sponsored by NASA.

- SPECIAL PUBLICATION. Scientific, technical, or historical information from NASA programs, projects, and missions, often concerned with subjects having substantial public interest.

- TECHNICAL TRANSLATION. English-language translations of foreign scientific and technical material pertinent to NASA's mission.

For more information about the NASA STI program, see the following:

- Access the NASA STI program home page at http://www.sti.nasa.gov

- E-mail your question to help@sti.nasa.gov

- Fax your question to the NASA STI Information Desk at 757-864-6500

- Telephone the NASA STI Information Desk at 757-864-9658

- Write to:
  NASA STI Program
  Mail Stop 148
  NASA Langley Research Center
  Hampton, VA 23681-2199

NASA/TP—2020-220152

Compass Final Report: Venus Bridge Orbiter and Surface Study (V-BOSS)

Gary W. Hunter
Glenn Research Center, Cleveland, Ohio

Noam Izenberg
Johns Hopkins University, Applied Physics Laboratory, Baltimore, Maryland

Steven R. Oleson and J.M. Newman
Glenn Research Center, Cleveland, Ohio

Martha Gilmore
Wesleyan University, Middletown, Connecticut

Kandis Lea Jessup
Southwest Research Institute, Boulder, Colorado

Robert Herrick
University of Alaska, Fairbanks, Alaska

Jeffrey Balcerski
Ohio Aerospace Institute, Brook Park, Ohio

Anthony Colozza
Vantage Partners, LLC, Brook Park, Ohio

Brent Faller and James Fincannon
Glenn Research Center, Cleveland, Ohio

James Fittje and John Gyekenyesi
Vantage Partners, LLC, Brook Park, Ohio

Robert Jones, Brandon Klefman, Geoffrey Landis, Michael Martini, Steven McCarty, and Thomas Packard
Glenn Research Center, Cleveland, Ohio

David Smith
Vantage Partners, LLC, Brook Park, Ohio

Elizabeth Turnbull
Glenn Research Center, Cleveland, Ohio

National Aeronautics and
Space Administration

Glenn Research Center
Cleveland, Ohio 44135

May 2020

This report contains preliminary findings, subject to revision as analysis proceeds.

Level of Review: This material has been technically reviewed by a committee of peers.

Available from

NASA STI Program
Mail Stop 148
NASA Langley Research Center
Hampton, VA 23681-2199

National Technical Information Service
5285 Port Royal Road
Springfield, VA 22161
703-605-6000

This report is available in electronic form at http://www.sti.nasa.gov/ and http://ntrs.nasa.gov/

Contents

Compass Final Report: Venus Bridge Orbiter and Surface Study (V-BOSS)

Gary W. Hunter
National Aeronautics and Space Administration
Glenn Research Center
Cleveland, Ohio 44135

Noam Izenberg
Johns Hopkins University
Applied Physics Laboratory
Baltimore, Maryland 21218

Steven R. Oleson and J.M. Newman
National Aeronautics and Space Administration
Glenn Research Center
Cleveland, Ohio 44135

Martha Gilmore
Wesleyan University
Middletown, Connecticut 06459

Kandis Lea Jessup
Southwest Research Institute
Boulder, Colorado 80302

Robert Herrick
University of Alaska
Fairbanks, Alaska 99775

Jeffrey Balcerski
Ohio Aerospace Institute
Brook Park, Ohio 44142

Anthony Colozza
Vantage Partners, LLC
Brook Park, Ohio 44142

Brent Faller and James Fincannon
National Aeronautics and Space Administration
Glenn Research Center
Cleveland, Ohio 44135

James Fittje and John Gyekenyesi
Vantage Partners, LLC
Brook Park, Ohio 44142

Robert Jones, Brandon Klefman, Geoffrey Landis,
Michael Martini, Steven McCarty, and Thomas Packard
National Aeronautics and Space Administration
Glenn Research Center
Cleveland, Ohio 44135

David Smith
Vantage Partners, LLC
Brook Park, Ohio 44142

Elizabeth Turnbull
National Aeronautics and Space Administration
Glenn Research Center
Cleveland, Ohio 44135

Summary

The Venus Bridge Orbiter and Surface Study (V-BOSS) Compass concurrent engineering design team study shows that new, high-priority Venus science can be achieved using a linked Orbiter + Surface Element (Lander) mission concept within a $200 million cost cap with assumptions. This is feasible through optimizing investment in early technologies and platforms, such as the Long-Lived In-Situ Solar System Explorer (LLISSE), leveraging known and flight-ready technology, and the overall use of simple, small, and robust systems in innovative approaches to Venus exploration. This architecture allows a range of science investigations through modification of Orbiter-Lander platforms in this study through choice of other instruments (often sensors), science themes, or operational modes. In particular, a fundamental strength of this approach is to provide science not available in other ways by using simplified architectures, including rugged systems operable in situ on the Venus surface (Figure 1). Such investigations would be pathfinders for more complex, and more expensive, future missions. Additionally, the results of this study can be used to further champion the need, value, and return of early investment technology programs for the hard problem of in situ investigations on Venus.

1.0 Introduction

The Venus Bridge Team formed by Venus Exploration Analysis Group (VEXAG) was directed by NASA Headquarters to evaluate if useful Venus exploration, independent of the Discovery, New Frontiers, and Flagship solicitations, can be performed within a $200 million cost cap. An extensive study has been performed by Compass team of a linked-mission concept of a Lander + Orbiter. The Venus

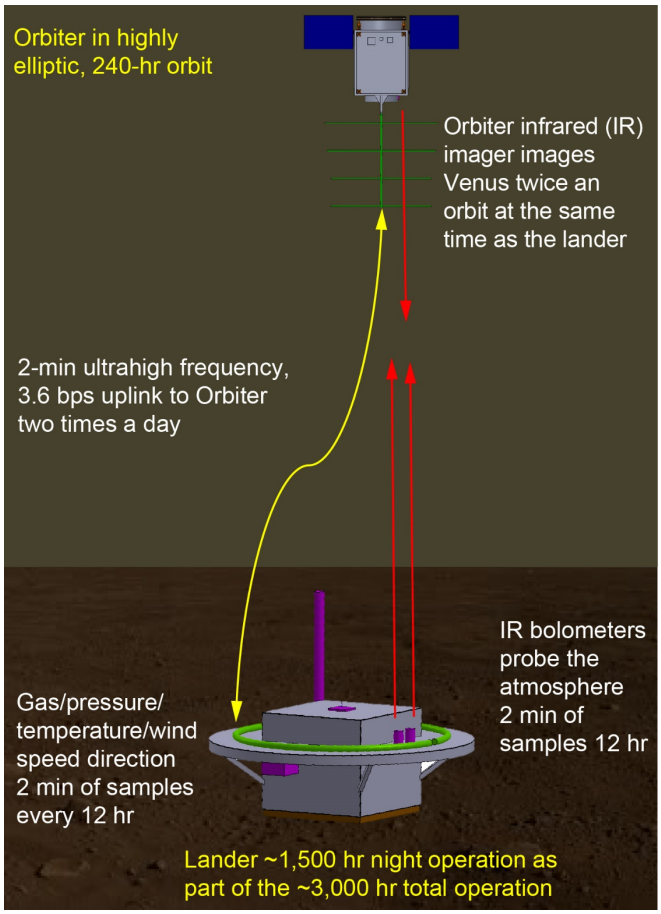

Figure 1.—Venus Bridge Orbiter and Surface Study (V-BOSS) coupled Orbiter-Lander concept.

Bridge Orbiter and Surface Study (V-BOSS) Compass study assumed the parameters of the overall Venus Bridge activity: one or more small missions performing important science investigations with launch dates in the early-to-mid 2020s within a $200 million cost cap. Preliminary results of this study were presented at the 2017 VEXAG meeting.

The Compass study used the facilities and methodology established in similar studies during the history of this team, and included collaboration with planetary scientists and technologists with expertise in relevant Venus and planetary missions. The core of the study took place over a 2 ½-week period, not including pre- and post-preparation and analysis, held in October and early November. The Compass team provided high-level guidance on restrictions for potential instruments, while the V-BOSS Science team identified science goals and candidate instruments along with a science traceability matrix. The overall mission concept includes establishment of an Orbiter into a stable Venus orbit to serve as a communication relay and conduct orbital science, delivery of a surface Lander to the Venus surface, and coordination/linking between the two mission elements to increase the overall science delivered. Furthermore, the concept of Landers maximizing science return through data acquisition upon descent was considered.

The approach of this Compass study is not to advocate for a single mission concept, but examine generic missions optimizing the science delivered, new technology demonstrations, and the impact on future Venus exploration. However, in order to have firm cost and mission timelines a single reference design mission with Lander and Orbiter point designs was provided targeted for the $200 million cost cap. The results of the study and the various trades to evaluate mission concepts are summarized below. This study is intended to illustrate the potential benefits, limitations, risks, and technology needs of this overall Lander + Orbiter concept. Specific instrument, spacecraft (S/C), and mission concepts can potentially be considered as part of future studies and proposal calls by the NASA Science Mission Directorate (SMD) as it deems appropriate. Table 1 lists the system-level master equipment list (MEL) provided by this Compass study.

The Compass team was tasked by the Venus Bridge Team to create an independent concept design for a Venus Orbiter and Lander. The Orbiter and Lander stack is delivered towards the Moon on a secondary launch. Upon separation, the Orbiter carries the Lander through two lunar gravity assists (LGAs), and one powered Earth gravity assist (EGA). Thirty days prior to capture into a 10-day inclined Venusian orbit, the Lander/entry, descent, and landing (EDL) system separates from Orbiter. The Lander/EDL will enter in Venus's atmosphere while in sight of the Orbiter, and will land at 55° S at Venusian nighttime. The Lander will periodically take data and uplink to the Orbiter for relay to Earth, for a total mission duration of 1 Venusian day (120 Earth days).

2.0 Study Background and Assumptions

2.1 Report Perspective and Disclaimer

This report is meant to capture the study performed by the Compass team, recognizing that the level of effort and detail found in this report will reflect the limited depth of analysis that was possible to achieve during a concept design session. All of the data generated during the design study is captured within this report in order to retain it as a reference for future work.

TABLE 1.—VENUS BRIDGE ORBITER AND SURFACE STUDY (V-BOSS) SYSTEM-LEVEL MASTER EQUIPMENT LIST

Description	Total mass with margin, kg
V-BOSS	215.13
Lander	13.56
Science	0.66
Command and Data Handling (C&DH)	0.23
Communications and Tracking	0.56
Electrical Power (EP) subsystem	3.41
Structures and mechanisms	8.70
Entry, descent, and landing	10.44
EP Subsystem	0.27
Thermal control (nonpropellant)	10.00
Structures and mechanisms	0.17
Orbiter	191.13
Science	2.60
Attitude Determination and Control	3.34
C&DH	2.29
Communications and Tracking	7.03
EP subsystem	25.22
Thermal control (nonpropellant)	12.23
Propulsion (chemical hardware)	14.07
Propellant (chemical)	90.43
Structures and mechanisms	33.92

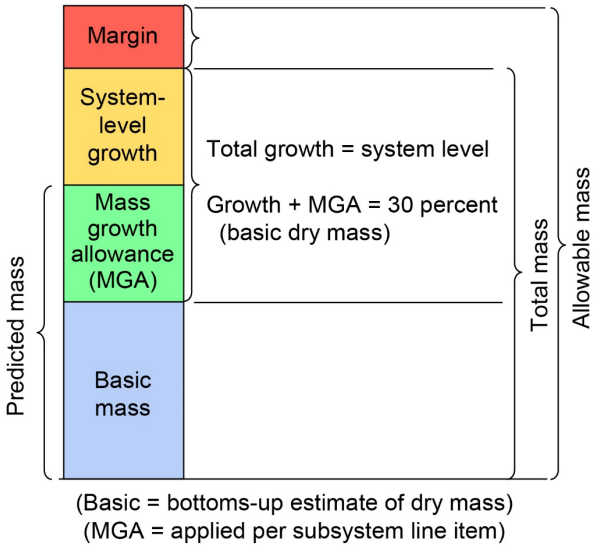

Figure 2.—Graphical illustration of definition of basic, predicted, total, and allowable mass.

TABLE 2.—DEFINITION OF MASSES TRACKED IN THE MASTER EQUIPMENT LIST

CBE[a] mass	MGA[b] growth	Predicted mass	Predicted dry mass
Mass data based on most recent baseline design (includes propellant)	Predicted change to basic mass of item phrased as percentage of CBE dry mass	CBE mass + MGA	CBE mass + MGA – propellant
CBE dry + propellant	MGA percent ∗ CBE dry = growth	CBE dry + propellant + growth	CBE dry + growth

[a]Current best estimate.
[b]Mass growth allowance.

2.2 Growth, Contingency, and Margin Policy

Table 2 expands definitions for the MEL column titles to provide information on the way masses are tracked through the MEL used in the Compass design sessions. These definitions are consistent with those in Figure 2 and Appendix B, Terms and Definitions. This table is an alternate way to present the same information to provide more clarity.

2.2.1 Mass Growth

The Compass team normally uses the American Institute of Aeronautics and Astronautics (AIAA) S–120–2006, Standard: Mass Properties Control for Space Systems, as the guideline for its mass growth calculations. Table 3 shows the percent mass growth of a piece of equipment according to a matrix that is specified down the left-hand column by level of design maturity and across the top by subsystem being assessed.

The Compass team's standard approach is to accommodate for a total growth of 30 percent or less on the dry mass of the entire system. The percent growth factors shown above are applied to each subsystem before an additional growth is carried at the system level in order to ensure an overall growth of 30 percent. Note that for designs requiring propellant, growth in the propellant mass is either carried in the propellant calculation itself or in the delta velocity (ΔV) used to calculate the propellant required to fly a mission.

2.2.2 Power Growth

The Compass team typically uses a 30-percent margin on the bottoms-up power requirements of the bus subsystems when modeling the amount of required power. The power system assumptions for this study are listed in Section 3.1.3.

TABLE 3.—MASS GROWTH ALLOWANCE (MGA) AND DEPLETION SCHEDULE (AIAA S–120–2006)

6	Maturity code	Design maturity (basis for mass determination)	MGA, percent												
			Electrical/electronic components			Structure	Brackets, clips, hardware	Battery	Solar array	Thermal control	Mechanisms	Propulsion	Wire harness	Instrumentation	ECLSS[a], crew systems
			0 to 5 kg	5 to 15 kg	>15 kg										
E	1	Estimated (1) An approximation based on rough sketches, parametric analysis, or undefined requirements; (2) a guess based on experience; (3) a value with unknown basis or pedigree	30	25	20	25	30	25	30	25	25	25	55	55	23
	2	Layout (1) A calculation or approximation based on conceptual designs (equivalent to layout drawings); (2) major modifications to existing hardware	25	20	15	15	20	15	20	20	15	15	30	30	15
C	3	Prerelease designs (1) Calculations based on a new design after initial sizing but prior to final structural or thermal analysis; (2) minor modification of existing hardware	20	15	10	10	15	10	10	15	10	10	25	25	10
	4	Released designs (1) Calculations based on a design after final signoff and release for procurement or production; (2) very minor modification of existing hardware; (3) catalog value	10	5	5	5	6	5	5	5	5	5	10	10	6
A	5	Existing hardware (1) Actual mass from another program, assuming that hardware will satisfy the requirements of the current program with no changes; (2) values based on measured masses of qualification hardware	3	3	3	3	3	3	3	2	3	3	5	5	4
	6	Actual mass Measured hardware	No MGA—use appropriate measurement uncertainty values												
	7	Customer-furnished equipment or specification value	Typically a not-to-exceed value is provided; however, contractor has option to include MGA if justified												

[a]Environmental Control and Life Support System.

2.3 Redundancy Assumptions

The S/C is designed to be zero fault tolerant in the design of the subsystems, as appropriate for a mission of this cost class.

The mission was designed to meet a large number of constraints imposed from both technical and scientific drivers. In order to keep launch costs down, an Earth entry sequence was designed that could be achieved by launching as a secondary payload on a trajectory targeting the Moon. From there, modest S/C propulsive capability combined with multiple lunar and EGAs would target an Earth escape trajectory with enough energy to reach Venus. Before arrival at Venus, the Lander would separate from the Orbiter and a small maneuver would provide separation between the Venus arrival time of each element to enable the Orbiter to track the entry of the Lander after orbit insertion.

2.3.1 Mission Analysis Assumptions

A number of assumptions were made while designing the mission. For the launch phase, it is assumed that the S/C is placed on a trajectory with the appropriate energy to target a lunar flyby. This could come from either a direct launch to the Moon, or from being injected into a number of highly elliptical phasing orbits that would target the required flyby some number of revolution after launch, enabling a wider launch window.

For arrival at Venus, assumptions were made for the Lander entry and the orientation of the Orbiter and Lander.

Orbiter Assumptions:

1. Capture must be into a 10-day period orbit with 400-km periapsis altitude.
2. Venus orbit insertion (VOI) must be visible from Earth.
3. Orbiter must observe the Lander entry to relay data.
4. Orbiter first apoapsis latitude should be equal to that of the landing location.
5. Orbiter first apoapsis longitude should be 60° greater than that of the landing location.

Assumptions 4 and 5 are necessary to maximize the time during which the Orbiter apoapsis passes above the Lander while Venus rotates.

Lander Assumptions:

1. Venus atmospheric entry interface altitude is 300 km.
2. Venus atmospheric entry angle must be less than 45°.
3. Final landing location is 250 km downrange from the atmospheric entry point.
4. Landing location must be between ±70°.
5. Landing location can be at any longitude.
6. Time of Venus day at landing location must be between –75° and –180° from the dawn terminator.

The last three of these assumptions flow from the science goals of the mission.

2.3.2 Mission Details

Rather than requiring a high-energy (characteristic energy $C_3 \approx 7$ to 10 km^2/s^2) direct launch to Venus, the baseline mission design begins with a comparatively low-energy launch towards the Moon ($C_3 \approx -1.5$ km^2/s^2). The launch towards the Moon targets an LGA to increase energy and send the S/C on a ballistic solar loop, where the Sun's gravity perturbs the trajectory in such a way to target a second LGA 112 days later. The second LGA adds more energy and targets a close approach to Earth 2 days later, where a ≈300 m/s chemical burn sends the S/C on a ballistic trajectory to Venus. This departure strategy allows the S/C to fly as a secondary payload on launches towards the Moon, which are assumed to be more common than other routes to Venus. There are, however, specific planetary alignment requirements that may impose difficult departure window constraints. This was deemed an acceptable trade for the potential of more, relatively less expensive launch opportunities, though further analysis is required to better understand these potential impacts. Using this strategy, the S/C is able to reach a departure characteristic energy of 7.1 km^2/s^2.

Three days after the final departure burn, the S/C has left the Earth's sphere of influence on a 132-day ballistic trajectory to Venus. The Lander is released from the Orbiter 28 days before entry, at which point the Orbiter performs a maneuver to divert from the Venus intercept trajectory and target VOI ahead of the Lander entry. Geometry constraints force the Orbiter to complete the 795 m/s VOI on the sunlit side of Venus approximately 2 hr before the Lander reaches the entry interface on the nightside of Venus. The 2-hr separation is necessary for the Orbiter to observe the Lander entry after completing its critical Earth-observable VOI burn. After VOI, the Orbiter is in a 10-day period elliptical orbit with an inclination (INC) of 122° oriented such that the apoapsis latitude matches that of the Lander and the apoapsis longitude is offset by ~60° from the Lander. This latitude/longitude arrangement enables consistent Orbiter-Lander coverage over the 120-day mission as Venus slowly rotates.

VOI Details:

- Date: May 8, 2025, at 14:22 Coordinated Universal Time (UTC)
- ΔV: 795 m/s
- Post-VOI orbital elements:
  - Semi-major axis (SMA) = $1.831417537483480 \times 10^5$
  - Eccentricity (ECC) = $9.647472594095532 \times 10^{-1}$

- INC = $1.225843513736866\times10^{2}$
- Right ascension of the ascending node (RAAN) = $4.498363824442468\times10^{1}$
- Argument of periapsis (AOP) = $9.489433939887820\times10^{1}$

The Lander enters the atmosphere approximately 2 hr after VOI at 10.8 km/s with a flight path angle of 45°, targeting a landing site optimized for minimum Orbiter VOI ΔV. The optimal landing location, assumed as 250 km downrange of atmospheric entry, was determined to be 55.1° S/261.6° E, which at the time of landing is –150° from the dawn terminator (approximately 50 Earth days).

2.3.3 Mission Analysis Event Timeline

The following is the mission analysis event timeline:

- First lunar flyby: September 2, 2024 (mission event time (MET) = 0 days)
- Second lunar flyby: December 23, 2024 (MET = 112 days)
- Power Earth flyby: December 25, 2024 (MET = 114 days)
- Depart Earth sphere of influence: December 28, 2024 (MET = 117 days)
- Lander separation: April 10, 2025 (MET = 221 days)
- VOI: May 8, 2025, at 14:22 UTC (MET = 249 days)
- Lander entry: May 8, 2025, at 16:27 UTC (MET = 249 days)

Figure 3 is an illustration of the trajectory solved for the MET dates and times labeled at the appropriate places along the trajectory. Figure 4 to Figure 6 provide detailed graphics of the Venus arrival phase, including Lander separation, VOI, and Lander entry.

2.3.4 Mission Analysis Analytic Methods

The mission design was completed using Copernicus, a general trajectory optimization tool capable of designing and optimizing missions at various levels of detail.

The interplanetary (i.e., post-Earth escape) and Venus arrival phases of the mission were first designed and optimized end to end due to the highly constrained arrival geometry, using a point mass gravity model for Venus and the Sun.

The Earth departure sequence was then designed and optimized using a patched conics approach for the LGAs, with point mass gravity from the Earth and Sun. The required departure right ascension and declination at Earth escape were targeted based on that which was required from the interplanetary trajectory.

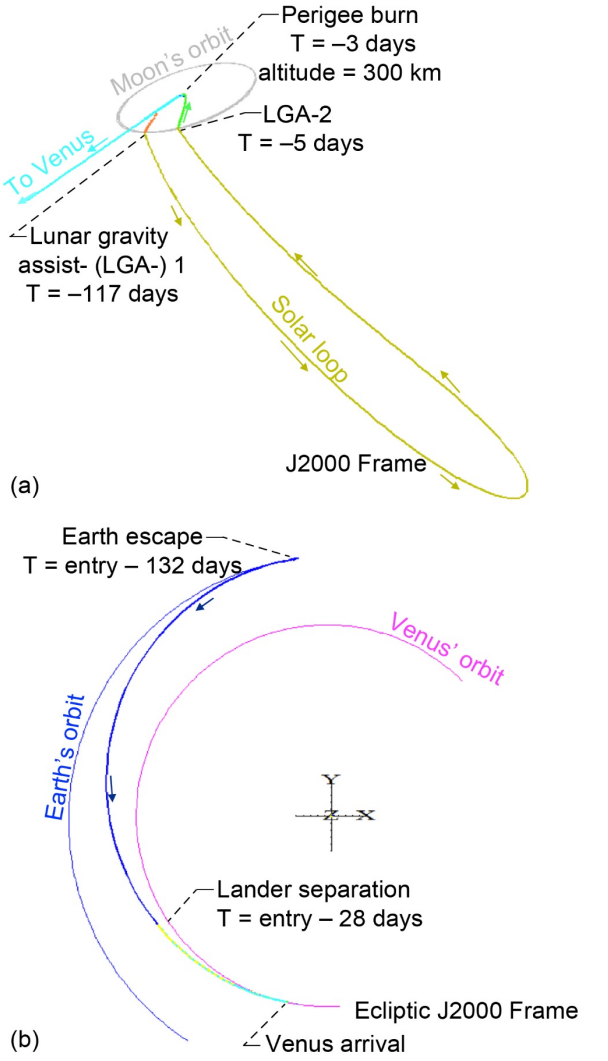

Figure 3.—Departure sequence and cruise overviews. (a) Earth departure sequence. (b) Interplanetary cruise.

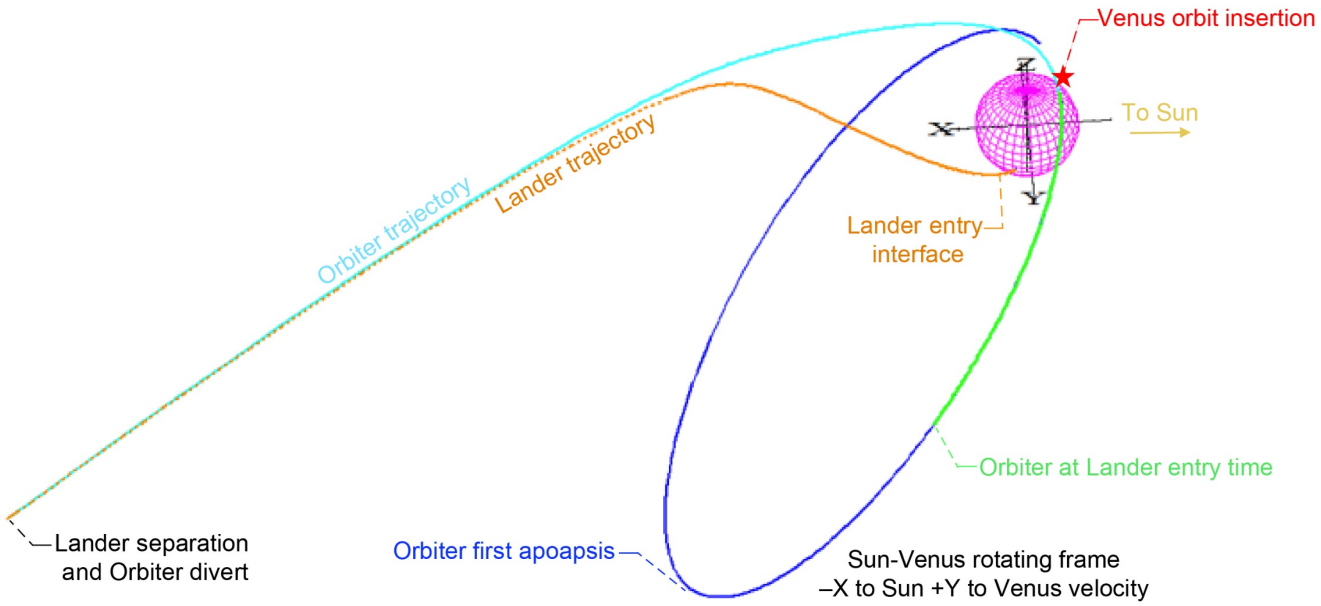

Figure 4.—Venus arrival sequence overview showing separation of Lander and position of Orbiter at Lander entry.

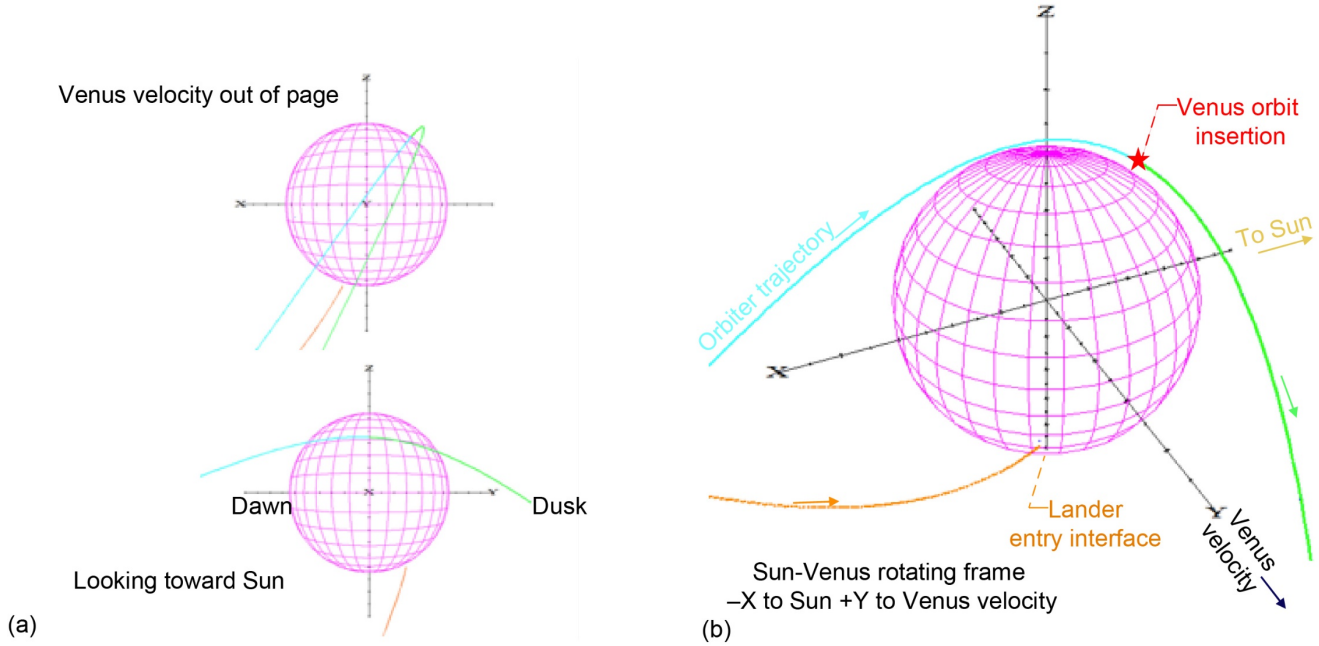

Figure 5.—Venus orbit insertion and landing location detailed views. (a) Looking toward Sun. (b) Sun-Venus rotating frame (–X to Sun and +Y to Venus velocity).

A parallel monotonic basin-hopping global optimization technique was used throughout the design in order to locate feasible solutions and further optimize the highly constrained mission. All maneuvers were designed as impulsive.

2.3.5 Mission Delta Velocity (ΔV) Details

A summary of the mission ΔVs for the V-BOSS mission can be seen in Table 4. The mission is broken into five phases. Phase 1 starts just after separation from the launch vehicle and

includes the Earth-Moon portion of the trajectory, including escape from the Earth-Moon system. Phase 2 is the heliocentric transfer trajectory from the Earth-Moon system to Venus. Phase 3 occurs just prior to VOI and encompasses the Lander/EDL package deployment event. Phase 4 sets up and performs the VOI maneuver, placing the Orbiter in a 10-day highly elliptical orbit around Venus. Phase 5 accounts for any orbital maintenance required to hold the orbit around Venus within acceptable bounds during the remainder of the mission.

It was assumed the launch vehicle would place the vehicle on a trans-lunar trajectory. The initial angular rates imparted onto the vehicle during separation from the launch vehicle were assumed to be 0.5°/s about each of the three body axes. These are nulled via Reaction Control System (RCS) thrusters. An approximated 10 m/s of ΔV was used to account for any corrections needed to target appropriate lunar flyby points, shown as lunar flyby correction 1 and 2 in Table 4. Finally, the Earth departure burn is a conservative estimate of the ΔV necessary to set up a heliocentric transfer trajectory from Earth to Venus. It accounts for any preburn targeting that may need to occur.

The heliocentric trajectory is fairly quiet in terms of dynamic events. Estimates of the necessary midcourse corrections were derived from the Venus Express and Magellan missions, both of which were successful missions to Venus. The S/C is three-axis controlled due to stringent science pointing requirements and the numerous times the Orbiter would need to orient itself for communication with the Deep Space Network (DSN) and the Lander. The reaction wheels onboard the vehicle are assumed to perform these slew maneuvers.

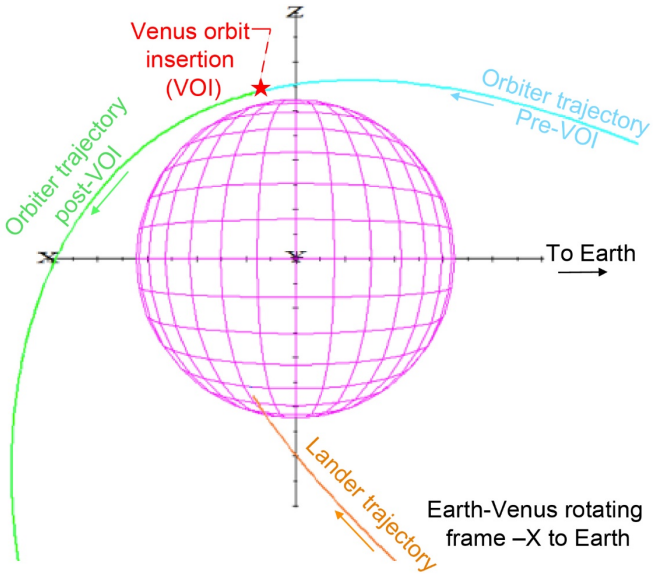

Figure 6.—Venus orbit insertion (VOI) demonstrating Earth visibility of critical event detailed view.

TABLE 4.—MISSION DELTA VELOCITY (ΔV) SUMMARY

Phase no.	Phase name	Pre-event mass, kg	Main ΔV, m/s	ACS[a] ΔV, m/s	Main I_{sp}[b], s	ACS I_{sp}, s	Main prop, kg	ACS prop, kg
1	Null tipoff rates	214	-----	0.5	---	200	----	0.058
	Trans-lunar injection (TLI) orbit insertion dispersion correction	214	-----	----	---	---	----	-----
	Lunar flyby correction 1	214	-----	10.0	---	200	----	1.154
	Lunar flyby correction 2	213	-----	----	---	---	----	-----
	Earth departure burn	213	350.0	----	240	---	31.2	-----
2	Midcourse correction 1	184	-----	5.0	---	200	----	.495
	Midcourse correction 2	183	-----	5.0	---	200	----	.494
3	Deploy direction attitude maneuver	183	-----	0.5	---	200	----	.049
	Deploy spin up	183	-----	1.0	---	200	----	.099
	Lander deploy	162	-----	.0	---	200	----	.000
	Orbiter spin down	162	-----	1.0	---	200	----	.085
4	Reorient for course correction	162	-----	.5	---	200	----	.043
	Course correction	161	-----	1.0	---	200	----	.085
	Venus orbit insertion	161	795.0	.0	240	---	47.9	-----
5	Orbital maintenance	115	-----	10.0	---	200	----	.606
	Total		1,145.0	35.0			79.1	3.2

[a]Attitude Control System.
[b]Specific impulse.

Analysis of the EDL package deploy event involved researching the similar Huygens deploy event during the Cassini-Huygens mission to Saturn. The inertial stabilization associated with spinning an object about its major principal axis is useful for setting up a desired orientation for the atmospheric entry phase. The Huygens probe was spun up via a spin table, and then deployed from Cassini after a certain minimum revolution per minute had been surpassed. For V-BOSS, the Orbiter/EDL package is spun up about the major principal axis via RCS thrusters until a revolution rate of 7 rpm is achieved. At this time, the EDL package (includes the Lander) is deployed via a spring mechanism. Another aspect taken from the Cassini-Huygens mission was the time at which the deploy occurred, relative to entry into the Venusian atmosphere. The estimated propellant required for the deploy event and subsequent despin is shown in Table 4.

The heliocentric trajectory is set up such that the S/C would enter the Venusian atmosphere at a certain range of latitude and longitude. Thus, the trajectory is developed such that the Lander constraints are satisfied. Therefore, a course correction maneuver was necessary to set up the VOI burn. The course correction burn occurs shortly after the deploy event in order to reduce the amount of propellant necessary to set up the VOI target point. The VOI burn is sized to place the Orbiter in a highly elliptical 10-day orbit.

Once in orbit about Venus, the Orbiter performs science, transfers data to the DSN, and acts as a relay for the Lander/backshell. Any attitude maneuvers associated with these activities are assumed to be handled by the onboard reaction wheels. The Orbiter attitude and orbit will be perturbed by environmental effects, primarily solar radiation pressure. The reaction wheels will frequently become saturated if used to counteract these torques. Therefore, 10 m/s of ΔV was allotted to account for desaturating the wheels and to perform any orbit raising maneuvers that may arise due to the effects of atmospheric drag reducing the periapsis of the orbit.

2.3.6 Concept of Operations (CONOPS)

The V-BOSS concept includes both an Orbiter and a Lander (Figure 7). The Lander is encapsulated in an entry and descent system. The Orbiter performs three main functions. First, it carries the encapsulated Lander through launch and transit to Venus and delivers the Lander to the proper insertion conditions for landing on Venus. Second it provides communications relay from the Lander back to Earth from atmospheric insertion, through landing, and periodically (~2 min every 12 hr) for ~120 days after landing. Due to the simplicity of the Lander, there is no downlink to the Lander from the Orbiter. Finally, the Orbiter carries its own infrared (IR) instrument, which works in concert with the Lander uplooking IR instrument.

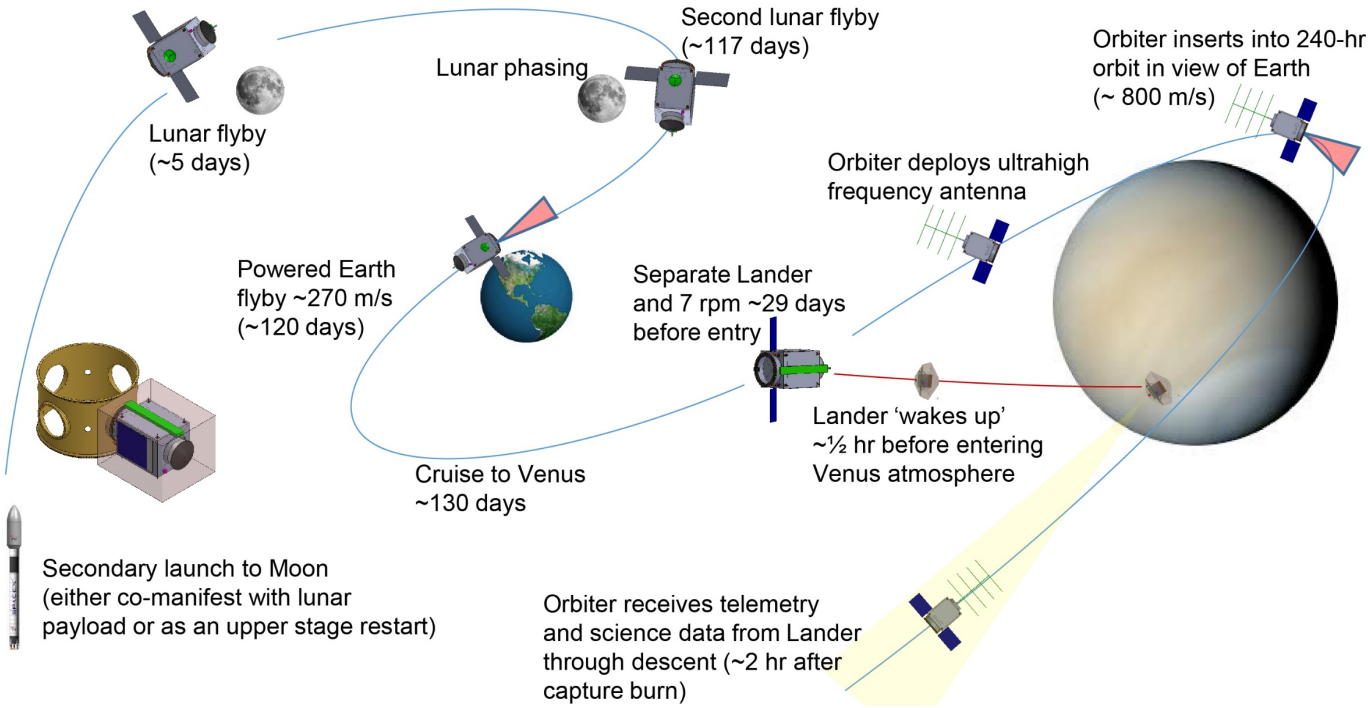

Figure 7.—Launch, transit, and delivery concept of operations.

2.3.6.1 Launch

Based on the launch and trajectory trades, a secondary ride with a lunar mission was chosen as the fastest, most likely, and lowest cost option. A representative launch date in the range of 2024 to 2025 was chosen with a secondary lunar mission or possibly Interstellar Mapping and Acceleration Probe (IMAP) Solar Terrestrial Probe-5 (STP–5). Attached to an Evolved Expendable Launch Vehicle (EELV) Secondary Payload Adapter (ESPA) Grande on a medium launcher with a 5-m fairing, the V-BOSS is launched toward the Moon with a C_3 of approximately –2 km^2/s^2. After separation of the primary payload, V-BOSS itself is separated from the ESPA Grande, deploys arrays, and begins commissioning.

2.3.6.2 Transit

After commissioning, the Orbiter performs the necessary midcourse corrections to enable a lunar flyby about 5 days after launch. The Orbiter points its fixed medium gain antenna at Earth while gimbaling its solar arrays (SAs) to maximize S/C power. The aeroshell/Lander are in quiescent mode—not to be activated until approaching Venus. The Orbiter performs an unpowered phasing loop to enable a second lunar flyby at 117 days. This sets up an Earth close approach when combined with a propulsive burn to provide sufficient ΔV to enable an escape trajectory towards Venus. After a coasting cruise of about 130 days, the Orbiter is about a month away from Venus intercept and begins deployment operations for the Lander.

Aeroshell/Lander Deployment

Based on Earth positioning and commands, the Orbiter points the aeroshell/Lander in the appropriate direction to intercept the Venus atmosphere and spins itself and the aeroshell/Lander up to a 7-rpm rotation to stabilize the aeroshell/Lander for its 29-day solo trip the rest of the way to Venus. At this point, the aeroshell/Lander are released from the Orbiter and a ~29-day backshell timer is activated. The Orbiter performs a despin maneuver and then a course correction to change its Venus intercept to allow a capture burn near Venus.

2.3.6.3 Orbiter Venus Capture

During the 29-day cruise to Venus, the Orbiter deploys its ultrahigh frequency (UHF) antenna to provide a link with the soon to be activated Lander. The Orbiter then performs a capture burn using its monopropellant system while in view of Earth. The critical event parameters are transmitted back to Earth using the omnidirectional antennas. Once captured in its 240-hr orbit, the Orbiter prepares to track and relay the event parameters of the Lander as it transits the atmosphere and lands on Venus.

2.3.6.4 Entry, Descent, and Landing (EDL)

After its 29-day spun cruise to Venus, the aeroshell timer activates a pyrolytic heater to activate a thermal battery pack on the backshell, which in turn activates the Lander for the first time since its loading on the launch vehicle. This activation occurs ½ hr before entering the Venus atmosphere. Once activated, the Lander provides status data back to the Orbiter for the critical EDL events. Communications are made using the Lander communications system through a radiofrequency (RF) transparent backshell at a rate of ~36 bps. Estimates show that the spun stabilized aeroshell would encounter the atmosphere at 11 km/s at a ~45° angle and incur up to 300g of deceleration as it slows in the upper Venus atmosphere. Temperature and atmospheric density begins to rise as the still-packaged Lander descends. A communication uplink providing temperature, pressure, and Lander health is continually transmitted up to the newly captured Orbiter for relay back to Earth. A pressure switch detects the Venus pressure of 25 km (~25 min after entry) and deploys the backshell dragflaps to allow the backshell/Lander to slow and the heatshield to be jettisoned (Figure 8). At 20 km (~37 min after entry), a second pressure switch releases the Lander from the backshell for its solo descent to the surface. A built-in dragflap provides sufficient Lander deceleration during its final descent to the surface. Once released, additional Lander science instruments are activated (chemical sensors and IR bolometers) for the final descent to the surface. The IR bolometer data during descent will work in concert with the Orbiter's downlooking bolometer. This final descent portion for the Lander is estimated to take about ¾ of an hour. Uplink communications to the Orbiter continue during this phase to uplink additional science data since the Lander has no data storage system. The Lander should land ~120 km downrange from the atmospheric insertion point and land at a speed of ~5 m/s. Landing site selection is important so that a maximum slope of <13° and minimal debris will be encountered by the small Lander. Final deceleration of the Lander is performed by a crush pad on the bottom of the Lander.

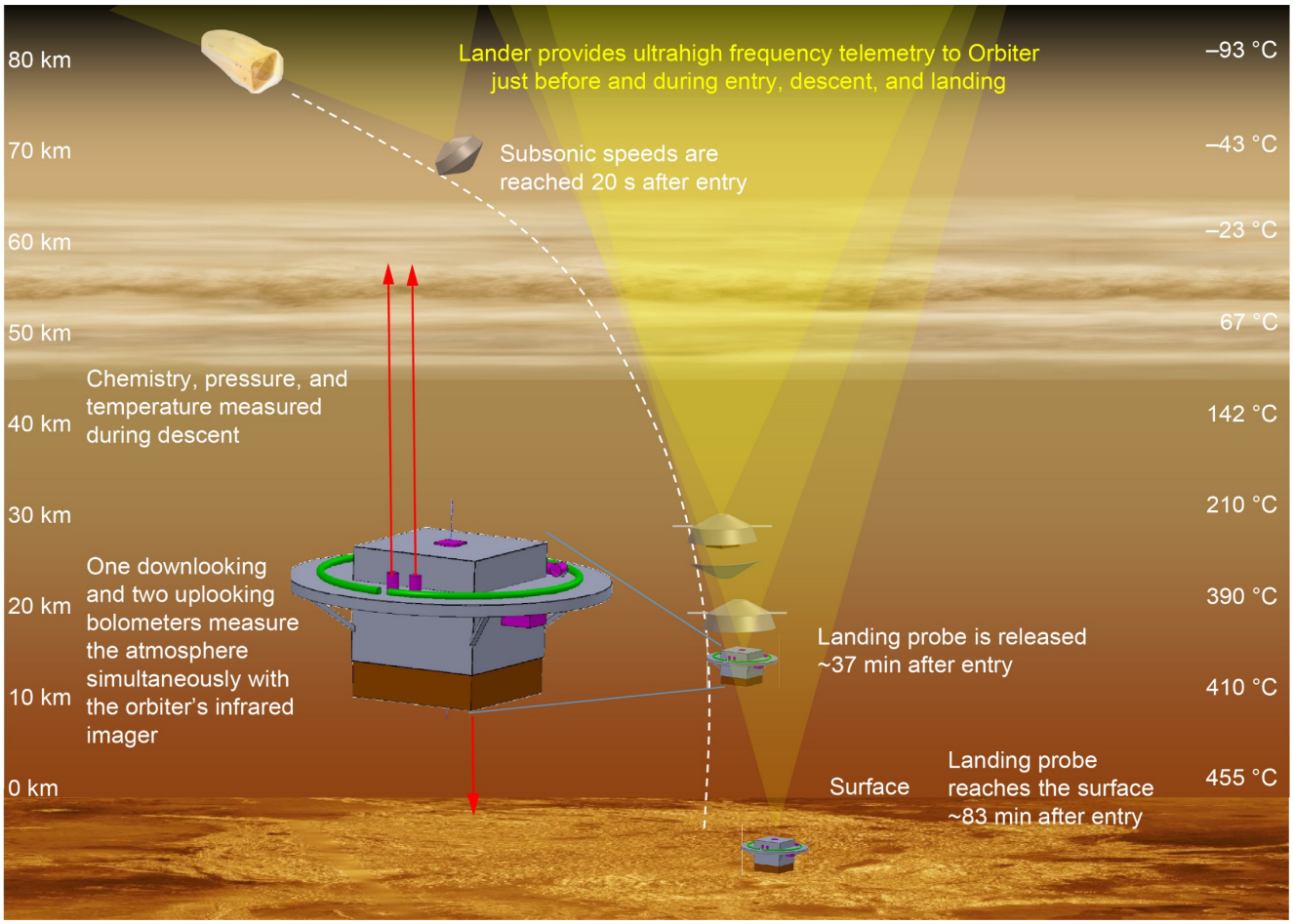

Figure 8.—Entry, descent, and landing.

2.3.6.5 Landed Operations

Given the constraints of the launch date, the requirement to view the Orbiter during insertion and the Orbiter to relay from the Lander during descent as well as land in darkness at 50 Earth days before dawn, a landing site near Helen Planitia (55° S, 261° E) was chosen. Other sites are possible, assuming additional analysis efforts. The landed lifetime desired is 120 Earth days (a Venus solar day). This has a large impact on landed operations due to use of battery power for the Lander. To maximize the lifetime, three mission phases were chosen: a 5-hr continuous operation just after landing, an uplink for 2 min every hour for the next 72 hr, followed by the long-duration operations of 2 min every 12 hr for the rest of the 120 days (Figure 9). During this first 5 hr, the wind sensor is deployed and its data joins the rest of the periodic data taken for the duration of the landed mission. The key to minimizing energy needs is a low-power timer circuit (~15 mW), which provides simultaneous science and communications for a 2-min duration. After the 2 min, the timer is reset and the science and communications deactivated. As mentioned elsewhere, high-temperature data storage is prohibitively energy intense as would be a receiver operating continuously. As such, the 2-min realtime data uplink every 12 hr to an Orbiter should have minimal data loss given the Orbiter's highly elliptical, 240-hr orbit. The Lander will experience sunrise on Venus at roughly halfway through its mission. The Lander will operate until its battery energy is exhausted.

2.3.6.6 Orbiter Operations at Venus

Once captured in orbit, the Venus Orbiter will store and relay data from the Lander back to Earth. The Orbiter will listen for data for the three mission phases described above. Once a Lander uplink is sensed, the Orbiter will also activate its IR sensor to allow corroborating the data between the upward-looking Lander and the downward-looking Orbiter. The Orbiter will need to have its UHF antenna pointed towards the Lander during its entry, descent, and landing as well as during its operations. This will require storing the uplinked data for later

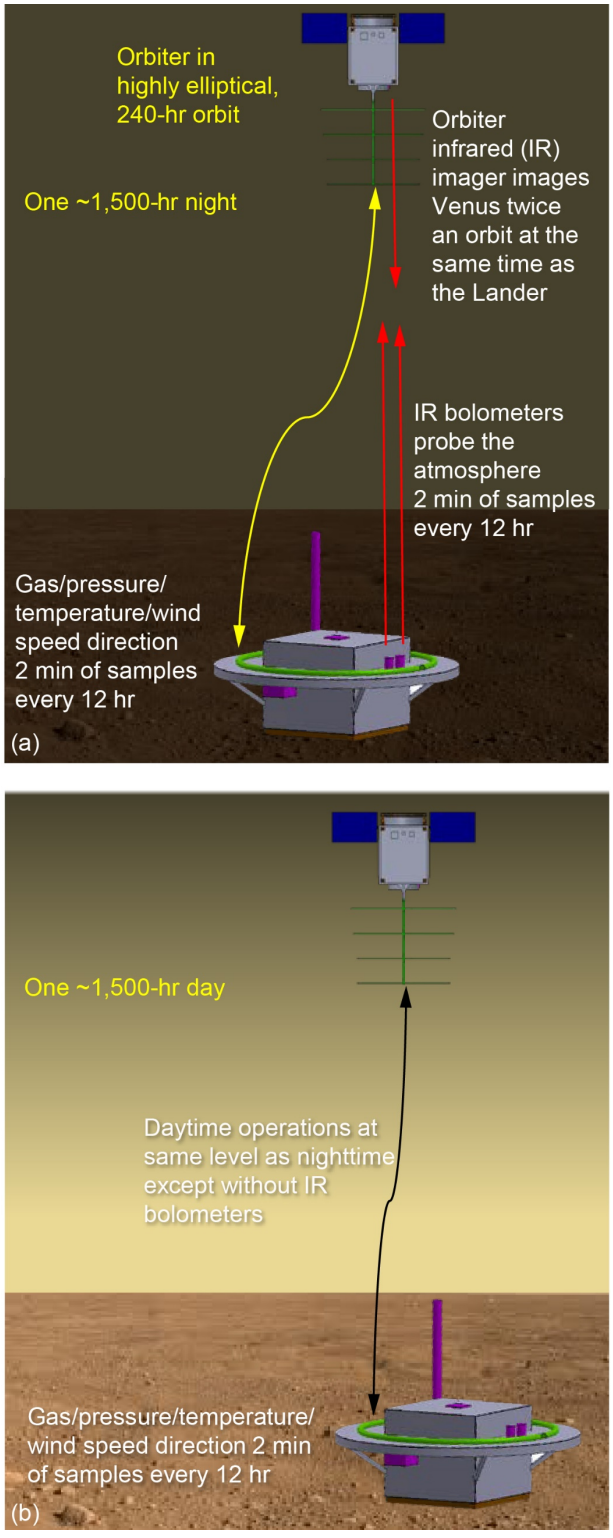

Figure 9.—Landed operations. (a) Nighttime. (b) Daytime.

relay to Earth. The 72-hr phase should generate about 9 Mb of Lander data with an additional 240 kb of Lander data every 5 days for the 2 min every 12 hr data collection phase. Added to this is the Orbiter IR imaging data at around 3 Mb for every matched image with the Lander, amounting to about 6 Mb per day. All this data can be sent back to Earth using the DSN at about 200 bps for a single 8-hr pass once each day. The initial 72-hr data can be included over the life of the mission in this data stream. Coordinating pointing and listening for the 2 min every 12 hr Lander uplinks with the fixed UHF antenna can be interleaved with pointing the satellite's fixed medium gain X-band antenna for 8 hr back to Earth over each 240-hr orbit once the fixed Lander uplink cadence is detected, eliminating lost uplinks. Some uplinks may be lost during the Orbiter's periapsis pass, but these should be minimal. The Orbiter will point its SAs and either UHF or medium gain X-band antenna by rolling the S/C and turning its SA gimbals. Orbit maintenance and wheel dumps will be performed periodically by the monopropellant system. Currently, a budget of 10 m/s is allotted for orbit maintenance. Once the Lander has become inactive, the Orbiter's primary mission is over, but it could be extended to provide additional IR data or data relay capabilities given sufficient propellant reserves. Further work needs to be done to assess Orbiter disposal. It is most likely that once propellant is exhausted, solar/third body perturbations will either lower the orbit to impact the atmosphere or raise it away from future low-orbiting assets.

2.4 System Design Trade Space

2.4.1 Architecture Trades

While the main objective of the Venus Bridge concept point design was to determine if a $200 million cost cap is achievable for an Orbiter/Lander combination with meaningful science, many trades were made, both at architectural and subsystem levels to settle on the chosen point design. These options provide valuable insight into other possible Venus Bridge Orbiter/Lander combinations. Trajectory and subsystem trades are discussed in detail in their appropriate sections. Overarching architecture trades will be discussed here.

2.4.1.1 Orbiter Delivery

There are many paths from Earth to Venus for a small satellite with Lander. Figure 10 shows some of them. The first that springs to mind is launching as a secondary with a primary Venus Orbiter. Such a path makes even more sense if the Lander is part of the primary Orbiter, which also provides delivery and communications relay. This was thought to be outside the spirit of Venus Bridge. Another seemingly attractive way would be to hitch a ride with an S/C using Venus during a

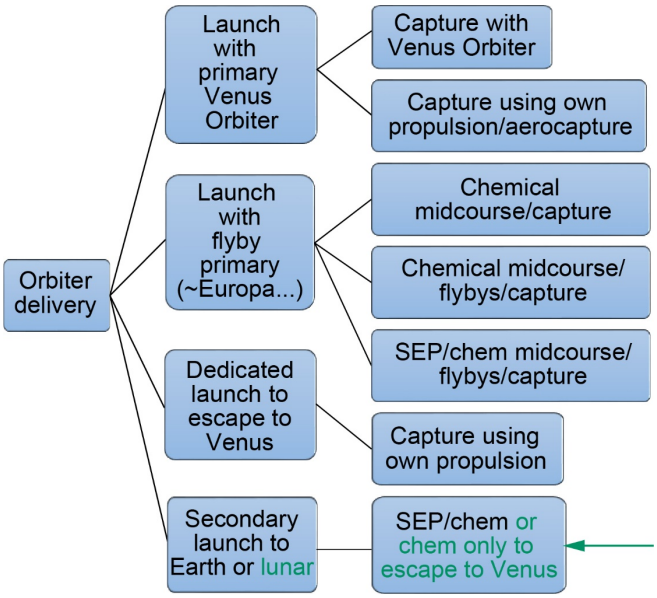

Figure 10.—Orbiter delivery trade, where SEP is solar electric propulsion.

gravity assist. However, the primary S/C usually will be flying by Venus at high velocities, making the capture propellant excessive. (As a carrier for a short-lived Lander, a Venus flyby might make sense, but the Lander would probably need its own propulsion system to intercept Venus, to avoid risking the primary S/C.) The capture propellant could be reduced if the first Venus flyby were modified for the Orbiter with a return later to capture (similar to the Japanese satellite Akatsuki). This would add more time to the trajectory. Given an inexpensive, small launch vehicle, a dedicated launch for the Orbiter/Lander is the most straightforward, but an affordable small launch vehicle is not yet available—perhaps in the next decade. From an affordability and frequency standpoint, a secondary launch to a geostationary transfer orbit is very attractive but does require additional propellant to escape Earth. An even more attractive secondary launch, which may not be as frequent but would greatly reduce the propellant requirements, would be a secondary lunar launch. With the new space council initiative on lunar missions, more opportunities might appear in the next decade. A lunar mission provides almost enough energy to escape Earth and also provides the bonus of lunar and EGAs.

2.4.1.2 Venus Operational Orbit

Operating orbit at Venus was also traded. While landers and rovers on Mars can use a low-altitude Orbiter link once a day, thus minimizing the communications link energy, the battery-powered Venus Lander must minimize its energy use in order to last 120 Earth days. As such it cannot be listening for an Orbiter to say it is ready for data uplink since having the receiver on continuously would take too much energy. Thus, it is best if the Orbiter is overhead as much as possible, which equates to an elliptic orbit with the apoapsis above the Lander. Combining this with a need to minimize propellant mass drove the design to be in a very highly elliptical (240-hr) orbit. This orbit provides >90-percent access time to the Orbiter from the Lander. In addition, this highly elliptical orbit is most easily accessed using an impulsive (chemical) propulsion system. While a solar electric propulsion (SEP) system could spiral into a high circular orbit, it would only have about one-half of the viewing time since there is no synchronous orbit for the very slow rotating Venus.

2.5 Launch Configuration Details

There are three main elements that were designed for the Venus Bridge study: an Orbiter, an entry, descent, and landing (EDL) system (aeroshell), and the Lander itself. All three of these elements are to be launched as a single secondary payload on an ESPA ring. While it was desired to utilize a standard ESPA, the payload envelope associated with the standard ESPA does not provide sufficient volume for all three elements, thus requiring the use of an ESPA Grande. The size of the Orbiter is primarily driven by the diameter of the spherical monopropellant tank. Figure 11 shows various views of the V-BOSS launch configuration integrated to the ESPA Grande.

A 24-in. Lightband provides the interface between the ESPA Grande port and the Orbiter (Figure 12) and also serves as the separation mechanism between the two. A cylindrical structure extending off the top of the Orbiter provides the support structure for the EDL system containing the Lander. The separation system between the Orbiter and EDL system is not included in the computer-aided design (CAD) model for this study, but is included in the Structures and Mechanisms portion of the MEL, and thus included in the cost numbers for the V-BOSS design.

In order for the Orbiter to fit within the payload envelope associated with the ESPA Grande, several components need to be stowed for launch. These include the two solar array wings (SAWs) and the UHF Yagi antenna used for communication between the Orbiter and Lander during the surface operations phases of the mission. These deployable components for the various mission phase configurations can be seen in Figure 13.

Once separated from the ESPA Grande, the two SAWs are deployed. Each wing contains one solar panel that when stowed, lies parallel to the side of the Orbiter bus structure with the solar cells facing outward. This orientation allows for a limited amount of power to still be generated for the Orbiter in the event there is a deployment failure. Deployment is performed by a spring mechanism that allows the arrays to fall away 90° from the side of the bus. Solar tracking is performed by a single-axis gimbal at the base of each array wing.

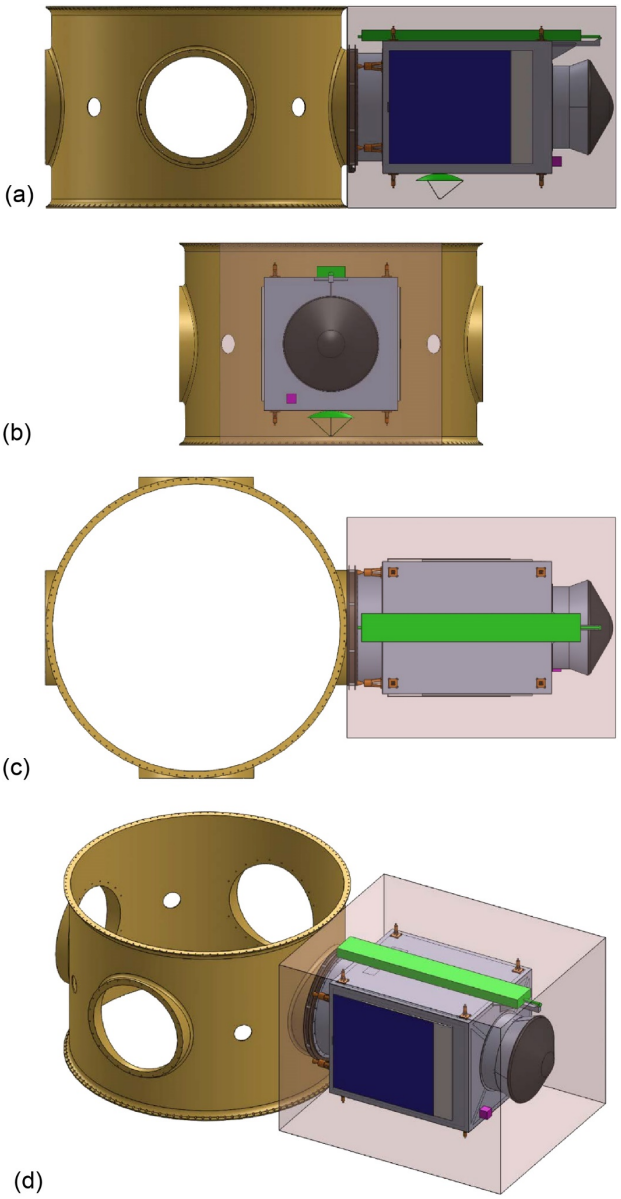

Figure 11.—Venus Bridge Orbiter and Surface Study (V-BOSS) launch configuration integrated to Evolved Expendable Launch Vehicle (EELV) Secondary Payload Adapter (ESPA) Grande. (a) Side view. (b) End view. (c) Top view. (d) Overview showing available payload volume.

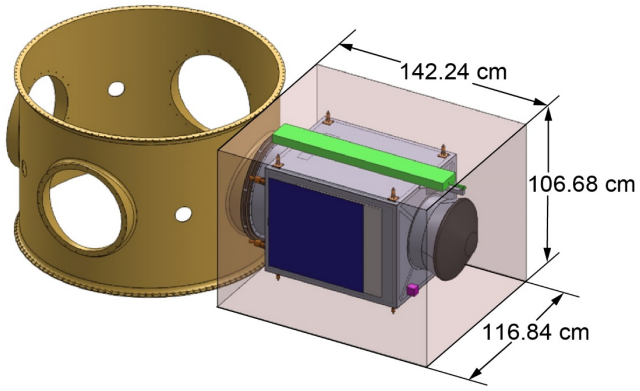

Figure 12.—Payload envelope with dimensions for Evolved Expendable Launch Vehicle (EELV) Secondary Payload Adapter (ESPA) Grande.

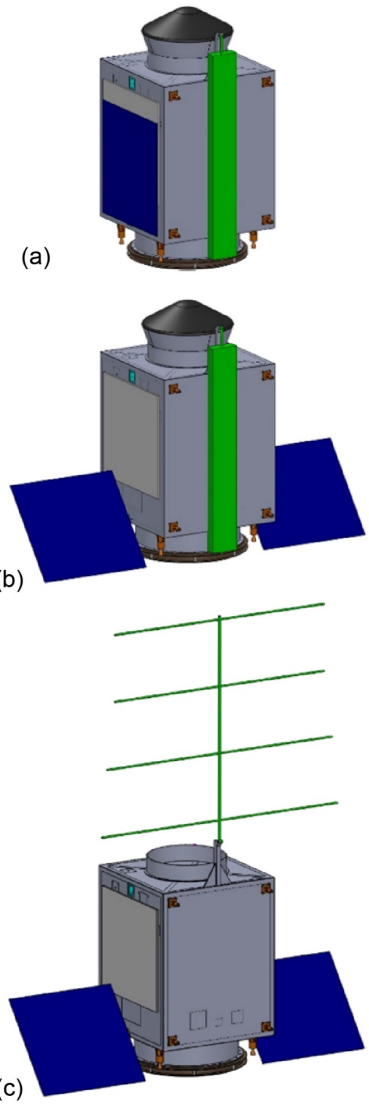

Figure 13.—Payload envelope for Evolved Expendable Launch Vehicle (EELV) Secondary Payload Adapter (ESPA) Grande. (a) Stowed. (b) Transit. (c) Venus orbit.

Once in orbit around Venus, and after separation of the EDL system, the UHF Yagi antenna is deployed. The elongated green rectangular box shown in Figure 13 represents the stowed envelope for the Yagi antenna. In order to fit within the payload envelope associated with the ESPA Grande, each member of the Yagi antenna must be stowed at launch. While some work went into determining an appropriate envelope for the stowed antenna, a detailed design of how each member would stow and deploy is beyond the scope of this study. Prior to deployment of each of the individual members that comprise the Yagi antenna, a spring mechanism is used to deploy the stowed antenna by rotating the antenna assembly 180° up from its stowed position along the side of the Orbiter bus. There is no gimbal associated with the Yagi antenna, thus, any pointing is achieved by using the RCS to point the entire Orbiter.

The EDL system contains the V-BOSS Lander and consists of the heat shield, backshell, and four deployable drag flaps contained on the backshell. These drag flaps are the only deployable components contained on the EDL system. Upon entering the Venus atmosphere, the four drag flaps are deployed to create the drag necessary to slow down the Lander during entry and descent. Due to the small size of the EDL system and the size of the Lander contained in the EDL system, a parachute could not be used to slow down the Lander during the descent phase. Figure 14 shows the EDL system with the drag flaps stowed and deployed while the dimensions of the heat shield and backshell are shown in Figure 15.

The Lander element of the V-BOSS design is contained within the EDL system. In order to fit within the aeroshell, the wind sensor needs to be stowed at launch as it is contained on a 20-cm-long boom. The wind sensor boom lays on the top of the drag flap structure, parallel to the surface, when stowed and utilizes a spring mechanism for deployment that rotates it 90° upward and perpendicular to the surface. This puts the wind sensor well above the Lander and into winds that are not affected by the Lander itself. There are no other components on the Lander that need to be deployed once on the surface of Venus. Figure 16 shows the Lander in the stowed and deployed configurations. Note that the image for the deployed Lander shows the crush pad, located on the bottom of the Lander, in the crushed (or displaced) state as it would be after landing on the surface.

Additional images of the stowed configurations for the Orbiter, EDL system, and Lander can be found in Appendix C.

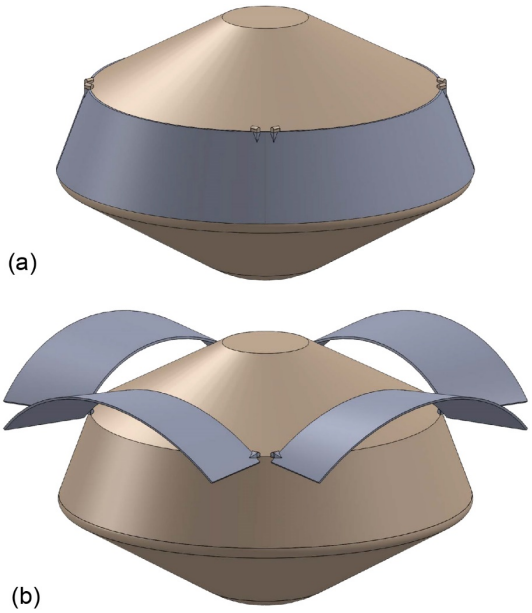

Figure 14.—Entry, descent, and landing system configurations. (a) Stowed. (b) Deployed.

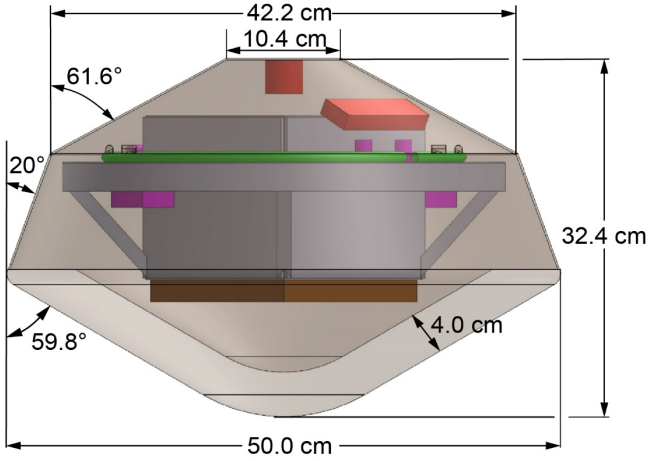

Figure 15.—Heat shield and backshell dimensions.

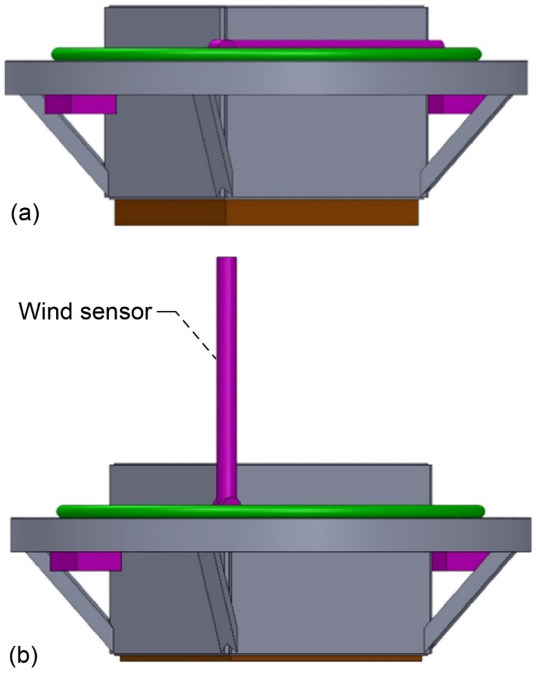

Figure 16.—Lander configurations. (a) Stowed. (b) Deployed.

3.0 Baseline Design

3.1 Top-Level Design

3.1.1 Master Equipment List (MEL)

The MEL lists the three major elements in terms of the major subsystems within them. The entire S/C assembly, which contains the Lander, EDL system, and Orbiter, is listed as work breakdown structure (WBS) Element 06. The Lander itself is listed in the MEL as WBS element 06.1. The EDL system is listed as WBS element 06.2. The Orbiter is listed as WBS element 06.3. Table 5 shows the MEL listing of all three elements designed by the Compass team.

3.1.2 Spacecraft (S/C) Total Mass Summary

The MEL shown in Table 6 captures the bottoms-up estimation of current best estimate (CBE) and growth percentage that the subsystem designers calculated for each line subsystem. Section 4.0 provides additional detail about the basic and total masses of the different subsystems and of the entire V-BOSS platform after mass growth percentage is applied. In order to meet the total required mass growth of 30 percent, an allocation is necessary for growth on basic dry mass at the system level, in addition to the growth calculated on each individual subsystem. This additional system-level mass is counted as part of the inert mass to be flown along the required trajectory. Therefore, the additional system-level growth mass impacts the total propellant required for the mission design.

The system-level summary for the baseline case, which includes the additional system-level growth, is shown in Table 6. With 30-percent growth on the basic dry mass, the total mass is 226.9 kg. The inert mass and dry mass is also shown. After summarizing the bottoms-up masses from Table 6, an additional system-level growth was applied and shown in Table 6. In order to reach the 30-percent total MGA on basic mass of the required for this study, additional system-level margin growth mass was carried for each element, as shown in Table 6.

3.1.3 Power Equipment List (PEL)

To model the power systems in this design study, 10 modes of operation were defined. These modes were defined based on the mission profile and they identify which items and subsystems are operating, and which items are dormant, at any time throughout the mission. The definitions of these modes are shown in Table 7.

Table 8 shows the assumptions about the power requirements in all the modes of operation. The power requirements from the bottoms-up analysis on listed in Table 8 are used by the power system designers (described in Sec. 4.7) to size the SAs and other power system components.

TABLE 5.—MASTER EQUIPMENT LIST WORK BREAKDOWN STRUCTURE (WBS) FORMAT

WBS no.	Description Venus Bridge Orbiter and Surface Study (V-BOSS)
06	V-BOSS
06.1	Lander
06.1.1	Science
06.1.3	Command & Data Handling
06.1.4	Communications and Tracking
06.1.5	Electrical Power Subsystem
06.1.11	Structures and Mechanisms
06.2	EDL
06.2.5	Electrical Power Subsystem
06.2.6	Thermal Control (Nonpropellant)
06.2.11	Structures and Mechanisms
06.3	Orbiter
06.3.1	Science
06.3.2	Attitude Determination and Control
06.3.3	Command & Data Handling
06.3.4	Communications and Tracking
06.3.5	Electrical Power Subsystem
06.3.6	Thermal Control (Nonpropellant)
06.3.7	Propulsion (Chemical Hardware)
06.3.8	Propellant (Chemical)
06.3.11	Structures and Mechanisms

TABLE 6.—BASELINE CASE SUMMARY

MEL[a] summary: Venus Bridge Orbiter and Surface Study (V-BOSS)	Lander	EDL[b]	Orbiter	Total
Main subsystems	Basic mass, kg	Basic mass, kg	Basic mass, kg	Total basic mass, kg
Science	0.5	0.0	2.0	2.5
Attitude Determination and Control (AD&C)	0.0	0.0	3.2	3.2
Command and Data Handling (C&DH)	0.2	0.0	2.0	2.2
Communications and Tracking	0.4	0.0	6.3	6.7
Electrical Power (EP) Subsystem	2.6	0.2	18.7	21.5
Thermal Control (Nonpropellant)	0.0	8.5	10.4	18.8
Propulsion (Chemical Hardware)	0.0	0.0	13.3	13.3
Propellant (Chemical)	0.0	0.0	90.4	90.4
Propulsion (EP Hardware)	0.0	0.0	0.0	0.0
Propellant (EP)	0.0	0.0	0.0	0.0
Structures And Mechanisms	7.5	0.1	29.1	36.7
Element total	11.1	8.8	175.4	195.4
Element dry mass (no propellant, consumables)	11.1	8.8	85.0	105.0
Element propellant	0.0	0.0	90.4	90.4
Element mass growth allowance (aggregate)	2.4	1.6	15.7	19.7
Additional system-level growth (for 30-percent total)	0.9	1.0	9.8	11.8
Total wet mass with 30-percent growth	14.5	11.5	200.9	226.9

[a]Master equipment list.
[b]Entry, descent, and landing.

TABLE 7.—DEFINITION OF POWER MODES

Power mode title	Description	Duration
Orbiter/EDL[a] + Lander separation	Orbiter separates from EDL + Lander	30 min
EDL/Lander entry	Begins at Orbiter/EDL + Lander separate, includes stack entry, and ends when EDL separation from Lander	29 Earth days
Orbiter insertion burn	Orbit insertion burn	20 min
Lander baseline mode	Full power for the first 8 hr (first 1 hr during descent) and then transmit once every hour for the first 3 days	72 hr
Lander standby	Lander goes into a standby/timer mode, instruments are off	12 hr
Lander science and communications	All instruments are on and Lander is communicating the data	2 min
Orbiter eclipse		15 min
Orbiter science	Orbiter instruments are active and taking data (take a picture every 12 hr when Lander is communicating)	5 min
Orbiter communications	Orbiter is communicating with Earth (once every 24 hr)	8 hr
Orbiter standby	Orbiter is not communicating with Earth, but includes Orbiter receiver	10 Earth days

[a]Entry, descent, and landing.

TABLE 8.—POWER EQUIPMENT LIST (DOES NOT REFLECT 30-PERCENT POWER MARGIN)

Power mode name (W)	Orbiter/ EDL[a] + Lander separation	EDL/ Lander entry	Orbiter insertion burn	Lander baseline mode	Lander standby	Lander science and comm	Orbiter eclipse	Orbiter science	Orbiter comm	Orbiter standby
Power mode duration	30 min	29 Earth days	20 min	72 hr	12 hr	2 min	15 min	5 min	8 hr	10 Earth days
V-BOSS	150.68	9.68	252.73	17.13	9.50	17.13	39.88	45.68	90.68	40.68
Lander	0.00	0.00	2.05	7.65	0.02	7.65	0.00	0.00	0.00	0.00
Science	0.00	0.00	0.50	1.30	0.00	1.30	0.00	0.00	0.00	0.00
C&DH[b]	0.00	0.00	1.55	1.95	0.02	1.95	0.00	0.00	0.00	0.00
Communications and Tracking	0.00	0.00	0.00	4.40	0.00	4.40	0.00	0.00	0.00	0.00
Electrical Power (EP) subsystem	0.00	0.00	0.00	0.00	0.00	0.00	0.00	0.00	0.00	0.00
Structures and mechanisms	0.00	0.00	0.00	0.00	0.00	0.00	0.00	0.00	0.00	0.00
EDL	0.00	0.20	0.00	0.00	0.00	0.00	0.00	0.00	0.00	0.00
EP subsystem	0.00	0.00	0.00	0.00	0.00	0.00	0.00	0.00	0.00	0.00
Thermal control (nonpropellant)	0.00	0.20	0.00	0.00	0.00	0.00	0.00	0.00	0.00	0.00
Structures and mechanisms	0.00	0.00	0.00	0.00	0.00	0.00	0.00	0.00	0.00	0.00
Orbiter	150.68	9.48	250.68	9.48	9.48	9.48	39.88	45.68	90.68	40.68
Science	0.00	0.00	0.00	0.00	0.00	0.00	0.00	5.00	0.00	0.00
AD&C[c]	21.10	0.00	21.10	0.00	0.00	0.00	20.30	21.10	21.10	21.10
C&DH	8.98	8.98	8.98	8.98	8.98	8.98	8.98	8.98	8.98	8.98
Communications and Tracking	50.00	0.00	50.00	0.00	0.00	0.00	0.00	0.00	50.00	0.00
EP subsystem	10.10	0.00	10.10	0.00	0.00	0.00	10.10	10.10	10.10	10.10
Thermal control (nonpropellant)	0.00	0.00	0.00	0.00	0.00	0.00	0.00	0.00	0.00	0.00
Propulsion (chemical hardware)	60.50	0.50	160.50	0.50	0.50	0.50	0.50	0.50	0.50	0.50
Propellant (chemical)	0.00	0.00	0.00	0.00	0.00	0.00	0.00	0.00	0.00	0.00
Structures and mechanisms	0.00	0.00	0.00	0.00	0.00	0.00	0.00	0.00	0.00	0.00

[a]Entry, descent, and landing.

[b]Command and Data Handling.

[c]Attitude Determination and Control.

3.2 Concept Drawing and Description

3.2.1 Orbiter Configuration

The bus structure for the Orbiter comprises a rectangular space frame, six face sheets that close in the space frame, and two cylindrical structures, one centered on the top of the rectangular bus and the other on the bottom. Nearly all of the S/C components are mounted to the six face sheets, making for a relatively easy assembly. Figure 17 shows a transparent view of the Orbiter structures with all of the system components.

The spherical propellant tank is mounted to four structural members that extend inwards from the vertical members of the space frame via four tab mounts equally spaced around the tank circumference. A band runs the full circumference of the tank to provide additional support. Extending up from the edge of the top of the bus is a structural member to which the UHF Yagi antenna is mounted. This member allows the Yagi antenna clearance from the bus when deployed and also allows the length of the stowed antenna to stay within the ESPA Grande payload envelope as the stowed antenna envelope is longer than the rectangular bus structure.

The top cylindrical structure provides the interface to the EDL system. The backshell portion of the EDL system extends down into the cylindrical structure and sits nearly flush with the top face sheet on the bus. This allows the EDL system, when integrated with the Orbiter, to remain within the provided payload envelope for the ESPA Grande. A detailed CAD design for the interface and separation mechanism between the Orbiter and Lander was considered beyond the scope of this initial study.

The cylindrical structure located on the bottom of the bus structure provides the interface to the passive side of the 24-in. Lightband, which when combined with the active side, provides the interface and separation mechanism between the Orbiter and the ESPA Grande. The height of this cylindrical structure is driven by the length of the four RCS thrusters extending below the rectangular bus structure, and thus keeping the thrusters above the separation plane of the Lightband.

A more detailed discussion on the structural design of the Orbiter can be found in Section 4.9.

Figure 18 shows the maximum dimensions of the Orbiter in the deployed configuration. Additional dimensions for the Orbiter, specifically focusing on the bus sizes, can be found in Appendix C.

Those system components that are located on the outside of the bus structure include the two SAWs, two radiator panels, a UHF Yagi antenna, an X-band dish antenna, a star tracker (though mounted inside, it has an outside field-of-view), an IR spectrometer, eight 1-N RCS thrusters, four 22-N RCS thrusters, and a 24-in. Lightband. These external components can be seen in Figure 19.

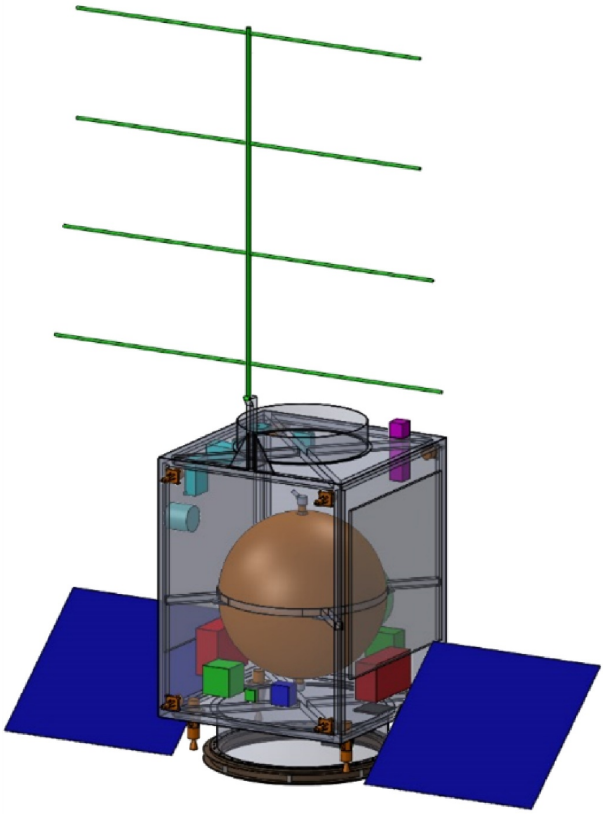

Figure 17.—Transparent closeup of Orbiter bus.

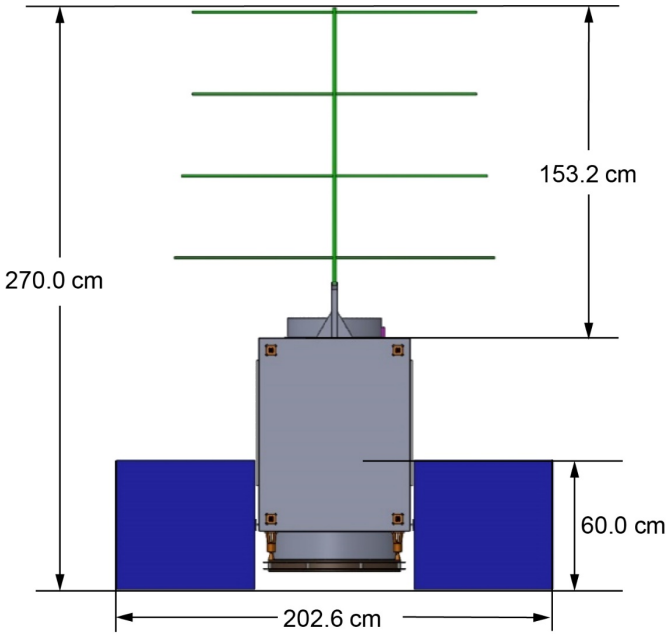

Figure 18.—Maximum dimensions for deployed Orbiter.

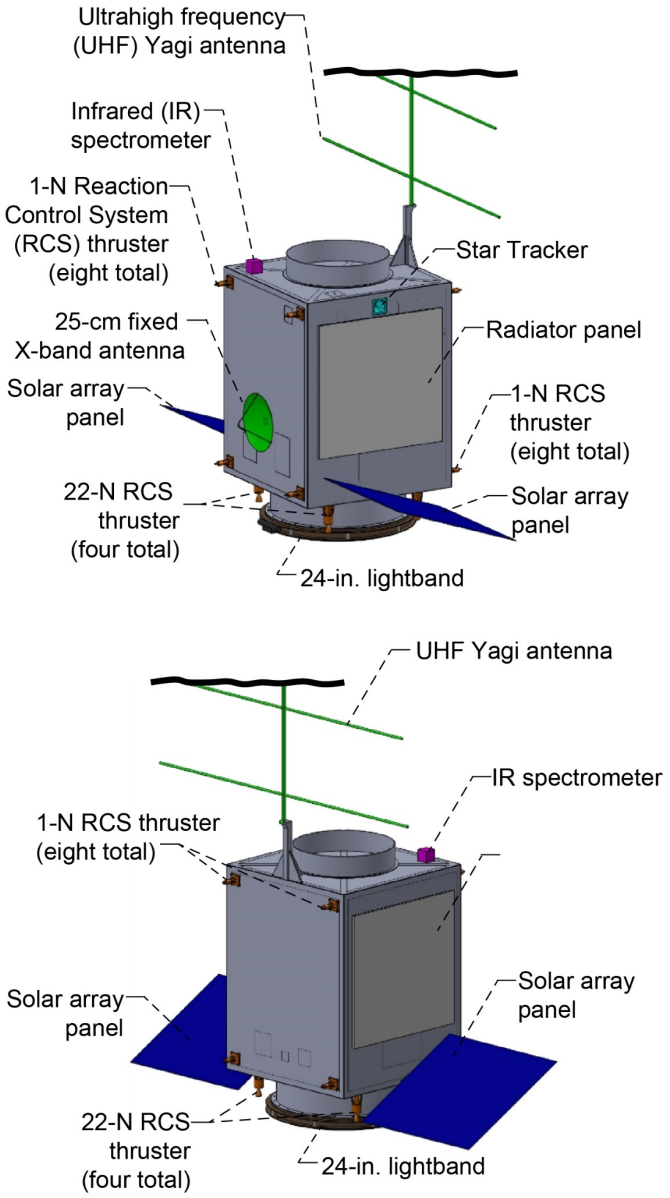

Figure 19.—Rotated views of Orbiter, showing external components.

Each of the two SA wings are located on opposite sides of the bus structure. A single-axis gimbal, located inside the bottom of the rectangular bus structure, provides the interface for the array wings and allows for solar tracking throughout the mission. Also located on the same sides as the SA wings, and mounted directly to the bus face sheets, are the two fixed radiator panels that provide the rejection of the waste heat created by all of the bus electronics. This location ensures that while the arrays are tracking the Sun, the radiators will always have a perpendicular view of the Sun. In addition to having a perpendicular view of the Sun, this location ensures the radiators will not have a view of Venus as the UHF Yagi antenna located at the top of the bus will be pointed towards Venus while communicating with the Lander. More details on the SA and radiator designs can be found in Section 4.7, Electrical Power (EP) Subsystem and Section 4.10, Thermal Control.

As mentioned previously, the UHF Yagi antenna is located on the top of the bus structure and will be pointed at Venus while communicating with the Lander. Communications back to Earth are done with a 25-cm-diameter fixed X-band dish antenna. This antenna is mounted directly to the face sheet on a side of the bus adjacent to the arrays and radiators. Antenna pointing for the X-band system is done by pointing the entire S/C. More details on the communications system can be found in Section 4.4.

The single star tracker is located just above one of the radiator panels on the side of the rectangular bus structure. While mounted inside the bus structure, the star tracker has an external field-of-view, and is thus included with the external components. By placing the star tracker above the radiator panel, it assures that the SA will never enter its field-of-view. This location also ensures, as with the radiator, that the star tracker will never be pointed at the Sun or Venus, but will have a clear view of deep space. A detailed discussion on the star tracker can be found in Section 4.6.

Located on the top of the bus structure near a corner opposite the UHF Yagi antenna is the IR spectrometer. While most of the unit is contained inside the bus, a portion protrudes out above the top face sheet. This location, similar to the Yagi antenna, allows the IR spectrometer to examine the Venus surface as the top of the S/C will be pointed at Venus while in orbit. By placing the IR spectrometer in a corner opposite the Yagi antenna, it will have a field-of-view that is unobstructed by the Yagi antenna as well as the cylindrical structure used to interface with the EDL system. A more detailed discussion on the IR spectrometer can be found in Section 4.1.

The eight 1-N RCS thrusters are located on the two sides of the rectangular bus structure that do not contain the SAs and radiators. There are four thrusters per side, each at the corner of the rectangular bus structure, and all are mounted with their thrust vectors perpendicular to the face sheet. These sides were selected to contain the thrusters so as to not have any interference with the SAs contained on the other two sides. At the bottom of the rectangular bus structure are the four 22-N RCS thrusters. They are located out at the corners of the bottom face sheet with thrust vectors perpendicular to that face sheet. These larger thrusters perform the major maneuver burns during the mission as well as assist the eight 1-N thrusters in adjusting the attitude of the Orbiter as needed. A more detailed description of the RCS can be found in Section 4.8.

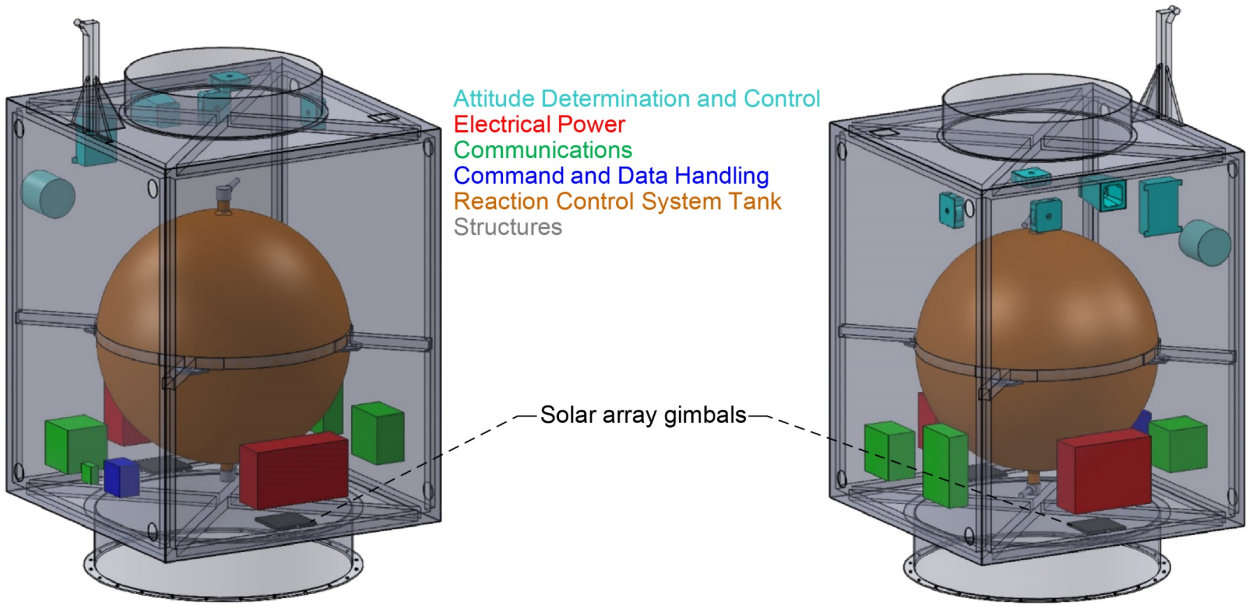

Figure 20.—Internal system components of Orbiter.

The last external component is the 24-in. Lightband, located on the end of the cylindrical structure on the bottom of the rectangular bus structure. The Lightband serves as the interface and separation system between the Orbiter and ESPA Grande. More details on the Lightband can be found in Section 4.9.

Those components contained inside the Orbiter bus structure include a spherical propellant tank, the Guidance, Navigation and Control (GN&C) system components, all of the Command and Data Handling (C&DH) system components, the communications electronics, the battery and Power Management and Distribution (PMAD) unit, and the two SA gimbals. Figure 20 shows two transparent views of the Orbiter bus with all of the internal components color coded by system. With the exception of the propellant tanks, all of the internal components are mounted directly to the inside face of any of the six face sheets. The spherical propellant tank is located inside the bus along the vertical centerline of the Orbiter and near the bottom of the bus. Locating the tank as close to the bottom of the bus as possible pushes the center of gravity (CG) location closer to the interface with the ESPA Grande, providing a shorter moment arm when the launch stack is cantilevered from the ESPA Grande port. As mentioned earlier, the tank utilizes four tabs equally spaced around the tank circumference. These tabs are each mounted to a structural member extending from the vertical member of the rectangular space frame. More details on the propellant tank and RCS can be found in Section 4.8.

The GN&C system consists of three reaction wheels, an inertial measurement unit (IMU), a star tracker, and the electronics unit associated with the star tracker. While the star tracker optical head was discussed as an external component due to it having a view of deep space, it is mentioned here as well since it is mounted to structures internal to the bus. The electronics unit associated with the star tracker is mounted directly to the inside of the face sheet right next to the star tracker optical head. Right next to the star tracker electronics unit, mounted to the inside of the same face sheet, is the IMU. Also mounted on that same face sheet is one of the three reaction wheels. The second reaction wheel is mounted to the adjacent side face sheet, with the third wheel mounted to the top face sheet. These locations ensure that the spin axes for all three wheels are perpendicular to one another. A more detailed description of the GN&C system can be found in Section 4.6.

The compact peripheral component interconnect (cPCI) enclosure for the C&DH system, the battery and PMAD unit for the EP system, and all the communications electronics are mounted to the four side face sheets near the bottom of the Orbiter bus. Locating these components near the bottom of the bus pushes the CG location closer to the interface with ESPA Grande at launch. More details on these systems can be found in their relative sections later in this document.

Finally, the two SA gimbals are located at the bottom of the bus structure, on opposite sides from one another (as are the SAs). They provide single-axis control for the SAs. More detail on the gimbals and the entire power system can be found in Section 4.7.

3.2.2 Lander Configuration

The bus structure for the Lander comprises an L-bar frame that nearly forms a cube. This frame is used for mounting all of

the internal components contained within the Lander bus and is closed out by six face sheets that are mounted to the outside of the frame. A drag flap is utilized to further decrease the landing velocity during the final stage of descent. L-frame structural members make up the frame for the 40-cm-diameter drag flap, while four square tubes extending from the drag flap frame down to the bottom corners of the bus carry the vertical loads placed on the drag flap. A structural face sheet is placed on top of the drag flap frame and is used for mounting all of the external components on the Lander. Figure 21 shows two transparent views of the Lander structures with all of the system components. A more detailed discussion on the structural design for the Lander can be found in Section 4.9.

Overall deployed dimensions of the Lander are shown in Figure 22. Note that these dimensions are given after the 2-cm crush pad, located on the bottom of the Lander, has already been displaced 1.6 cm at landing.

Those components located externally to the Lander bus include a wind sensor and boom, three IR bolometers, a pressure and temperature science suite, a reaction chemistry instrument, a UHF loop antenna, and a crush pad. These external components are shown in Figure 23.

The wind sensor sits atop a ~20-cm-long boom extending from the top of the drag flap, allowing for wind data to be collected on winds that are not influenced by the Lander. Also located on the top of the drag flap are two of the IR bolometers, with the third IR bolometer mounted to the underside of the drag flap for use on the descent stage of the mission. The pressure and temperature suite is mounted to the underside of the drag flap with the reaction chemistry instrument, also mounted to the underside of the drag flap, 180° from it. This balances out the masses of the two instruments to help stabilize the Lander through descent and landing. A more detailed discussion on the science instruments can be found in Section 4.1, Science Context and Instrument Package.

Communication to the Orbiter is performed by the UHF loop antenna mounted to the top of the drag flap. A 1-m circumference for the loop antennas was selected as it is the largest circumference that will fit on the deck and allow for the proper communication link with the Orbiter. A more detailed discussion on the communications system can be found in Section 4.4.

Located on the very bottom of the bus is the crush pad. This pad is designed to decelerate the vehicle to achieve an acceptable landing force. Prior to landing, the crush pad is 4 cm thick, and displaces 1.6 cm through the landing process. More details on the crush pad can be found in Section 4.9.

Those components that are contained inside the bus structure include the battery, C&DH enclosure, and the UHF Transmitter. The internal components can be seen in Figure 24.

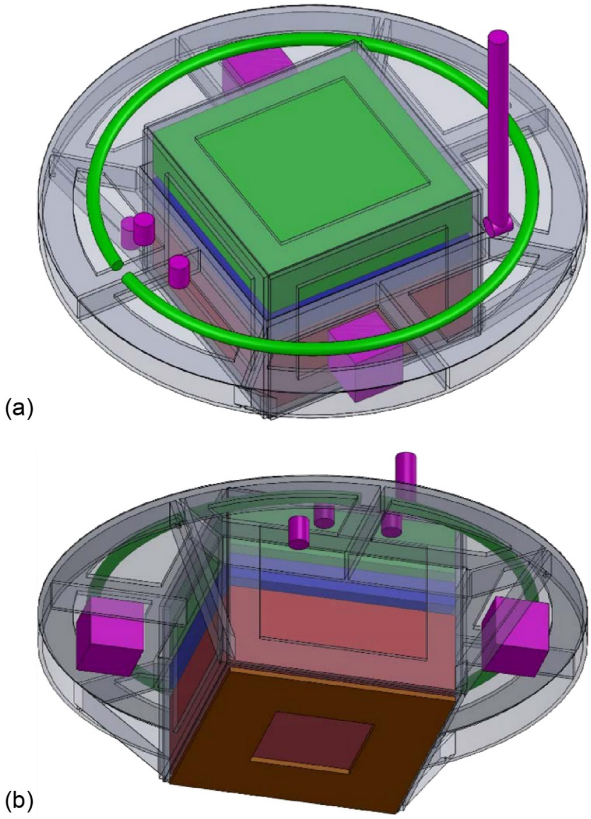

Figure 21.—Transparent views of Lander design. (a) Top view. (b) Bottom view.

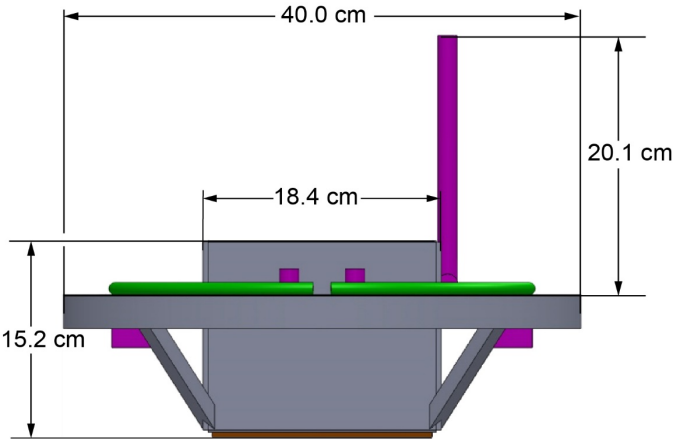

Figure 22.—Dimensions of Lander once on Venus surface.

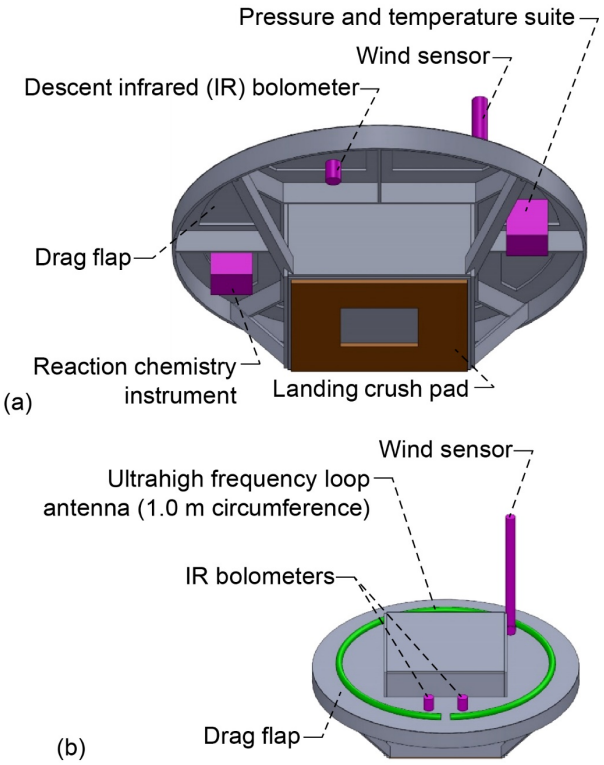

Figure 23.—External components on Lander. (a) Bottom view. (b) Top view.

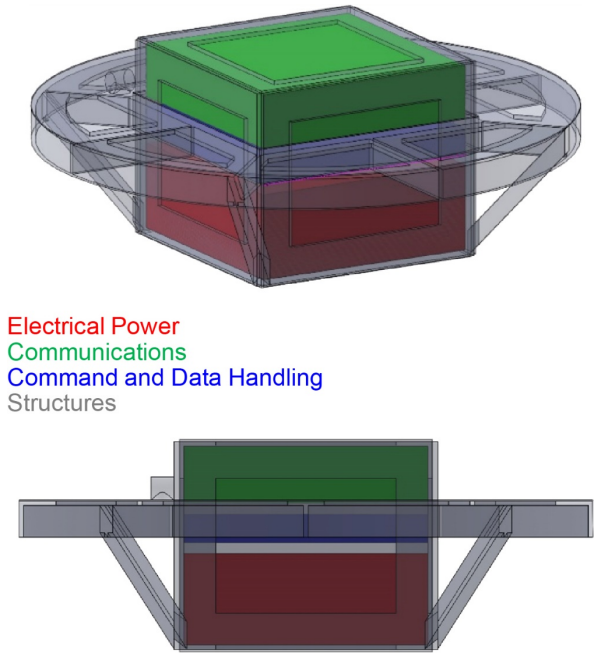

Figure 24.—Internal components on Lander.

Located at the bottom of the bus is the battery. As it is the heaviest component on the Lander, placing it at the bottom provides more stability for the Lander during the entry phase of the mission as well as once landed on the surface of Venus. Directly above the battery is the box containing the electronics that make up the C&DH system, and directly above that is the UHF Transmitter. All three elements were designed to have the 17-cm-long sides so that they fit within the L-bar frame that makes up the bus structure. More details on these three components can be found in their associated system sections later in this document.

4.0 Subsystem Breakdown

4.1 Science Context and Instrument Package

The approach to determining the science objectives of this study was to understand and maximize the science viable from a coupled Orbiter-Lander mission given the overall Venus Bridge framework. Coupling of Orbiter-Lander science in a meaningful way was considered a key objective and drove all aspects of the study. Although it is understood that the science produced from a mission is proportional to the mission class, the Venus Bridge approach is not a standard mission class and a core question of this study was whether viable science from such a coupled Orbiter-Lander mission could be obtained.

In order to formulate the science approach, two major assumptions were made. (1) The Orbiter would have a science instrument scaled appropriately for the size of the mission, and the operation of the Orbiter would in part be determined by the coupled science objectives. Limited technology development was assumed for the Orbiter system, and the candidate instruments, although not as complex as would be found in a larger mission class, would be required to provide valuable information relevant to significant science questions. (2) The Lander would be based on high-temperature technologies, such as electronics, sensors, communication, and power, operational for extended periods using the Long-Lived In-Situ Solar System Explorer (LLISSE) system as a baseline. These technologies are presently being actively developed as part of the LLISSE activity for possible use in Venera-D in the mid-2020s, and a similar timeframe for that technology maturation and availability was assumed for this V-BOSS study.

A preliminary Instrument Suite as shown in Table 9 was identified as a baseline for possible science investigations. This preliminary Instrument Suite identified a range of basic targeted measurements of interest to address relevant Venus science questions. Over the course of the study, this preliminary Instrument Suite was used as a guideline to identify methods to impact Venus science. In a number of cases, the instruments were either not viable given present technology development;

their implementation too complex to fit within the parameters of a single Venus Bridge Mission; or the choice of specific instruments over others, including those on this list, allowed improved coupling between Orbiter and Lander science. Given these limitations, and following the LLISSE model, significant effort was made to identify methods to provide relevant science data to address the measurement needs described in Table 9, but using simpler methods that could be implemented within the V-BOSS and technological constraints. The instruments selected for this study and their corresponding masses are listed in Table 10.

In order to assess the feasibility of the Venus Bridge concept, a specific point design with a chosen science theme was considered for the V-BOSS study. The science theme targeted a coupled Orbiter-Lander conceptualized to uniquely investigate mineralogy and surface atmosphere interactions over extended duration. However, this chosen theme is only an example. To emphasize this point, we present both a detailed description of the mission design and science return conceptualized for mineralogy and surface atmosphere theme (Sec. 4.1.1) as well as brief overview of an alternate Science Theme related to atmospheric circulation and dynamics (Sec. 4.2).

It should be strongly noted that the V-BOSS approach is not limited to the two science themes discussed in this report. It is envisioned that a range of science investigations could be possible through modification of Orbiter-Lander platforms investigated in this Compass study through the choice of other instruments, science themes, or operational modes. Such choices may be as simple as swapping one instrument or sets of instruments out for another. The fundamental approach to the choice of such instruments (often sensors) is to provide science not available in other ways in a simplified system compatible with the V-BOSS approach. Such investigations would be pathfinders for more complex and more expensive future missions.

TABLE 9.—BASELINE PRELIMINARY INSTRUMENT SUITE

Mission goals	Instrument
Orbiter	
Identify ultraviolet (UV) absorber	UV bolometer
Determine surface mineralogy	Infrared (IR) bolometer
Descent Probe	
Determine atmospheric composition at lowest scale height	Chemical sensor suite with pressure, temperature
Identify UV absorber	Up/downwelling bolometer (UV)
Determine surface composition	Up/downwelling bolometer (CO_2 IR windows)
Measure wind speed and direction	Accelerometer
Lander	
Measure heat flow	Heat flow sensor
Measure seismicity over several months	Long-duration seismometer
Measure surface conductivity	Conductivity probe/spike
Measure wind speed over several months	Long-duration wind sensor
Local geologic context for interpreting Lander data	Panchromatic camera
Thickness, compressibility of soil	Measure soil compressibility during emplacement of heat flow plate and/or conductivity probe/spike
Constrain surface-atmosphere interactions	Chemical sensor suite with pressure, temperature
Measure surface mineralogy	X-ray diffraction (XRD), alpha particle x-ray spectrometer (APXS)

TABLE 10.—SCIENCE MASTER EQUIPMENT LIST

Description	Quantity	Unit mass, kg	Basic mass, kg	Growth, %	Growth, kg	Total mass, kg
Lander	-	----	11.15	21.6	2.41	13.56
Science	-	----	0.51	30.0	0.15	0.66
Science package group one	-	----	0.51	30.0	0.15	0.66
Chemical wind pressure/temperature suite	1	0.35	0.35	30.0	0.11	0.46
Infrared (IR) bolometer	3	0.02	0.06	30.0	0.02	0.08
Reaction chemistry instrument	1	0.10	0.10	30.0	0.03	0.13
Orbiter	-	----	175.44	8.9	15.70	191.13
Science	-	----	2.00	30.0	0.60	2.60
Science package group one	-	----	2.00	30.0	0.60	2.60
IR spectrometer	1	2.00	2.00	30.0	0.60	2.60

4.1.1 Mineralogy and Surface Atmosphere Interactions Theme

The Science Traceability Matrix for the mineralogy and surface/atmosphere interactions theme is shown in Table 11. Mapping of the surface with diffraction-limited horizontal resolution of ~60 km can distinguish major differences in surface mineralogy by utilizing an IR emissivity imaging camera on the Orbiter and then calibrating those images based on the IR flux measurements from the Lander. Using this scheme, new and relevant insights regarding the mineralogy of Venus's crust may be obtained. Moreover, access to newly recorded surface maps can be compared to the IR measurements obtained from previous missions and provide critical data needed to interpret the composition of specific high-priority geologic targets such as tesserae or coronae. Additional detail on chemistry and composition of the landing site may be accomplished by completing in situ reaction chemistry experiments of known samples using contemporary advancements in solid-state chemistry. This testing will provide essential data to investigate and define mineral stability regimes at the surface and the effect of the Venus atmosphere on known geological materials.

This section will discuss details related to the Science Mission Components and resulting Science Return in this point design. The operational considerations to carry out this mission, such as the orbit type, are described elsewhere in this report. The technology maturity and possible pathways for development are also addressed elsewhere in this report.

4.1.2 Science Mission Components

There are three mission components that examine different science aspects of Venus mineralogy and surface atmosphere interactions: Orbiter, Descent Profile, and Long-Lived Lander. All three phases complement each other and provide new science related to the mission theme.

4.1.2.1 Orbiter

The Orbiter will constrain surface composition of large regions through orbital multispectral IR mapping. The IR mapping will use four channels at selected wavelengths for which the atmosphere is mostly transparent, and one reference channel, at a resolution 50 km per pixel. This data will constrain composition through spectral analyses and thermal modeling. Only IR data collected observing the nightside of the planet is useful for surface studies, and the orbit is planned to maximize coverage of nighttime observations. The Orbiter must communicate with Lander during descent and landing. The Orbiter will collect data for the landing site, especially during periods of data transfer from the Lander, to allow comparison of orbital measurements and real-time surface properties.

4.1.2.2 Descent Profile Measurements

Selected Lander sensors will be activated during descent to allow an atmospheric composition, pressure, temperature, and IR radiance profile to be taken during descent to the surface. This will allow determination of the concentration of selected high-interest species down to the lowest scale height correlated with temperature and pressure. In parallel, two IR bolometers with wavelengths matching that of two elements of the Orbiter IR mapping system, and a third IR bolometer looking down at one wavelength, will profile the IR radiance profile over the transition to the surface. These Lander IR measurements will be simultaneous with the Orbital IR measurements to allow correlation between the Orbiter measurements through the atmosphere and their profile at various heights.

4.1.2.3 Long-Lived Lander

The Lander will investigate a range of meteorological, radiance, and mineralogical properties over one Venus solar day (day/night). The full meteorological package provides concentrations of selected high-interest species, combined with pressure and temperature as well as wind speed and direction, thus constraining atmospheric variability at the surface boundary over a long duration. These measurements will also characterize surface-atmosphere interactions/dynamics and equilibrium conditions over the same time period, including the transition from night to day. A microsensor platform, based on the atmospheric chemical sensor structure, will monitor exposed mineral samples over an extended period and electrically characterize surface mineralogical reactions occurring in the samples. The IR bolometers will provide upward-looking data correlated with two wavelengths of Orbiter IR mapping system and the downward IR bolometer will provide upwelling irradiance.

TABLE 11.—SCIENCE TRACEABILITY MATRIX FOR THE MINERALOGY AND SURFACE ATMOSPHERE INTERACTIONS THEME

Decadal goals	VEXAG[a] goals	Mission goals	Instrument	Measurement
Orbiter				
How have the myriad chemical and physical processes that shaped the solar system operated, interacted, and evolved over time?	Understand what the chemistry and mineralogy of the crust tell us about processes that shaped the surface of Venus over time	Constrain surface mineralogy	MIREM: Multispectral IR Emissivity Mapper, with four channels (one channel outside IR window for control)	Radiant flux in four specific wavelength bands
Probe (descent: data collection at <20 km)				
What governed the accretion, supply of water, chemistry, and internal differentiation of the inner planets and the evolution of their atmospheres, and what roles did bombardment by large projectiles play?	Understand atmospheric evolution. Characterize the Venus greenhouse. Characterize how the interior, surface, and atmosphere interact	Determine atmospheric composition at lower scale height	V-Chem (on descent): atmospheric chemical sensor suite: fO_2, CO, SOx, H_2O, OCS, HCl, HF, NO, pressure, temperature	Vertical T, P profiles Abundance profile of major and trace species and oxygen fugacity
Can understanding the roles of physics, chemistry, geology, and dynamics in driving planetary atmospheres and climates lead to a better understanding of climate change on Earth?	Understand what the chemistry and mineralogy of the crust tell us about processes that shaped the surface of Venus over time. Characterize current processes in the atmosphere	Radiance profile with altitude at selected wavelengths. Correlation with Orbiter measurement	V-Rad (activated on descent) IR radiance bolometers: two looking up and one looking down	Upward and downward IR radiant flux in bands matching the Orbiter
Probe (landed)				
How have the myriad chemical and physical processes that shaped the solar system operated, interacted, and evolved over time?	Understand atmospheric evolution. Characterize the Venus Greenhouse. Characterize how the interior, surface, and atmosphere interact	Constrain surface-atmosphere interactions	V-Chem: long-duration atmospheric chemical sensor suite: fO_2, CO, SOx, H_2O, OCS, HCl, HF, NO, pressure, temperature	Long-term monitoring of chemical composition at surface, variability of species abundances with temperature and pressure
	Characterize current processes in the atmosphere	Measure wind speed and direction over several months	V-Wind: long-duration wind sensor	Long-term wind speed and direction measurements
	Understand what the chemistry and mineralogy of the crust tell us about processes that shaped the surface of Venus over time	Constrain the atmospheric radiance energy over a long time duration	V-Rad: (remains active after landing) IR radiance bolometers: two uplooking and one downlooking	Upward and downward IR radiant flux in specified bands
Did Mars or Venus host ancient aqueous environments conducive to early life, and is there evidence that life emerged?	Understand what the chemistry and mineralogy of the crust tell us about processes that shaped the surface of Venus over time	Measure surface mineralogy reactions	V-Lab: microplatforms that monitor selected standard geological samples for reaction chemistry testing	Reaction chemistry via electrochemical measurements (current-voltage, capacitance-voltage)

[a]Venus Exploration Analysis Group.

4.1.3 Science Return

4.1.3.1 Major Atmospheric Science Return

The Science Mission Components aim to address the following VEXAG goals related to atmospheric science:

- Characterize current processes in the atmosphere
- Understand atmospheric evolution; characterize the Venus greenhouse
- Characterize how the interior, surface, and atmosphere interact

New observations of planetary-scale gravity waves (GWs) from Akatsuki bring into question the stability of the Venus atmosphere, its impact on our understanding of the exchange of momentum between the surface and the atmosphere, and the way in which the atmosphere evolves diurnally over long time scales (defining the climate) (Refs. 1 to 23). There are two types of stability that contribute to the propagation/demise, and thus the visibility of planetary scale GWs on Venus: temperature stability and wave front stability. The wave front stability is determined as a function of the product of the zonal wind velocity (U) and the Brunt-Vaisala frequency (N), which is the frequency at which a displaced air parcel will oscillate when displaced vertically within a statically stable (nonturbulent) atmospheric environment. The value of N is a function of the temperature gradient. Theoretical models show that in the afternoon when the surface temperature is stable and hot, the high temperatures lead to a high N value, one high enough that the product of $U{\cdot}N$ is nearly equivalent to the height of the mountains, and this creates maximum mountain stress (and air lift) and initiates the GW. What causes the GW to continue to propagate is dependent on the stability of the atmosphere through which the GW travels, for example, travel through instability (turbulent) regions will depress the GW, but travel through stable (laminar) regions allows the GW to propagate. On Venus, GW travel on both the dayside and nightside, and the mechanism that initiates the GW is different in the dayside and nightside.

As noted by Marcq (Ref. 2), "A better characterization of the lower atmosphere dynamics and temperature field is required to understand how these waves can propagate in the first place, and cannot be determined from remote sensing alone. The need for an in-situ mission in the atmosphere of Venus and on the surface is consequently more pressing than ever." Thus, to begin to understand the energy and momentum vectors that allow this motion, the temperature, radiant flux, and species profiles need to be mapped from the surface into the upper atmosphere. In particular, mapping of the atmospheric conditions at the surface level requires an in situ element that can trace changes in the atmospheric behavior (temperature, wind, and pressure) and the energy budget as a function of local time through a full solar day on Venus (~4 months). A combined program of in situ measurements of the atmospheric characteristics at the surface, with detailed observations of the energy sources and cloud motions, can provide critical empirical data needed to better resolve and interpret what the momentum exchange is at the surface and how that impacts the atmospheric circulation at other altitudes.

Related to atmospheric characterization of chemical species, the Decadal Survey identifies as a high priority a mission to "understand the physics and chemistry of Venus's atmosphere, especially the abundance of its trace gases, sulfur" (Ref. 4). Currently, scientists do not know "the elemental… compositions of species in Venus's atmosphere, especially… nitrogen-, hydrogen-, carbon- and sulfur-bearing species" (Ref. 5). The presence of SO_x is thought to provide potential geological information on the presence of volcanoes (Ref. 6), and NO may indicate lightning (Refs. 7 and 8), but further study is needed to confirm these hypotheses. A mission, like Venus In Situ Explorer (VISE), that "focuses on the detailed characterization of the surface, deep atmosphere and their interaction" (Ref. 9) is targeted by Decadal. Answering gaps in atmospheric science requires "in situ measurements, such as can be performed during atmospheric transit by Landers like VISE, using balloons, and/or dropsondes/probes" (Ref. 10). Furthermore, VEXAG Exploration Investigations III.B.3-4 include determination of "the abundances and altitude profiles of reactive atmospheric species (OCS,...SO_2,…HCl, HF)… H_2O" as well as CO (Ref. 11). The V-BOSS approach targets a number of the species above for quantitative measurements.

4.1.3.2 Major Mineralogical Science Return

The Science Mission Components aim to address the following VEXAG goals related to mineralogical science:

- Understand what the chemistry and mineralogy of the crust tell us about processes that shaped the surface of Venus over time.
- Characterize how the interior, surface, and atmosphere interact.

IR spectroscopy is able to identify minerals within geologic materials based on the vibrations of different chemical bonds within the mineral. This technique is also effective at identifying rock types due to the fact that rocks are composed of minerals. Orbital observations of the surface in the IR while looking up from the surface in the IR allow for a better correction for the clouds to calibrate the orbital data. This can be satisfied with the orbital mapping and IR upward-looking bolometers on the Lander. Since little chemical and mineralogical data from the surface of Venus exists, there is a

vast number of specific questions regarding these aspects of the planet. The combination of an orbital and Lander approach, while not able to answer all of these questions in one mission, can answer some questions and provide a more focused framework for our pursuit of geological understanding of Venus. For example, the orbital IR measurements can determine the kinds of rocks and minerals present in large-scale regions on the surface and their distribution. This data in itself is meaningful, as different type of rocks and minerals indicate the occurrence of different geologic processes, but it also can be combined with other datasets such as the previously acquired radar altimetry to understand the compositions of specific surface landforms (e.g., tesserae and coronae). Lander IR measurements are capable of similar rock and mineral identifications, but on a local scale and can likely resolve features (e.g., outcrops) that are beyond the resolution of the orbital measurements. Such data can speak to the local-scale variability of the Venus surface.

A second method to understand the geology of the Venus surface will involve in situ reaction chemistry experiments. The approach relies on the same principle as the chemical species gas sensors: a substrate with a temperature detector and heater on which there is a solid-state material. In the case of chemical sensing, the solid-state material is a stable material with a reaction chemistry and sensor structure that is tailored to be selective to a given gaseous species of interest. The electrical properties, such as capacitance or conductivity, of the material are monitored and changes in the electrical properties of the material are proportional to concentration of the gaseous species. In the case of the in situ reaction chemistry experiment, in order to better understand the geology of the Venusian surface, geological materials will be chosen whose core properties may change over time upon exposure to the Venus atmosphere. Changes in a geological material as monitored through electrical measurements will give an indication of its reaction chemistry in the Venus environment. Comparison of the reaction chemistry between different material types will provide an improved understanding of the effect of the Venus surface atmosphere on known geological materials. In situ electrochemical measurements have been significant in Mars exploration, with experiments such as the Wet Chemistry Laboratories in the 2007 Phoenix Mars Scout Lander (Ref. 12). Venus surface conditions presently preclude such a complicated experiment, but information can be obtained on geologically relevant samples through simpler impedance measurements (Ref. 13). The objective here is to investigate materials whose state may transition upon exposure to the Venus environment and monitor those changes electrically over extended periods.

4.2 Alternate Science Theme

One alternate science theme that can be accomplished with the core Orbit/Lander platforms using the LLISSE model is an indepth study of the physical drivers of Venus's Atmospheric Circulation and Dynamics, which ultimately defines the mechanisms that drive Venus's atmospheric superrotation. A study of this theme responds to VEXAG goals to (a) characterize current processes in the atmosphere; (b) understand atmospheric evolution; and (c) characterize how the interior, surface, and atmosphere interact. To accomplish these goals requires coordinated remote and in situ observations on the time scale of a solar day on Venus (~4 Earth months) or more and the following instrument/measurement/architecture trades (relative to Table 11):

- Orbiter
  - An ultraviolet (UV) and near-infrared (NIR) spectral imaging versus Multispectral Infrared Emissivity Mapper (MIREM)
- Descent probe
  - Radiant flux profile at UV, IR and visible wavelengths versus IR only
  - Wind speed profiles versus multispecies composition detection
  - Sensor tuned to H_2SO_4 aerosol, CO_2 abundance profile
  - Sensors to obtain profile of aerosol particle size ranges
- Lander
  - Self-lit UV-visible spectrometer versus mineral reaction platforms
  - Aerosol sensors from descent remain active for entire life of the Lander
- Launch
  - Initial arrival should be designed for the probe/Lander to be released on the dayside to maximize coordination with dayside UV observations of the cloud tops; however, the Orbiter will take advantage of both dayside and nightside observing within the initial 4-month mission period; while the availability of LLISSE measurements on the nightside are predicate only on the lifetime of LLISSE.

Venus's atmospheric circulation and dynamics are driven by solar energy deposition, primarily accomplished via UV light absorption, and the overall atmospheric radiant energy budget at each altitude from the surface to thermosphere—which is influenced by the H_2SO_4 aerosol/haze and CO_2 abundance profiles. Therefore, with the trades listed above, and the previously defined descent and landing capabilities, the following critical measurements could be achieved:

- Detailed UV, IR, and visual radiant flux profiles (single trajectory) in coordination with cloud top motions.
- Long-term mapping of the atmospheric wind speeds over a range of altitudes via multiwavelength imaging.
- Long-term mapping of the spatial distribution of the species dominantly responsible for energy deposition in the atmosphere via UV spectroscopy.
- Long-term record of the temporal variance in the aerosols abundance and radiant energy budget in the deep atmosphere needed to understand relation between the two atmospheric properties and the overlying cloud circulation.
- A distinct trace of the temporal variance in the abundance of UV-absorbing materials at the surface needed to better understand source of the absorber, which is believed to be transported to cloud tops from lower atmosphere and to be linked to something that originated on the surface such as $FeCl_3$ or even a remnant microorganism from Venus's habitable period. Understanding if the UV absorber is from historic biogeneic sources links directly to understanding if extant life ever existed on Venus.

These measurements, along with the boundary layer interaction measurements that are part of the baseline LLISSE design, can provide many of the critical measurements needed to advance modeling of Venus's circulation and dynamics. These measurements represent the essential data needed to advance our understanding of the mechanisms that produce and maintain Venus's atmospheric superrotation. Such alternate missions would require their own point design, including trades and costing, to understand the specifics of what could be accomplished. Other science themes may also be considered. Thus, a major conclusion of the study is that a range of significant science can be obtained based on core Orbit/Lander platforms using the LLISSE model within the Venus Bridge Framework with the mineralogy and surface atmosphere interactions theme being just one example.

4.3 Technology Development and Maturity

4.3.1 Orbiter System

MIREM, with four channels (one channel outside IR window for control) is based on experiences with relevant past instruments on the Galileo and Venus Express missions and published literature on IR instruments proposed for NASA's Discovery and New Frontiers calls and European Space Agency's (ESA's) M5 call.

4.3.2 Lander System

The V-BOSS Lander approach assumes the continued development and maturation to technology readiness level (TRL) 6 of the LLISSE. Although the specific design of V-BOSS is different from the LLISSE design due to its different targeted application and functionality, the V-BOSS Lander is based on the LLISSE model and approach. Thus, in order to understand the technical viability of V-BOSS, one needs to understand the technical viability of the core LLISSE system. Beyond that, one then needs to understand the technical readiness of the specific technology components used in V-BOSS that are not in LLISSE.

4.3.2.1 Long-Lived In-Situ Solar System Explorer (LLISSE) Technology Development and Maturity

LLISSE has a goal of developing and demonstrating proof-of-concept probes that will function in Venus surface conditions and do so for long time periods (weeks to months). These probes will be designed, fabricated, and demonstrated by test to operate in Venus conditions. To accomplish these goals, LLISSE leverages the NASA Glenn Research Center high-temperature electronics, sensors, power, and communications in an innovative operations model to collect and transmit science data for 60 Earth days or longer in Venus conditions. The LLISE development plan assumes a two-phase approach: a battery-only version to be proof-of-concept demonstrated in 2019 followed by a wind-powered version to be proof-of-concept demonstrated in 2021. While the battery-powered version of LLISSE is the most relevant to V-BOSS and will provide the core of the V-BOSS functionality, some aspects of LLISSE, such as a higher frequency communication system and aspects of power management, are scheduled to be developed and demonstrated as part of the wind-powered version of LLISEE. This is highlighted in Table 12, which shows the planned development of a range of LLISSE components relevant to V-BOSS, as well as identifying V-BOSS components not presently being developed in LLISSE, and possible funding sources. It is upon the demonstration of the broad range of LLISSE components in Venus relevant environments for extended periods that not only missions such as LLISSE can be envisioned, but also a new range of future planetary exploration concepts. Description of the technology readiness of both LLISSE core technology and V-BOSS-specific capabilities is provided below.

A core to LLISSE system operation is high-temperature electronics for sensors, data handling, communications, and power management. These electronics are based on the world's first microcircuits of moderate complexity that have shown extended operation in Venus relevant conditions (Refs. 14 and 15). These circuits have been recently upscaled in complexity to over hundreds of transistors per chip with two metal interconnect layers, and have now demonstrated operation for thousands of hours at 500 °C in Earth air ovens (Ref. 15), and very recently for 60 days in the Glenn Extreme Environments Rig (GEER)

TABLE 12.—TECHNOLOGY READINESS LEVEL (TRL) FOR LANDER INSTRUMENT SUITES AND BOTH LONG-LIVED IN-SITU SOLAR SYSTEM EXPLORER (LLISSE) AND VENUS BRIDGE ORBITER AND SURFACE STUDY (V-BOSS), INCLUDING CURRENT TRL, ESTIMATED TRL 6 DEMONSTRATION, AND EITHER ONGOING OR POSSIBLE FUNDING SOURCES

Technology	Current TRL	Estimated component TRL 6	Modification from LLISSE for V-BOSS	Funding source: ongoing (O) and potential (P)
Electronic circuits (SiC): sensors and data handling	4 to 5	August 2019	None	LLISSE (O)
Electronic circuits (SiC): power management	3 to 4	September 2021	None	LLISSE (O)
Communications (100 MHz)	3 to 4	September 2021	None	LLISSE (O)
MIREM[a] spectral imager	3 to 4	2021 to 2022	None	IRAD[b]/MatISSE[c] (P)
Wind sensor	4	August 2019	None	LLISSE (O)
Temperature sensor	4 to 5	August 2019	None	LLISSE (O)
Pressure sensor	4 to 5	August 2019	None	LLISSE (O)
Chemical sensors	5	August 2019	None	LLISSE/ HOTTech[d] (O)
LLISSE bolometer	3 to 4	September 2021	None	LLISSE (O)
V-Rad (V-BOSS infrared bolometer)	3 to 4	TBD[e]	• Modify LLISSE bolometer structure for specific filters • Verify system operation with filters	MatISSE (P)
V-Lab (V-BOSS surface reaction measurement)	4	TBD	• Identify high-temperature measurement approach for minerals in existing platform • Modify high-temperature circuits as needed	MatISSE (P)

[a]Multispectral Infrared Emissivity Mapper.
[b]Internal Research and Development.
[c]Maturation of Instruments for Solar System Exploration.
[d]Hot Operating Temperature Technology.
[e]To be determined.

simulated Venus surface conditions without any cooling or environmental protection (Refs. 16 and 17). This integrated circuit capability enables a wide range of very compact onboard mission electronics, including sensor signal amplification, digitization, and wireless transmission integrated circuits, to operate for months without any environmental sheltering from the harsh atmosphere found on the surface of Venus. Another important finding of the GEER tests is that it is inadequate to qualify parts for prolonged surface missions in reproduction of Venus atmospheric conditions (Refs 14 and 15). It is envisioned that prototype demonstration circuits specifically designed for most core aspects of LLISSE operation will be fabricated and preliminarily evaluated in 2018.

As part of this recent GEER testing, core components of the LLISSE sensor technology were tested in simulated Venus conditions for extended periods. These include first-generation sensor systems for surface wind speed, temperature, and pressure as well as specific sensors for atmospheric chemical composition (sulfur dioxide, hydrogen fluoride, carbon monoxide, and carbonyl sulfide). Analysis of the results of this testing for both the sensors and electronics is ongoing. Overall, valuable knowledge on the operability of the sensing approaches was gained combined with further characterization of candidate sensor materials stability to Venus conditions. To varying degrees, the preliminary viability of each chosen core sensor approach was supported. For example, the sulfur dioxide (SO_2) sensor (Makel Engineering, Inc.) (Ref. 16) responded to the intentional injections of SO_2 into the GEER chamber during the 60-day test in a manner suggesting real-time monitoring of the simulated Venus ambient conditions. However, notable further improvement of Venus-durable integrated circuit and sensor capabilities overall is planned and remains to be done in order to demonstrate a proof-of-concept LLISSE system.

The development of other LLISSE components is also progressing. Communication system designs including antennas are being investigated, coupled with modeling and limited component/materials testing. The LLISSE plan includes demonstration of communications at ~10 MHz in 2019, with further development, including appropriate circuits, for ~100 MHz communication capabilities by 2021. The development of the communications system will be closely coupled with the electronics development to enable higher frequency transmissions at adequate power levels. Furthermore, the battery system assumed in this study is based on NaS chemistry. The NaS battery has a long history of development for applications on Earth and has been space qualified. This

includes the demonstration test of the NaS battery in space that was done on space shuttle flight STS–87 in November 1997. The material system for the NaS battery allows high-temperature operation, and operation at 460 °C has been demonstrated at 92 bar pressure (Ref. 18). An energy density of 120 Wh/kg was assumed for this study, but higher power densities may be viable. However, further development, and demonstration in simulated Venus surface conditions, is needed for LLISSE applications. A contract (Ref. 19) has been awarded to an industry partner for battery development leading to a functional demonstration in GEER.

4.3.2.2 V-BOSS Lander Technology Development and Maturity

As seen in Table 12, a significant component of the Lander V-BOSS technology suite is under development as part of the LLISSE project. The innovation of V-BOSS is the tailoring of the core LLISSE model and approach towards the Mineralogy and Surface Atmosphere Interactions Science Theme, including coupling Lander and Orbiter data. Nonetheless, V-BOSS includes two modifications to the core LLISSE instrument platform that will require development beyond LLISSE that were added specifically to enhance science delivered for this theme: V-Rad and V-Lab. The technology challenges with each include the following:

V-Rad

LLISSE is presently developing a bolometer to measure radiance over a broad range of wavelengths. In order to couple radiance measurements between during descent and on the ground with the Orbiter, only specific IR wavelengths are of interest. Thus, the LLISSE bolometer would need to be modified to interrogate wavelengths matching those of the Orbiter. The approach identified to accomplish this is the inclusion of refractory filters tuned to the desired wavelengths to the baseline LLISSE bolometer. Thus, development work beyond LLISSE to enable V-Rad includes modification of the bolometer structure for inclusion of a filter, followed by verification of the resulting structure to not only detect the targeted IR wavelengths at the required sensitivity but also maintain durable operation in Venus decent and surface environments.

V-Lab

The LLISSE baseline includes a range of chemical sensors that depend on microplatforms for operation. These microplatforms, including temperature control, have electrode patterns on which are deposited sensing materials to allow detection of chemical species in the ambient. The sensing materials are intended to be stable in the Venus environment for significant periods of time. As noted in Section 4.1, both the microplatform and the sensing material for the SO_2 sensor have been tested in GEER for 60 days in simulated Venus conditions with demonstrated operation during the test. Although further analysis is necessary to understand the full implication of these results, it may be suggested that this microsensor platform has at least shown the viability to operate in simulated Venus conditions. In order to move from this chemical sensor platform to V-Lab, the ability to place minerals of interest on this microplatform would need to be demonstrated coupled with high-temperature circuits to provide relevant information on changes in mineral properties.

Table 12 notes that further maturation of V-Rad and V-Lab beyond LLISSE could take place in programs such as the Maturation of Instruments for Solar System Exploration (MatISSE). Other programs could be considered. However, a core point is that such activities would be modifications to existing platforms already being developed to TRL 6, not full-scale sensor development. This would limit potential development costs beyond LLISSE to no more than what would be requested under MatISSE, but potentially less. For example, core capabilities for V-Lab are presently being investigated. Initial tests are beginning in GEER to explore the ability to place materials not standardly used for chemical sensors on the microplatform and expose the platform to simulated Venus conditions to begin to explore the viability of such an approach. Such data, achieved while piggybacking on another test, could be a baseline for future development of V-Lab development.

4.4 Communications

4.4.1 Orbiter Communications

The communications requirement for the V-BOSS scenario is the design of a science data uplink from the Venus Lander to an Orbiter relay satellite. The Orbiter relay satellite will be a simplex link (receive only) from the Lander and a bidirectional link transmitting the science data to Earth.

4.4.2 Orbiter Communications Requirements

The communications subsystem design for the Orbiter relay satellite will consist of a dual system based around a zero fault tolerant space-qualified version of the Iris V2 Cubesat Deep Space Transponder, a General Dynamics X-band Solid State Regulated Power Amplifier, diplexer, a Yagi-Uda antenna, and a parabolic dish antenna. The Iris will be configured for both X-band operations to communicate (transmit/receive (Tx/Rx)) with Earth, and UHF/very high frequency (VHF) to communicate (Rx only) from the Lander. The features of the Iris platform include 0.5U volume, 1.1 kg mass, 26 W of direct current (DC) operating power consumption, and interoperability with the DSN at X-band frequencies. For Earth communications, the system includes a General Dynamics X-band Solid State

Regulated Power Amplifier. Features of the amplifier include a mass of 1.3 kg contained within approximately 1,000 cm^3, 65 W of DC operating power consumption, and throughput data rates of up to 8 kbps. The communication link to Earth is closed with a 0.25-m-diameter parabolic dish antenna (approx. 2 kg) mounted at zenith on the Orbiter platform and a 34-m DSN receive dish on Earth. The requirement for a data link to Earth is a minimum 2 kbps at a maximum distance of 0.7 AU. A 2- or 3-dB link margin is typically included in a space communications link for analysis, due to the uncertainty of the performance of components.

To receive data from the Lander, the Orbiter antenna will use a Yagi-Uda two-element antenna. The antenna will fit within an envelope of 12,000 cm^3 (stowed) and have a mass of approximately 1 kg. A Yagi-Uda antenna can typically be used when space is available and higher gain and directional applications are required to complete the link. The data link requirement is approximately 36 bps up to an Orbiter maximum distance of 360,000 km. A block diagram of the Lander and Orbiter communications system is included in Figure 25.

Table 13 shows the Orbiter communications MEL.

4.4.3 Lander Communications

The communications requirement for the V-BOSS scenario is the design of a science data uplink from the Venus Lander to an Orbiter relay satellite. The Orbiter relay satellite will be a simplex link (receive only) from the Lander and a bidirectional link transmitting the science data to Earth.

4.4.3.1 Lander Communications Requirements

The Lander communications system design will consist of a specialized transmitter and antenna (see Table 14). Because of the challenging high-temperature environment of the Venusian surface, the transmitter will be fabricated using a toolbox of signal conditioning, processing, and communications high-temperature SiC-integrated circuits that are currently being developed and tested. These circuits will operate in the UHF/VHF range (currently around 100 MHz center frequency). Packaging and component placement will be critical to the successful operation and longevity of these circuits to survive in the harsh Venusian atmosphere.

The UHF/VHF frequency range was chosen to have a better chance of successfully penetrating the harsh atmosphere to send sensor data to the Orbiter relay satellite. Because of these wavelengths, and to maximize successful data transfer from the surface, a 1.0-m-circumference loop antenna (approx. 0.2 kg) was chosen for the Lander. This represents approximately a one-half wave antenna for the system, which within the Lander volume limitations maximizes the power transfer of the Lander antenna signal to the Orbiter antenna. Since these transmit power levels are so low on the Lander (approx. 0.5 W), it is recommended to investigate the possibility and effect of electroplating the Lander antenna with gold or another alloy to significantly reduce the electrical resistivity of the antenna. Although, at these frequencies, the relative skin effect frequency depth of the antenna is negligible for commonly used metals, care must be exercised to minimize the formation

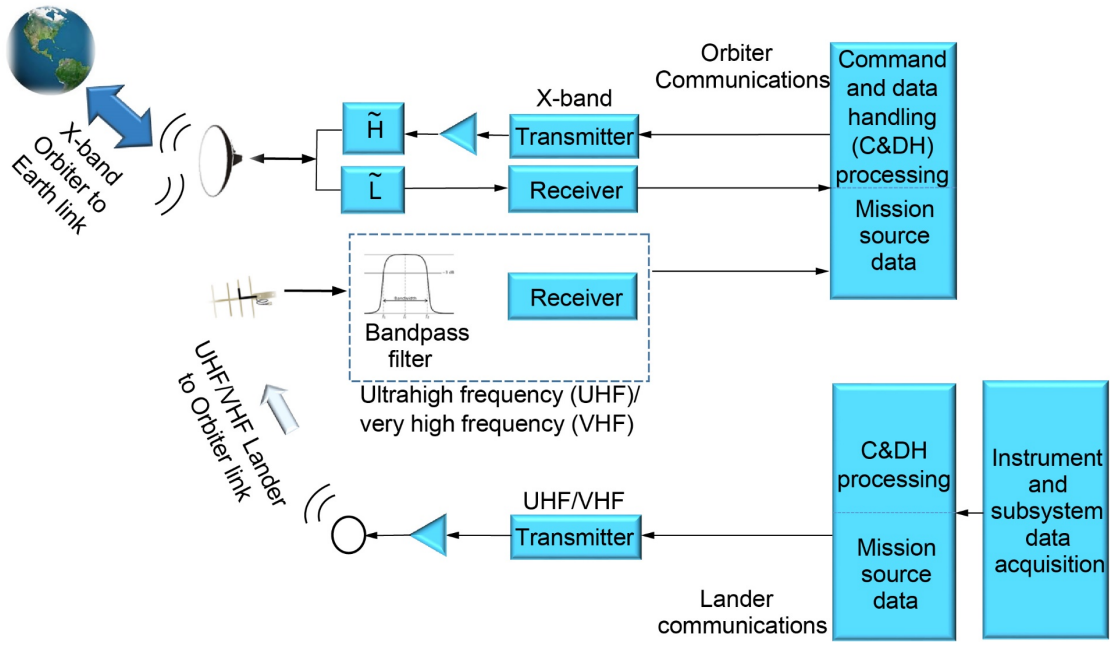

Figure 25.—Venus Lander and Orbiter communications.

TABLE 13.—ORBITER COMMUNICATIONS MASTER EQUIPMENT LIST

Description	Quantity	Unit mass, kg	Basic mass, kg	Growth, %	Growth, kg	Total mass, kg
Orbiter	-	----	175.44	8.9	15.70	191.13
Communications and Tracking	-	----	6.30	11.6	0.73	7.03
X-band system	-	----	6.30	11.6	0.73	7.03
X-band mini transceiver (Iris V2)	1	1.20	1.20	10.0	0.12	1.32
X-band solid-state parabolic dish antenna	1	1.30	1.30	10.0	0.13	1.43
X-band PA, 0.2 m	1	2.00	2.00	10.0	0.20	2.20
Diplexer	1	0.20	0.20	10.0	0.02	0.22
Cabling	1	0.10	0.10	10.0	0.01	0.11
Ultrahigh frequency (UHF) receiver only (Iris V2.1)	1	0.50	0.50	10.0	0.05	0.55
UHF directional antenna	1	1.00	1.00	20.0	0.20	1.20

TABLE 14.—LANDER COMMUNICATIONS MASTER EQUIPMENT LIST

Description	Quantity	Unit mass, kg	Basic mass, kg	Growth, %	Growth, kg	Total mass, kg
Lander	-	----	11.15	21.6	2.41	13.56
Communications and Tracking	-	----	0.43	30.0	0.13	0.56
Ultrahigh frequency (UHF) system	-	----	0.43	30.0	0.13	0.56
UHF Transmitter, advanced circuitry	1	0.30	0.30	30.0	0.09	0.39
Antenna, loop, 1 m	1	0.12	0.12	30.0	0.04	0.16
Cabling	1	0.01	0.01	30.0	0.00	0.01

of electrically resistant oxide compounds on the antenna surface in the harsh atmosphere that could interfere with electrical connections, and thus attenuate the signal.

4.5 Command and Data Handling (C&DH)

The C&DH system for the V-BOSS mission provided command and control systems for both the orbiting S/C and Lander while operating in transit to Venus and during descent. The high-temperature electronics are used for C&DH functions while the Lander is on the surface of Venus. The technology is discussed in Section 4.3.2.1. For operation in transit and the initial entry to Venus, the operating temperature range for the C&DH electronics will be between 233 to 323 K.

The electronic components will also need to be radiation tolerant for the life of the mission. Since there are no radiation belts surrounding Venus and the radiation environment in deep space transit to Venus is fairly low with just solar particle events as the main concern for radiation damage. Depending on the timing of the mission with the Sun's solar cycle, the background cosmic rays will vary. However, these levels are very low, on the order of 0.6 to 1.6 rad/yr (Ref. 20), depending on the state of the solar cycle.

The components used to comprise the Orbiter C&DH system include (see Table 15)

- Single board control computer with integral storage memory
- Controller cards: telemetry, data interface, time generator, gimbal control, and thrust valve
- Data collection card
- Backplane with power supply
- Wiring harness and connectors

These components are selected to meet the functional requirements and to minimize the power consumption and volume. Low power consumption components were utilized where possible to try and meet the requirements of the transfer S/C. The breakdown of the components and their layout are illustrated in Figure 26. The controller cards are stacked into a backplane that supplies power and data transfer to and from the cards. The card stack is housed in an enclosure that provides the power and data ports to the external components that are being controlled or monitored. An example of the card stack and enclosure is shown in Figure 27.

TABLE 15.—ORBITER AND LANDER COMMAND AND DATA HANDLING (C&DH) MASTER EQUIPMENT LIST

Description	Quantity	Unit mass, kg	Basic mass, kg	Growth, %	Growth, kg	Total mass, kg
Orbiter	-	-----	175.44	8.9	15.70	191.13
C&DH	-	-----	2.00	14.3	0.29	2.29
C&DH hardware	-	-----	1.90	15.0	0.29	2.19
Andrews Model 160 Flight Computer	1	0.10	0.10	15.0	0.02	0.12
Data interface unit	1	0.30	0.30	15.0	0.05	0.35
Time generation unit	1	0.10	0.10	15.0	0.02	0.12
Command and control harness (data)	1	0.60	0.60	15.0	0.09	0.69
cPCI[a] enclosure with power supply	1	0.50	0.50	15.0	0.08	0.58
Gimbal control card	1	0.10	0.10	15.0	0.02	0.12
Thrust valve card	1	0.10	0.10	15.0	0.02	0.12
Pyro card	1	0.10	0.10	15.0	0.02	0.12
Instrumentation and wiring	-	-----	0.10	0.0	0.00	0.10
48-channel AD/DA/SDI[b] card	1	0.10	0.10	0.0	0.00	0.10
Lander	-	-----	11.15	21.6	2.41	13.56
C&DH	-	-----	0.18	27.8	0.05	0.23
C&DH hardware	-	-----	0.16	27.4	0.04	0.20
Die	1	0.00	0.00	20.0	0.00	0.00
Package	1	0.01	0.01	20.0	0.00	0.02
Lid	1	0.01	0.01	20.0	0.00	0.01
Circuit board	1	0.02	0.02	20.0	0.00	0.02
Box	1	0.08	0.08	30.0	0.02	0.10
Timing circuit	1	0.04	0.04	30.0	0.01	0.05
Instrumentation and wiring	-	-----	0.03	30.0	0.01	0.03
Miscellaneous cabling	1	0.03	0.03	30.0	0.01	0.03

[a]Compact peripheral component interconnect.
[b]Analog-to-digital/digital-to-analog/serial digital interface.

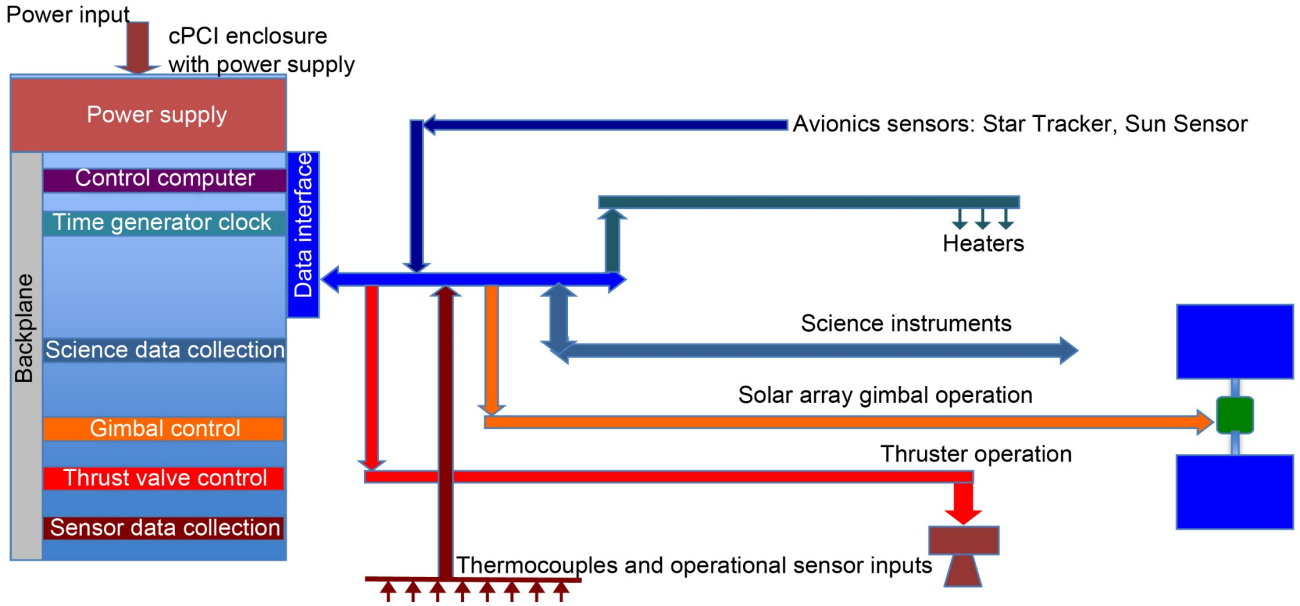

Figure 26.—Orbiter Command and Data Handling components and general layout, where cPCI is compact peripheral component interconnect.

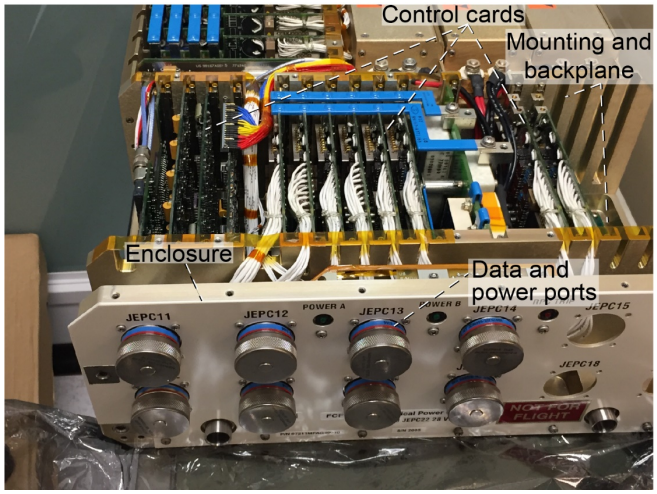

Figure 27.—Orbiter Command and Data Handling card stack and enclosure examples.

A number of different control cards were needed for operating and controlling the S/C. The S/C control begins with the onboard computer. For this application, an Andrews 160 off-the-shelf flight control computer was baselined. This card is a low-cost, highly functional processing card for controlling all aspects of the S/C and interfacing with the other designated controller cards. This controller uses dual PPC405 processors running at 400 MHz with Linux as the operating system. It contains 64 MB of synchronous dynamic random access memory (SDRAM), 16 GB compact flash nonvolatile memory, and a number of interfaces such as RS–22, RS–485, Serial Peripheral Interface (SPI), Inter-Integrated Circuit (I2C) and general-purpose input/output (GPIO).

The time generator clock is used to supply time interval data for syncing the operation of the different science and operational components of the S/C. The time generator is used as a reference for the timing of all functions of the S/C.

The gimbal and valve controllers are used to control the operation of the S/C SA gimbals and the propellant flow control valves for the propulsion system. These controllers provide precise operational control of the array gimbals for positioning the SA and the propellant control valves for the attitude control of the S/C.

The sensor and science data collection consists of a 48-channel analog-to-digital/digital-to-analog/serial digital interface (AD/DA/SDI) card for interfacing with the S/C sensors and science instruments.

The C&DH for the Lander is limited in scope. The Lander provides and transmits data for descent, baseline science, and measurement over an extended duration. To minimize power consumption and system volume, the system utilizes only the basic components needed to complete the mission based on the LLISSE model of simple systems based on high-temperature electronics. The main components include

- Sleep timer for descent
- Baseline science timer
- Sleep timer for extended operations
- Awake/sleep power bus switches
- Sensor analog amplifiers
- Digital converters
- Data stream registers and control
- RF transmitter

The objective of the Lander CD&H system is to monitor, process, and communicate data from the V-BOSS sensor array throughout the mission during high-temperature operations. A notional CD&H controller schematic is shown in Figure 28. As described in Section 4.1 and shown in Figure 28, the data provided are from a number of sensors: temperature, pressure, chemical species analysis, IR bolometers, wind sensors, and V-Lab. The core of the CD&H system functionality is science control and data processing/transfer from these various Lander sensors. This functionality is activated through a triggering mechanism to process and communicate information from the V-BOSS sensor array during different operational modes throughout the missions as described in the CONOPS in Section 2.3.6. In particular, the operational modes where the sensor data is provided are (1) during descent for 1 hr, (2) baseline science upon landing for 72 hr, and (3) long-duration science every 12 hr for 2 min for the rest of the mission until the batteries are exhausted.

A simplified electronics block diagram describing how the science control and data processing/transfer is achieved is shown in Figure 29. The circuits involved are high-temperature SiC electronics. As described in Section 4.7, during descent, a conventional battery is used to transition to a high-temperature battery for Lander surface operations. The triggering of the processing and transfer of sensor data depend on a timer circuit; e.g., one based on charging of a capacitor, and transitioning between each mission operational mode. The timer circuit triggers a power bus switch, which then activates the processing and transfer of data carried out by the Awake Mode Circuit shown in Figure 29. The operation of the awake mode circuits is the same in each operational mode; the initiation and duration of its operation is controlled by the timers. This awake mode circuit receives and amplifies the various sensor signals, digitizes the signals, and communicates the data. A shift register sequentially samples each sensor input so that data from each sensor is provided multiple times during, for example, the 2-min period of data collection every 8 hr during the long-duration mission mode. The maturity and development of the electronics and communications circuits for this CD&H system is discussed in Section 4.3.

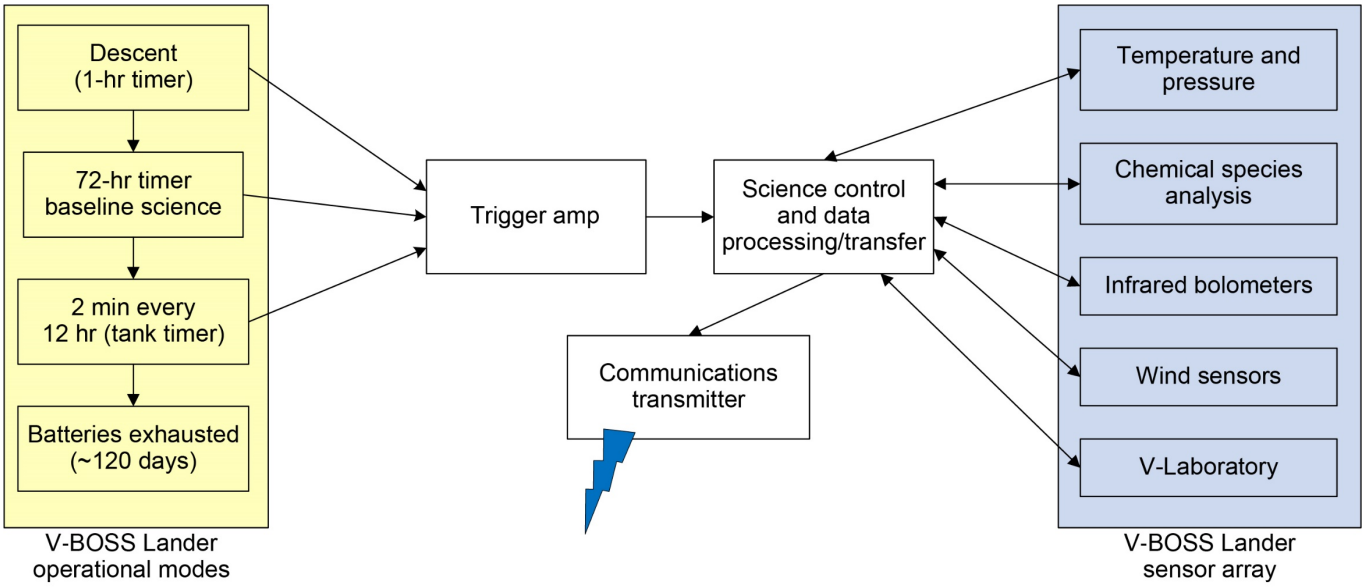

Figure 28.—Notional Command and Data Handling Lander controller schematic, where V-BOSS is Venus Bridge Orbiter and Surface Study.

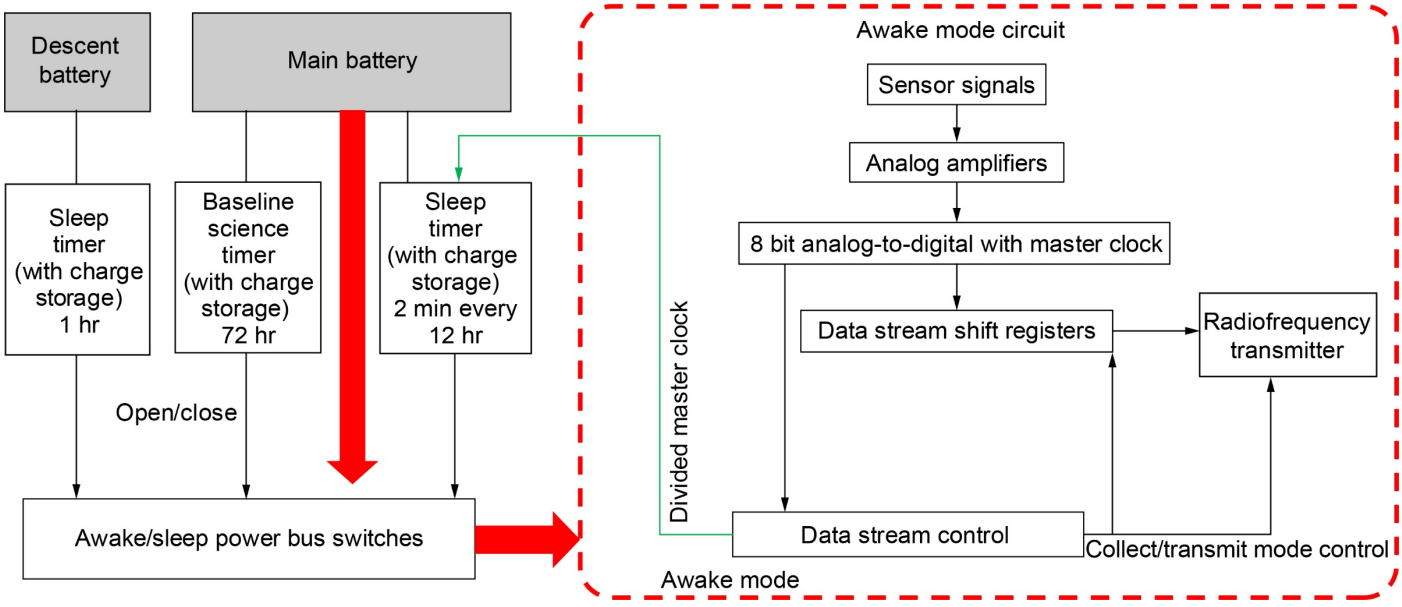

Figure 29.—Simplified electronics block diagram for the Lander Command and Data Handling system.

4.6 Guidance, Navigation and Control (GN&C)

The GN&C subsystem is responsible for determining and controlling the attitude and angular rate of the vehicle throughout all phases of the mission.

4.6.1 Guidance, Navigation and Control (GN&C) Requirements

The GN&C subsystem has the following requirements for the V-BOSS mission:

- Provide sufficient RCS control authority for critical mission events.
- Provide reasonable fine-control, via reaction wheels, for slew maneuvers and environmental torque cancellation.
- Maintain low jitter during IR imaging science operations.
- Be zero fault tolerant.

4.6.2 Guidance, Navigation and Control (GN&C) Assumptions

Sizing of the Attitude Control System (ACS) is very much dependent on the mass properties of the S/C as a whole. Several assumptions were made during the ACS design process due to the maturity of the system-level design.

As previously mentioned, estimation of the mass properties of the S/C during the various stages of the mission is necessary in order to gauge the size of the ACS. Therefore, the system moment of inertia (MOI) matrix was estimated by approximating the primary MOI drivers as basic geometric shapes positioned according to any available configuration data. All analyses assume the S/C acts as a rigid body.

The 1- and 22-N thrusters are assumed to have a 0.5-m moment arm. Constrained random dispersions are applied to the thruster locations and thrust values to determine an average value for the torques induced due to firing the thrusters. Additionally, a constant specific impulse (I_{sp}) and thrust are assumed for propellant system sizing purposes.

There is a lack of accurate atmospheric density measurements for the proposed 10-day orbital altitudes. Therefore, extrapolation of existing data-based models was used to determine the expected disturbance torque on the Orbiter due to atmospheric drag. Additionally, the orbit-lowering effect of drag was estimated from the Venus Express mission for orbit maintenance propellant budgeting purposes.

The EDL package deploy phase requires the S/C to be well balanced from a mass distribution standpoint. Ideally, the desired spin axis and the primary axis of the Orbiter/EDL package stack should be very closely aligned to avoid any coning or nutation. The undesirable effects of excessive coning and nutation could lead to unacceptably high landing zone errors. It was assumed there are only small differences between the Orbiter/EDL package primary axis and the spin axis.

4.6.3 Guidance, Navigation and Control (GN&C) Design and Master Equipment List (MEL)

The GN&C design for the Orbiter is zero fault tolerant and provides three-axis control over the S/C during the various phases of the mission. The ACS consists of three reaction wheels, eight 1-N thrusters, and four 22-N thrusters. Coarse attitude determination is assisted via six Sun sensors. Fine three-axis attitude determination is assisted via a single star tracker with one optical head. Finally, a single IMU containing three internal accelerometers and three internal gyroscopes is utilized. The attitude sensors are all high-TRL, off-the-shelf components in order to keep costs low. The system schematic is illustrated in Figure 30. Additionally, the selected components are able to handle the rotational and translational accelerations anticipated to occur throughout the mission.

The three reaction wheels are used for slew maneuvers, science pointing, and canceling environmental disturbance torques. The eight 1-N thrusters are used for spinning the S/C up and down during the EDL package deploy phase. The four 22-N thrusters are primarily used for translational burns. Due to the positioning of the thrusters, both the 1- and 22-N thrusters are used to desaturate the reaction wheels and to null the tipoff rates after separation from the launch vehicle. The Blue Canyon Technologies RWP100 reaction wheels were selected for their exceptionally low jitter, which is necessary during IR imaging operations. The relatively low momentum storage capabilities of the wheels results in frequent desaturations due to torques induced by solar radiation pressure, the primary driver in terms of environmental disturbance torques for the proposed orbit.

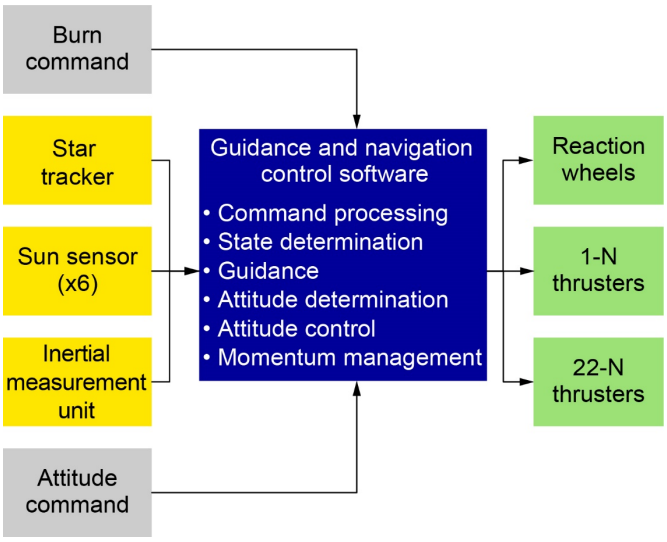

Figure 30.—Orbiter Attitude Determination and Control system schematic.

TABLE 16.—GUIDANCE, NAVIGATION AND CONTROL (GN&C) MASTER EQUIPMENT LIST

Description	Quantity	Unit mass, kg	Basic mass, kg	Growth, %	Growth, kg	Total mass, kg
Orbiter	-	----	175.44	8.9	15.70	191.13
Attitude Determination and Control	-	----	3.24	3.0	0.10	3.34
GN&C	-	----	3.24	3.0	.10	3.34
Inertial measurement unit	1	0.75	0.75	3.0	.02	0.77
Star tracker optical head	1	.25	.25	3.0	.01	.26
Star tracker electronics unit	1	.56	.56	3.0	.02	.58
Sun sensors	6	.03	.18	3.0	.01	.19
Reaction wheels	3	.50	1.50	3.0	.05	1.55

The Technical University of Denmark Micro Advanced Stellar Compass consists of a single data processing unit and one optical head. The unit is able to support multiple optical heads and provides 0.7 arcsec (1-σ) of attitude accuracy. Attitude measurements between star tracker updates and knowledge of body rates is provided by three solid-state fiber optic gyros contained in the LN–200S IMU. Also contained in the IMU are three solid-state silicon accelerometers that provide linear acceleration measurements. The GN&C system MEL can be seen in Table 16.

4.6.4 Guidance, Navigation and Control (GN&C) Analytical Methods

The GN&C design is based on several sources, including historical data from the Magellan and Venus Express missions, previous Compass studies, and calculations performed in a Microsoft Excel spreadsheet, which is purpose-built for Compass studies. There were several aspects of the mission that drove the GN&C design, the largest being the IR imaging operations.

A representative estimate of the S/C MOI was determined by separately modeling major components as basic geometric shapes, determining individual component MOIs, then using the parallel axis theorem to determine the overall MOI relative to an arbitrary body frame. As previously mentioned, component positions relative to a body frame were determined from available configuration data.

The three environmental torques considered were solar radiation pressure torque, aerodynamic drag torque, and gravity gradient torque. Additionally, torques induced due to offset thruster placement and off-nominal thruster performance were considered. Conservative estimates of the environmental torques were calculated by using worst-case orientations in order to determine the maximum torque values that are expected to be encountered during the mission. The dominant disturbance torque contributor was solar radiation pressure due to its constancy and the proposed placement of the SAs. Random dispersions of the thruster operation (±1-percent position per axis and ±1-percent thrust value) resulted in an approximately normal distribution of torque magnitudes. The mean value of this distribution was calculated and used as a typical torque induced during translational burns.

The IR imaging operations were the primary driver for sizing the reaction wheels, minimizing jitter being the primary goal. An off-the-shelf reaction wheel with very low jitter, relative to similar options, was selected for two reasons. First, an indepth jitter analysis would require fairly precise knowledge of the mass characteristics of the S/C to properly constrain the static and dynamic imbalances. Second, custom-designed hardware would drive costs up. An assessment of the maximum change in true anomaly versus the maximum slew rate provided by the reaction wheels was conducted to verify the selected reaction wheels could properly track a location on the surface of Venus for a discrete amount of time. It should be noted this assessment assumed the Orbiter would track the center of the planet; however, the low spin rate of the planet and excess margin in the maximum slew rate over the maximum change in true anomaly renders the assessment valid.

4.6.5 Guidance, Navigation and Control (GN&C) Risk Inputs

The star tracker provides the only high-accuracy measurement of the S/C inertial attitude. In case the single optical head is blinded by the Sun, high-accuracy attitude knowledge would be lost, which may result in diminished science return during IR imaging operations.

4.6.6 Guidance, Navigation and Control (GN&C) Recommendation

The current thruster placement, in the absence of restorative torques, necessitates the use of a pair of 22-N thrusters to desaturate one of the reaction wheels. The thruster on time to perform this task is on the order of milliseconds and may be smaller than the minimum impulse bit of the thrusters. This may lead to overshooting and will lead to a translational ΔV as the thruster forces are uncoupled. These effects can be reduced if the aft 22-N thrusters are downsized or moved more inboard.

Additionally, a set of auxiliary RCS thrusters can be placed next to the 22-N thrusters for finer control over the axis in question.

An indepth analysis of the minimum rotational speed of the Orbiter/EDL package stack should be conducted to assure the EDL package has a sufficient spin rate to remain stable during entry. Additionally, an acceptable landing error ellipse analysis should be conducted to determine the acceptable error in the deploy direction. This will constrain how balanced the S/C needs to be during the spin-up portion of the deploy phase.

A more refined estimate of the S/C MOI during the various phases of the mission will assist in reducing conservatism in torque estimates. Additionally, a flexible body model of the Orbiter and a propellant slosh model will give greater insight into the residual oscillations that may contribute to the effective jitter during IR imaging operations.

The frequent desaturation of the reaction wheels can be mitigated by selecting a quiescent attitude, which points either the fore or aft end of the Orbiter in the direction of the Sun.

Per the discussion in Section 4.6.5, it is recommended that an additional optic head be added to the star tracker system.

4.7 Electrical Power (EP) Subsystem

4.7.1 V-BOSS Orbiter

4.7.1.1 Orbiter Power Requirements

- The Orbiter EP system shall operate in Venus orbit for 120 Earth days.
- The Orbiter EP system shall operate during the 10-day orbit period of which 15 min is spent in eclipse and the remainder is spent in insolation.
- The Orbiter EP system shall provide the power levels shown in Table 17 to the Orbiter during the associated mission phases.

The Orbiter EP system was designed to operate for a total of 120 days in Venus orbit. The orbital period is 10 days with a maximum eclipse time of 15 min, making the orbit highly elliptical. The maximum power consumption for the Orbiter occurs during the orbital insertion burn at 330 W. Standby (10 days) and eclipse (15 min) modes required 55 W of power, while Orbiter communication operations (8 hr) requires 120 W of power.

TABLE 17.—ORBITER POWER MODES

Power mode[a]	Orbital insertion burn (mode 3)	Orbiter eclipse (mode 7)	Orbiter communications (mode 9)	Standby power (mode 10)
Power, W	330	54	120	55
Duration	30 min	15 min	8 hr	10 days

[a]All power modes include 30-percent growth allowance.

4.7.1.2 Orbiter Power Assumptions

The following assumptions were defined by the EP system lead for the Orbiter.

Solar arrays

- Scaled the SA design from the Venus Express SA design launched in late 2005.
- The front surface of the SA is evenly divided between active solar cells and optical surface reflectors for reducing the operational temperature of the array.
- The backside surface of the array is assumed to have optical surface reflectors covering the entire surface.
- The SA was sized for 190 W end of life (EOL) at Venus (0.723 AU, 100 W beginning of life (BOL) at Earth, 1 AU).
- The SA is divided into two wings.
- The SAs are Sun tracking and use an off-the-shelf single-axis solar array drive assembly (SADA) to articulate each wing separately.

Lithium-ion battery

- Assumed the battery is composed of Saft VES16 cells.
- The battery is oversized to provide power during the orbital insertion burn, since the SAs are not large enough to provide the full 330 W during the burn.
- Maximum depth of discharge (DOD) of 90 percent.

Power Management and Distribution (PMAD)

- The PMAD is designed based on off-the-shelf equipment designed by the TERMA Company and used on Mars Express and Venus Express.
- The power electronics box consists of multiple power cards, including a Power Distribution Unit (PDU), Battery Charge-Discharge Unit (BCDU), and an Array Regulator Unit (ARU).
- Assumed the harness mass was 25 percent of the total Orbiter EP system mass.

4.7.1.3 Orbiter Power Design and Master Equipment List (MEL)

EDL Power System Design

The Orbiter hardware includes the following components:

- SA (two wings)
- Honeybee single-axis SADA (one per wing)
- Li-ion battery composed of Saft VES16 cells
- TERMA Power Equipment Box
  - TERMA BCDU Card
  - TERMA ARU Card
- Harness

TABLE 18.—ORBITER ELECTRICAL POWER (EP) SYSTEM MASTER EQUIPMENT LIST

Description	Quantity	Unit mass, kg	Basic mass, kg	Growth, %	Growth, kg	Total mass, kg
Orbiter	-	----	175.44	8.9	15.70	191.13
EP subsystem	-	----	18.68	35.0	6.54	25.22
Power generation	-	----	5.86	30.0	1.76	7.62
Solar array	2	2.75	5.50	30.0	1.65	7.15
Single-axis gimbal	2	0.18	0.36	30.0	0.11	0.47
Power Management and Distribution	-	----	6.32	44.9	2.84	9.16
Power Distribution Unit	1	0.57	0.57	30.0	0.17	0.74
Battery Charge-Discharge Unit	1	0.55	0.55	30.0	0.17	0.72
Array Regulator Unit	1	0.50	0.50	30.0	0.15	0.65
Harness	1	4.70	4.70	50.0	2.35	7.05
Energy storage	-	----	6.50	30.0	1.95	8.45
Li-ion battery	1	6.50	6.50	30.0	1.95	8.45

TABLE 19.—LANDER POWER MODES

Power mode[a]	Startup mode	Baseline mode	Science/ communications operations	Standby
Power, W	10	10	10	0.02
Duration	First 8 hr after landing	Next 72 hr after startup, 2 min/hr	2 min	12 hr
Science and communications frequency	Continuous operation	Once per hour	Once every 12 hr	None
Total duration	8 hr	2.4 hr	7.6 hr	2,862 hr

[a]All power modes include 30-percent growth allowance.

All of the components of the power subsystem and their masses are shown in Table 18.

During insolation, the Orbiter EP system generates power using a SA. The SA was sized for 190 W EOL at Venus (0.723 AU, 100 W BOL at Earth, and 1 AU) with two wings and a wing area of 0.39 m^3 each. The SAs track the Sun using an off-the-shelf single-axis SADA with one gimbal per wing. During eclipses, the Orbiter is powered by a secondary (rechargeable) Li-ion battery. The total energy of the battery is 60 Wh. The PMAD of the Orbiter was designed using TERMA power equipment cards. The power box has a net efficiency of 92 percent and consumes a maximum of 10 W of parasitic power when operating.

Technology Maturity

Orbiter:

- SA = TRL 6
- Honeybee single-axis SADA = TRL 8
- Li-ion battery = TRL 9
- Power equipment box = TRL 9
  - PDU card = TRL 9
  - BCDU card = TRL 9
  - ARU card = TRL 9
- Harness = TRL 6

4.7.2 Lander Power Requirements

The Lander EP system shall operate for 120 Earth days on the surface of Venus, and it shall operate in four power modes: startup, baseline, standby, and science/communication operations. The modes and their associated power levels and durations are listed in Table 19.

The Lander EP system for the V-BOSS was designed such that the system operated in standby mode for the majority of the mission in order to minimize power consumption. Immediately following landing, the system ran science and communication operations continuously at 10 W for the first 8 hr. After this startup period, the system went into a baseline period entering standby mode and executing science and communication operations at 10 W once per hour. This baseline period lasted for a total of 72 hr. Finally, the Lander went into regular operations, entering a cycle of standby mode at 0.02 W for 12 hr then executing science and communication operations for 2 min at 10 W and returning to standby mode with the cycle continuing for 12 orbits at a 10-day orbit period.

4.7.3 Lander Power Assumptions

The following assumptions were defined by the EP system lead for the Lander.

- High-temperature NaS primary (nonrechargeable) battery
  - Assumed a specific energy of 120 Wh/kg and a specific volume of 150 Wh/L for the design of the NaS primary battery. This is the upper limit of a range provided by Energy Storage Technology for Future Space Science Missions, JPL D–30268 (Ref. 21).
  - The maximum DOD of the battery is assumed to be 90 percent.
- PMAD
  - Assumed an unregulated +25 V and –25 V bus for the Lander.
  - Assumed the harness mass is 14 percent of the total Lander EP system mass.

4.7.4 Lander Power Design and Master Equipment List (MEL)

The Lander hardware includes the following components:

- NaS primary battery
  - The total energy needed for the Lander battery is 269 Wh (includes DOD and 3-percent power system losses and 30-percent user power growth allowance). This is broken down to 91 Wh for startup, 27 Wh for baseline energy, 87 Wh for science and communication energy, and 64 Wh for standby energy.
  - The battery volume is approximately 1,800 cm^3.
- Harness

All of the components of the power subsystem and their masses are shown in Table 20.

Technology Maturity

- Lander
  - NaS Battery = TRL 4
  - Harness = TRL 6

4.7.5 V-BOSS Entry, Descent, and Landing (EDL)

4.7.5.1 Entry, Descent, and Landing (EDL) Power Requirements

- The EDL EP system shall provide 130 μW of power for 29 days (0.1 Wh) during the coasting phase after Orbiter separation up to Venus entry (Table 21).

4.7.5.2 Entry, Descent, and Landing (EDL) Power Assumptions

The following assumptions were defined by the EP system lead for the EDL.

- EDL timer
  - Assumed the EDL timer operated at 3.6 V and triggered ignition of the thermal battery.
  - The timer is powered using off-the-shelf primary Li battery cells.
  - The maximum DOD for the Li battery cells is 90 percent.
- Thermal battery
  - Assumed the thermal battery is used to heat up the high-temperature NaS battery for regular operation on the Venus surface.
  - Assumed the thermal battery provides 10 Wh of energy (it must also operate for 1 hr, which is unusually long for typical space-rated thermal batteries).
  - Assumed the thermal battery is a $LiFeS_2$ battery with a specific energy of 60 Wh/kg and a specific volume of 120 Wh/L.
- PMAD
  - Assumed the harness mass was 15 percent of the total EDL EP system mass.

4.7.5.3 Entry, Descent, and Landing (EDL) Power Design and Master Equipment List (MEL)

The EDL hardware includes the following components:

- $LiFeS_2$ Thermal Battery
- Saft primary Li (Li-$SOCl_2$) battery cell—LS 33600
- Harness

All of the components of the power subsystem and their masses are shown in Table 22.

Technology Maturity

- EDL
  - $LiFeS_2$ thermal battery = TRL 4
  - Primary Li battery cell = TRL 9
  - Harness = TRL 6

4.7.6 Power Analytical Methods

A spreadsheet power-sizing tool developed by the Compass team was utilized to design the power system. Figure 31 to Figure 33 illustrate the Lander, EDL, and Orbiter EP power system schematics, respectively.

TABLE 20.—ENTRY, DESCENT, AND LANDING AND LANDER ELECTRICAL POWER (EP) SUBSYSTEM MASTER EQUIPMENT LIST

Description	Quantity	Unit mass, kg	Basic mass, kg	Growth, %	Growth, kg	Total mass, kg
Lander	-	----	11.15	21.6	2.41	13.56
EP subsystem	-	----	2.57	32.5	0.84	3.41
Power Management and Distribution	-	----	0.32	50.0	0.16	0.48
Harness	1	0.32	0.32	50.0	0.16	0.48
Energy storage	-	----	2.25	30.0	0.68	2.93
Battery	1	2.25	2.25	30.0	0.68	2.93

TABLE 21.—ENTRY, DESCENT, AND LANDING (EDL) POWER MODE

Power mode[a]	EDL coast (PEL[b] power mode 2)
Power	130 µW
Duration	696 hr

[a]All power modes include 30-percent growth allowance.
[b]Power equipment list.

TABLE 22.—ELECTRICAL POWER (EP) SUBSYSTEM ENTRY, DESCENT, AND LANDING (EDL) MASTER EQUIPMENT LIST

Description	Quantity	Unit mass, kg	Basic mass, kg	Growth, %	Growth, kg	Total mass, kg
EDL	-	----	8.82	18.3	1.62	10.44
EP subsystem	-	----	0.20	32.6	0.07	0.27
Power Management and Distribution	-	----	0.03	50.0	0.01	0.04
Harness	1	0.03	0.03	50.0	0.01	0.04
Energy storage	-	----	0.18	30.0	0.05	0.23
Primary battery	1	0.01	0.01	30.0	0.00	0.01
Thermal battery	1	0.17	0.17	30.0	0.05	0.22

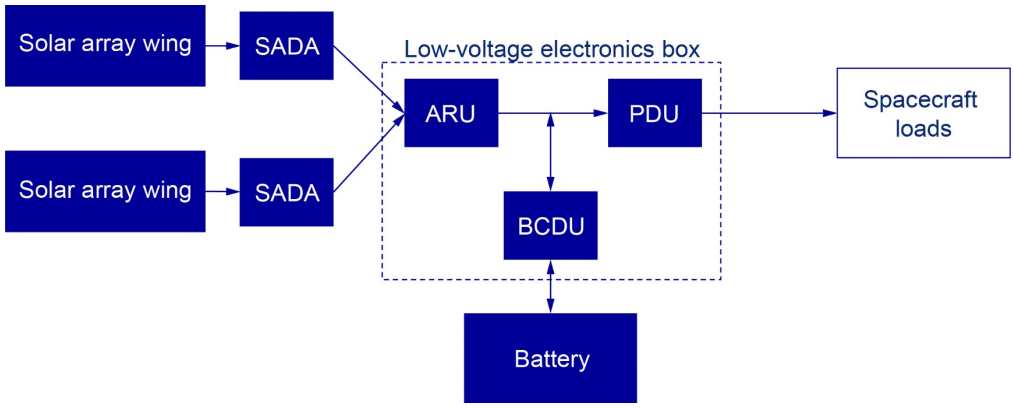

Figure 31.—Orbiter Electrical Power subsystem schematic, where ARU is Array Regulator Unit, BCDU is Battery Charge-Discharge Unit, PDU is Power Distribution Unit, and SADA is solar array drive assembly.

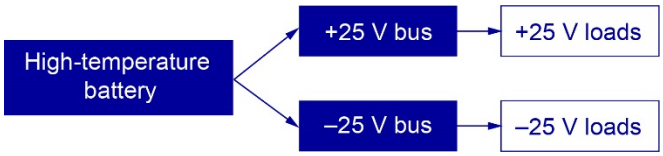

Figure 32.—Lander Electrical Power subsystem schematic.

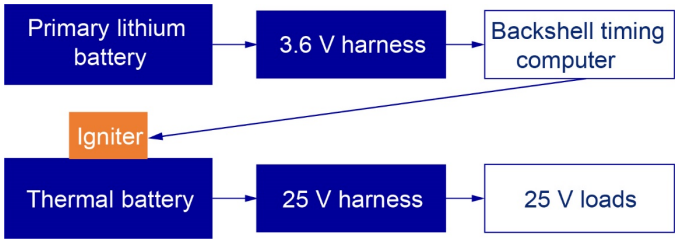

Figure 33.—Entry, descent, and landing Electrical Power subsystem schematic.

4.7.7 Power Risk Inputs

The following are the power risks:

- Lander NaS battery technology development
  - NaS batteries have flown once in the 1990s aboard the space shuttle as a technology demonstration, but have not flown as a primary energy source. The current market consists of only terrestrial batteries as there is no incentive to develop space-rated NaS batteries. It is unknown if the batteries require a pressure vessel to operate given the high Venus surface pressure. This will add significantly to the mass and volume if it is needed. Corrosion of the Venus surface environment may impact the battery as well. The operating cycle for the proposed battery differs significantly from any past NaS battery and it is unknown how this impacts its performance. The Venus surface temperature is significantly higher than the operating temperature of the battery and it is unknown how this affects its design or performance.
- EDL thermal battery technology development
  - The EDL thermal battery will require technology development as this type of battery (i.e., >1-hr operation) is not space rated.
- Orbiter SA and SADA temperature qualification
  - The SA and SADA for the Orbiter will require some development as the SA is scaled from an existing flight design, while the SADA may not be rated for the high Venus orbital temperatures. Further analysis of the Venus thermal environment will be needed to provide a better understanding of the additional technology development, which may be needed for the SAs and SADAs.

4.7.8 Power Recommendation

The following are the future work and recommendations from the power subsystem lead:

- Examine the Venus thermal environment to better understand the effect of high temperature on the power generation of the Orbiter's SAs and SADAs.
- Additional research is needed for NaS batteries to get a better understanding of how they operate to refine the accuracy of the power system models. This will provide a better estimate of the size and mass of the NaS battery on the Lander.
  - Since NaS batteries have only been developed for terrestrial or space shuttle use, we need to validate the ability of NaS battery to operate on Venus surface under high temperature and pressure. No known data exists for this testing. If it needs to be pressurized, then this will add greatly to its mass and volume. What are the temperature limits for Venus surface operations since this cannot be controlled? What are the corrosive impacts of the Venus surface on the battery? What is the lifetime of the battery for this application? What is the cell capacity? If a cell is 2 V and you need 25 V, then the battery must be heavier.
- Additional research is needed for the thermal batteries. Terrestrial thermal batteries are available, but further research into possible long-duration (1-hr) space-rated thermal batteries will improve the power system design and reduce risk.

As noted in Section 4.3.2.1, development of high-temperature battery systems is ongoing in LLISSE.

4.8 Orbiter Propulsion System

The primary purpose of the propulsion system is to provide adequate I_{sp} and thrust to accomplish the various maneuvers specified within the mission design. The system needs to store and deliver propellant at conditions and flow rates compatible with the selected thrusters, and do so in a manner that integrates well into the S/C. The propulsion system described here is a monopropellant AF–M315E blowdown system that performs both the major trajectory maneuvers and S/C orientation. The soon to be tested AF–M315E propellant (which is denser than

Hydrazine) was chosen due to the restricted volume on an ESPA Grande for an S/C.

4.8.1 Propulsion System Requirements

The Orbiter propulsion system is required to be zero fault tolerant to provide adequate propulsive performance to perform mission maneuvers and consist of commercial off-the-shelf (COTS) components, if possible, to minimize both cost and overall risk.

4.8.2 Propulsion System Assumptions

Although the Lander has no active propulsion, the Orbiter is assumed to use an AF–M315E based blowdown propulsion system with nitrogen pressurant gas, to minimize both volume and system mass. Both Earth departure and Venus orbital insertion maneuvers require significant propellant throughput to generate the ΔV required, and yet fine control with RCS is also required for S/C orientation. Thus, it is assumed that a set of larger thrusters will accomplish the major maneuvers, and smaller RCS thrusters will perform tipoff corrections, orbital maintenance, and the other lower ΔV maneuvers.

4.8.3 Propulsion System Design and Master Equipment List (MEL)

The propulsion system for the Orbiter is an AF–M315E based monopropellant blowdown system with two thrust classes of thrusters and a single COTS tank. AF–M315E is a hydroxyl ammonium nitrate (HAN-) based monopropellant developed by the Air Force Research Laboratory (AFRL). It is an ionic liquid that undergoes a glass transition at –80 °C, is much less toxic than hydrazine, and has an I_{sp} density 50 percent higher than hydrazine. This propellant has a low vapor toxicity, extremely low vapor pressure, and will not ignite unless the catalyst beds are heated to a temperature greater than 2,850 °C. Although AF–M315E is not considered a standard propellant, it is currently flight ready for the Green Propellant Infusion Mission (GPIM). A comparison of AF–M315E to both hydrazine and LMP–103S is shown in Table 23. Due to its properties, only single fault tolerance is required for flight systems (dual valve seat, no pyrotechnic valve required for isolation). Even though there is a systems-level requirement of zero fault tolerance, the single fault tolerant flight systems requirement is used in the feed system design detailed here.

TABLE 23.—STORABLE PROPELLANT COMPARISON

	Hydrazine	AF–M315E	LMP–103S
Primary ingredient	Hydrazine	Hydroxyl ammonium nitrate (HAN)	Ammonium dinitramine (ADN)
Composition	Hydrazine	USAF[a] proprietary methanol/ glycine/water blend	60- to 65-percent ADN 15- to 20-percent methanol 3- to 6-percent ammonia Remainder water
Density, g/cm^3	1.01	1.47	1.24
Freezing/boiling point	+1/+114 °C	<–40 °C / N/A	–6/120 °C
Vapor pressure, Pa	2,170 (300 K)	<0.013 (without H_2O, 300 K)	Ammonia/methanol/water
Toxicity	Highly toxic	Low toxicity	Low toxicity
Theoretical specific impulse (I_{sp}), s (e = 50:1, Pc = 300 psia)	242	266	252
Combustion temperature, K	1,227	2,713	1,873
Relative I_{sp} density	1.0	1.50	1.30
Cold start capability	Yes	No	No
Typical catalyst bed temperature, °C	90 to 300	285	340 to 360

[a]United States Air Force.

The thrusters used in this design are based on the Aerojet GR–1 and GR–22 thrusters designed for GPIM. The GR–1 thrusters have a nominal thrust of 1.0 N and a nominal I_{sp} of 210 s, while the GR–22 thrusters have a nominal thrust of 22.0 N and a nominal I_{sp} of 240 s. These thrusters are shown in Figure 36, and their nominal performance plots are shown in Figure 37.

The Orbiter propulsion system consists primarily of a single centrally mounted COTS membrane tank, eight small 1.0-N-class RCS thrusters located at the corners of the S/C frame, and four large 22.0-N-class thrusters as the aft on the vehicle near the adapter ring that are used primarily for the large ΔV maneuvers. The propellant tank and thruster placements are shown in Figure 34 and Figure 35.

These thrusters are fed propellant via a nominal single fault tolerant feed system that is stored in a single COTS ATK 80259–1. This tank is a 56.3-cm-diameter sphere with a 6Al-4V Ti alloy shell, an AF–E–322 membrane welded in at the equatorial midplane, is mounted to the S/C via equatorial tabs, and is nitrogen gas pressurized with a MOP of 24.13 bar. With the current propellant load of 89.6 kg, this tank is at 97-percent capacity and is shown in Figure 38.

The propellant load for the Orbiter is calculated by assuming that all maneuvers are conducted at a nominal I_{sp}, the large ΔV and all other maneuvers are accomplished using the 1.0-N-class thrusters. In addition to the propellant calculated by mission analysis, there is a 5-percent margin maneuvers are performed by the 22–N-class thrusters, added to primary propellant, 10-percent margin added to RCS propellant, and 3.5-percent residuals added to the total propellant load. The two primary maneuvers, Earth departure and VOI, are assumed to utilize all four of the larger thrusters, and are currently 13.9 and 21.4 min long, respectively. A summary of mission maneuvers and their corresponding propellant requirements is shown in Table 24. The development of these values is discussed throughout mission Section 2.3.1 to 2.3.5.

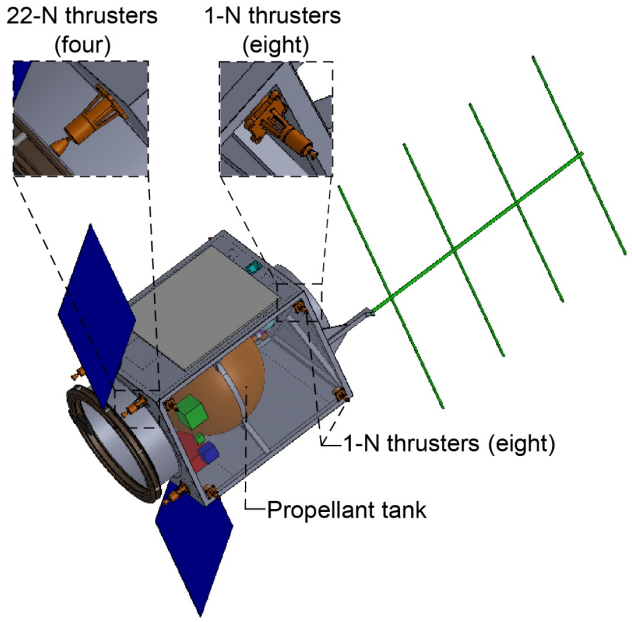

Figure 34.—Propulsion system configuration.

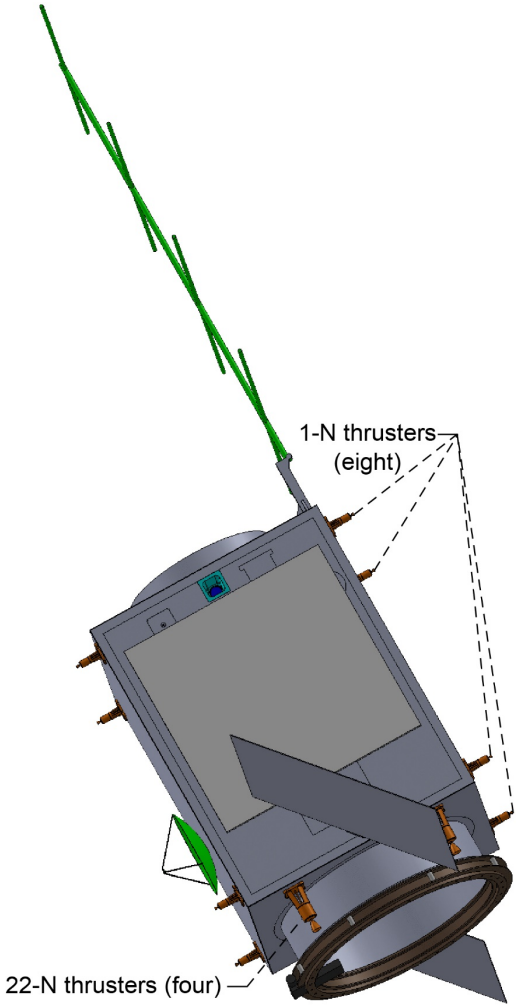

Figure 35.—Thruster locations.

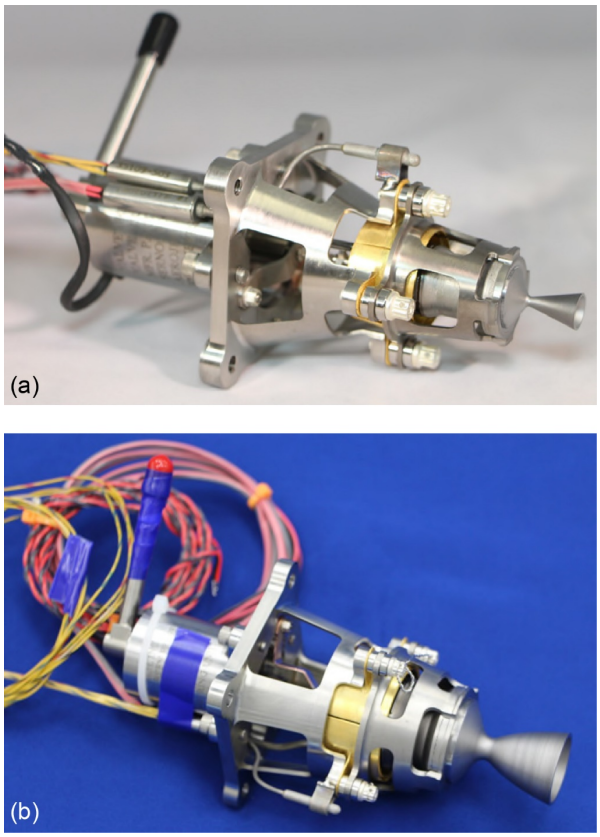

Figure 36.—AF–M315E-based Aerojet thrusters. (a) 1-N thruster. (b) 22-N thruster.

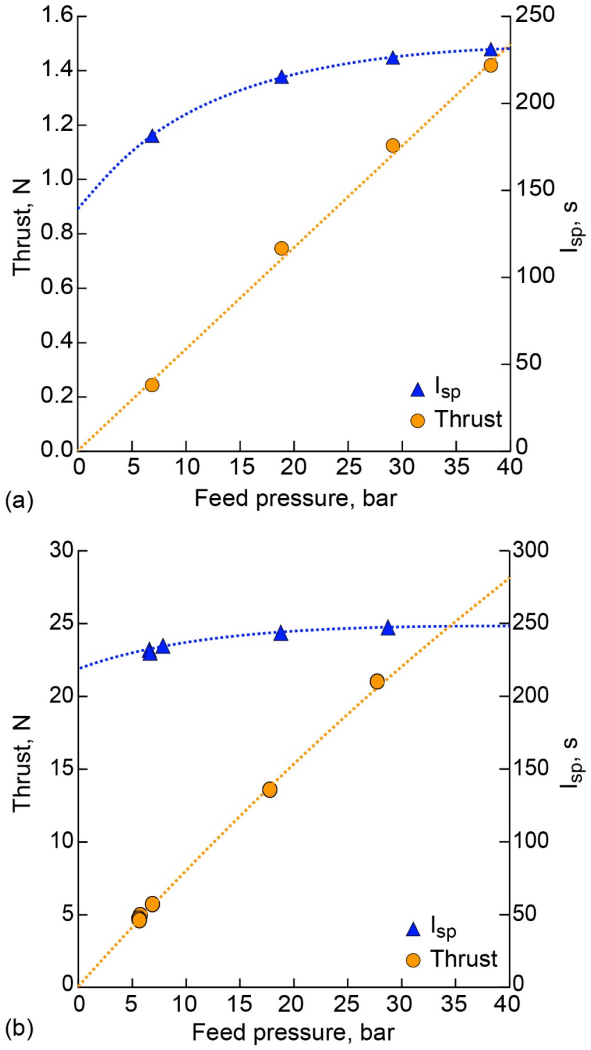

Figure 37.—Aerojet AF–M315E thruster performance. (a) GR–1 performance. (b) GR–22 performance.

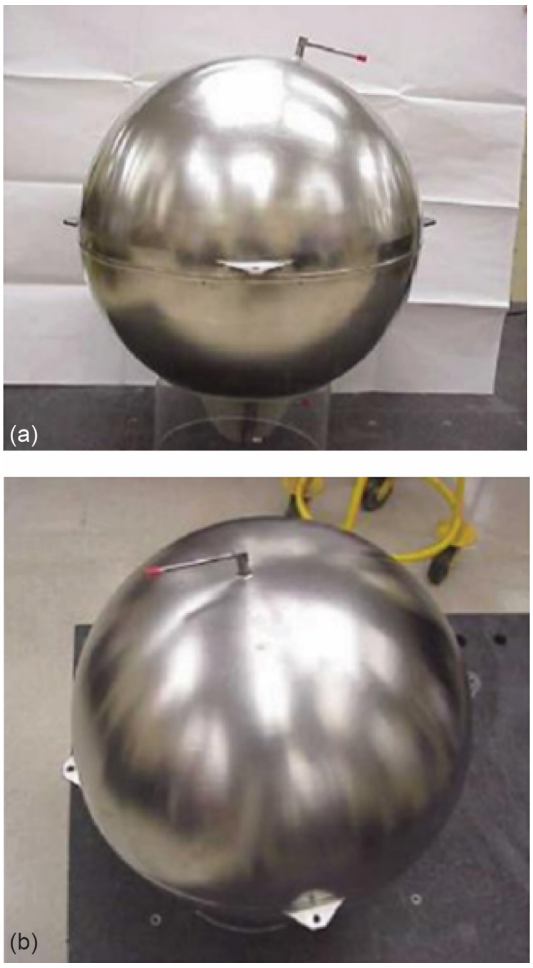

Figure 38.—ATK membrane tank Model 80259–1. (a) Front view. (b) Top view. (Used with permission.)

TABLE 24.—VENUS BRIDGE ORBITER AND SURFACE STUDY (V-BOSS) ORBITER DELTA VELOCITY (ΔV) SUMMARY

Description	ΔV, m/s	Nominal specific impulse, s	Required propellant, kg
Tipoff and corrections	10.5	210	1.21
Earth departure	350	240	31.2
Corrections and spin up/down	14	210	1.26
Venus orbit insertion	795	240	47.9
Orbital maintenance	10	210	0.61
Total usable propellant	---	---	82.3
Total with margin and residuals	---	---	89.6

The propellant is delivered to the thrusters via a simple single fault tolerant feed system with a nominal instrumentation suite and line heaters. Components are selected for AF–M315E compatibility, or chosen so that only simple material substations are required, as was done for GPIM. Being a blowdown system, there is no discreet pressurization system. The nitrogen gas that pressurizes the system is stored in the pressurant hemisphere of the propellant tank located on the opposite side of the membrane from the propellant. A preliminary piping and instrumentation diagram (P&ID) of the Orbiter propulsion system is shown in Figure 39.

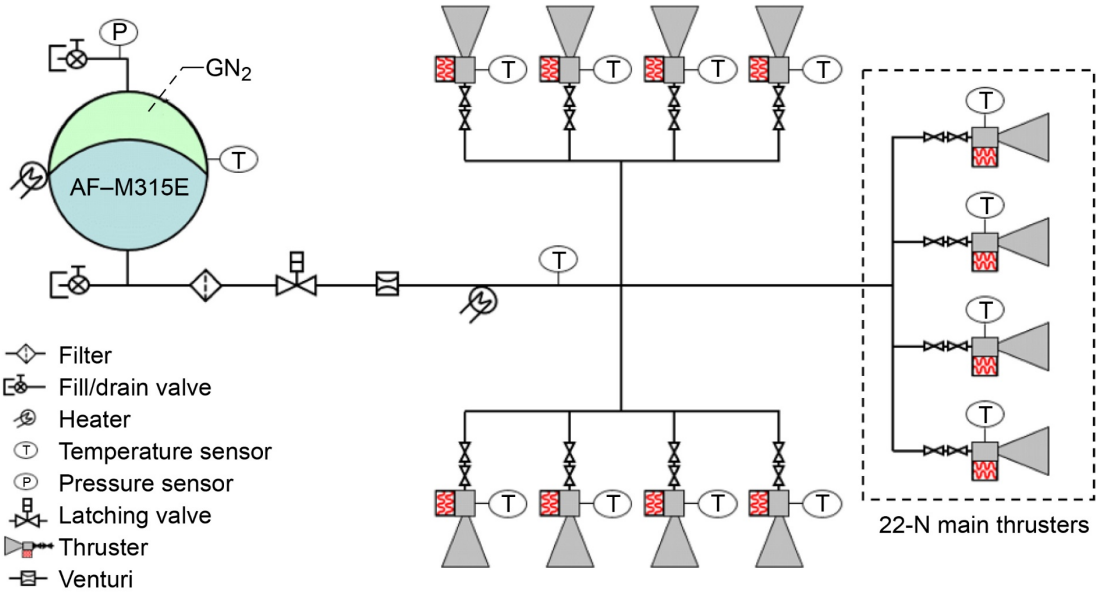

Figure 39.—Preliminary piping and instrumentation diagram.

TABLE 25.—ORBITER PROPULSION SYSTEM MASTER EQUIPMENT LIST

Description	Quantity	Unit mass, kg	Basic mass, kg	Growth, %	Growth, kg	Total mass, kg
Orbiter	-	-----	175.44	8.9	15.70	191.13
Propulsion (chemical hardware)	-	-----	13.28	5.9	0.79	14.07
Primary chemical system hardware	-	-----	13.28	5.9	0.79	14.07
Reaction Control System (RCS) hardware	-	-----	13.28	5.9	0.79	14.07
22-N AF–315E thrusters	4	0.65	2.60	3.0	0.08	2.68
1-N AF–315E thrusters	8	0.32	2.56	12.0	0.31	2.87
Feed system	1	1.77	1.77	12.0	0.21	1.98
ATK 80259–1 tank	1	6.35	6.35	3.0	0.19	6.54
Propellant (chemical)	-	-----	90.43	0.0	0.00	90.43
RCS propellant	-	-----	90.43	0.0	0.00	90.43
Fuel	-	-----	89.58	0.0	0.00	89.58
Fuel usable	1	82.28	82.28	0.0	0.00	82.28
Fuel margin	1	4.27	4.27	0.0	0.00	4.27
Fuel residuals (unused)	1	3.03	3.03	0.0	0.00	3.03
RCS pressurant	-	-----	0.85	0.0	0.00	0.85
Nitrogen pressurant gas	1	0.85	0.85	0.0	0.00	0.85

A complete MEL of the Orbiter propulsion system component quantity and masses, including propellant and pressurant gas, is listed in Table 25.

4.8.4 Propulsion System Trades

Two trades are conducted that compare the baseline AF–M315E system with a more traditional hydrazine-based blowdown system. In the first trade, ideally sized spherical membrane tanks are assumed with a 4:1 blowdown configuration. In the second trade, only COTS tanks are used. Both trades use Aerojet MR-106L and MR-103M hydrazine thrusters in place of the GR–22- and GR–1-based AF–M315E thrusters used in the design. For these two trades, the Orbiter and Lander have the same fixed, nonpropulsion, dry mass. Thus, only the effects of changing propellants, thrusters, tanks, and the impacts on the corresponding propulsion systems are explored.

First, the results of the ideal tank trade are shown in Table 26. Due to the lower I_{sp}, the hydrazine system required an additional 7.6 kg of propellant and an additional 35.6 L of tank volume. The resultant hydrazine tank is approximately 3.8 kg heavier, but the estimated feed system masses are the approximately same between the two designs. Overall, the hydrazine system is 9.8 kg heavier than the AF–M315E-based system.

Second, for the results of COTS tanks, only the propellant trade is shown in Table 27. The COTS tank-based hydrazine system requires an ATK 80505–1 diaphragm tank, which does fit in the S/C bus, but is so large that it is unclear if there is adequate room for all the other components. This configuration resulted in an additional 11.7 kg of propellant and a 21.5-kg increase in S/C wet mass relative to the AF–315E baseline.

The primary result of the propellant trade is that the AF–M315E-based system results in a smaller and lighter design relative to a comparable hydrazine-based system for this particular design. The ideal AF–M315E tank and the COTS tank (ATK model 80259–1) are very close in size, making it an excellent fit for this configuration and mission. In Figure 40, the COTS AF–M315E configuration is shown in comparison with both the ideal and COTS hydrazine tanks explored in these trades.

TABLE 26.—PROPELLANT TRADE WITH IDEAL TANKS

	AF–M314E			Hydrazine		
Main thrusters	GR–22	Thrust: 22 N	I_{sp}[a]: 240 s	MR-106L	Thrust: 22 N	I_{sp}: 230 s
Reaction Control System thrusters	GR–1	Thrust: 1.0 N	I_{sp}: 210 s	MR-103G	Thrust: 1.0 N	I_{sp}: 215 s
Estimated feed system mass	1.77 kg			1.77 kg		
Total propellant load (includes residuals)	89.58 kg			97.14 kg		
Required propellant volume	60.94 L			96.5 L		
Estimated ideal tank diameter and mass	53.2 cm/6.4 kg			61.8 cm/10.2 kg		
Ideal system dry mass	13.9 kg			17.0 kg		
System wet mass (with N_2 pressurant gas)	104.3 kg			114.1 kg		

[a]Specific impulse.

TABLE 27.—PROPELLANT TRADE WITH COMMERCIAL OFF-THE-SHELF (COTS) TANKS

	AF–M314E (current design)			Hydrazine		
Main thrusters	GR–22	Thrust: 22 N	I_{sp}[a]: 240 s	MR-106L	Thrust: 22 N	I_{sp}: 230 s
Reaction Control System thrusters	GR–1	Thrust: 1.0 N	I_{sp}: 210 s	MR-103M	Thrust: 1.0 N	I_{sp}: 215 s
Estimated feed system mass	1.77 kg			1.77 kg		
Total propellant load (includes residuals)	89.58 kg			101.3 kg		
Required propellant volume	60.94 L			100.2 L		
COTS tank diameter and mass (spherical)	ATK 80259–1 (97-percent fill 4:1 configuration)			ATK 80505–1 (96-percent fill, 4:1 configuration)		
	56.2 cm/6.4 kg			58.8 cm diam. by 72.3 cm/6.0 kg		
COTS system dry mass	13.4 kg			22.9 kg		
System wet mass (with N_2 pressurant gas)	103.7 kg			125.2 kg		

[a]Specific impulse.

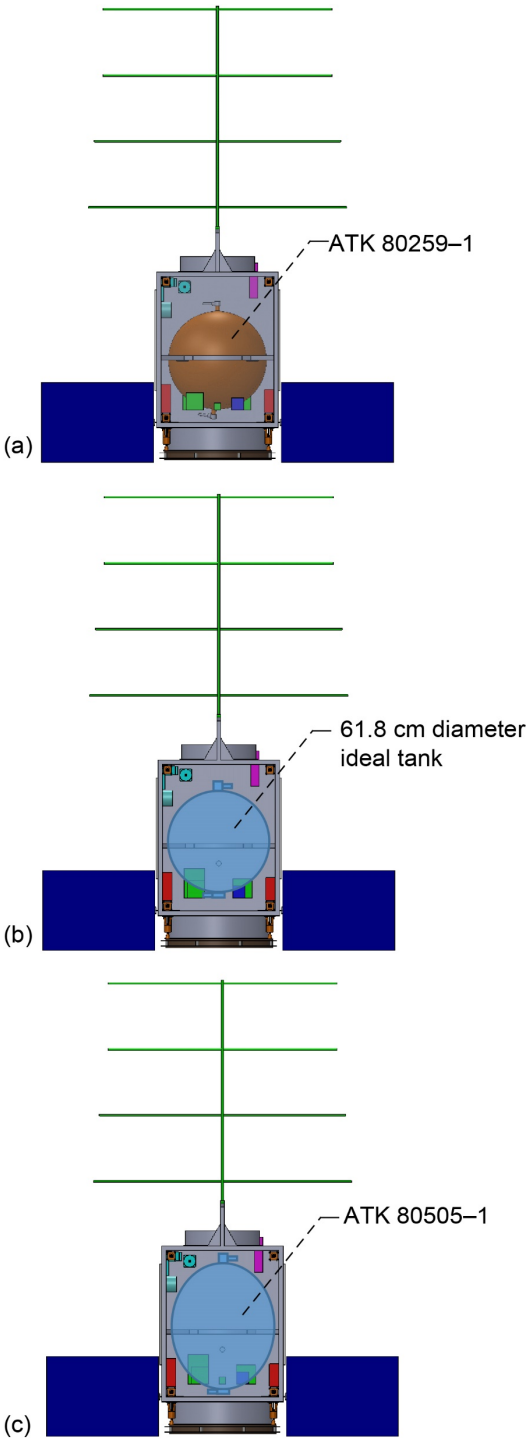

Figure 40.—Tank trade results comparison.
(a) Current design. (b) Ideal hydrazine tank.
(c) Commercial off-the-shelf hydrazine tank.

4.8.5 Propulsion System Analytical Methods

The methods used to design the propulsion system involve using a mix of published values, empirical data, and analytical tools. Published values and empirical data are used wherever possible, with analytical tools being employed as necessary. Empirical data is used to aid in the mass and size estimation of similar or derivative systems when published values are not available. Numerous NASA reports, AIAA standards, journal articles, and military specifications are used in this analysis, as well as custom analytical tools developed from basic physical relationships and conservation equations, with empirical-based inclusions for real-life hardware requirements (mounting bosses, flanges, etc.).

4.8.6 Propulsion System Risk Inputs

Due to the simplicity of the propulsion system design, the primary risk is materials compatibility with AF–M315E, which is mildly acidic and can cause leaching in some common aerospace materials. Long-term exposure tests currently underway have shown that many typical propulsion system materials, such as 6Al-4V Ti alloy, have sufficient compatibility for at least 3- to 5-year-long missions. AF–E–322 elastomeric membrane material was also found to meet AMS–R–83412A specification requirements for compatibility at elevated temperatures. Unfortunately, no ferromagnetic materials have shown compatibility to date. This led to minor design changes to some components used in the GPIM feed system, where appropriate material substitutions were made to a few subcomponents, or compatible coatings or claddings were applied. The work previously done under GPIM greatly reduces this propellant compatibility risk, and the careful selection of appropriate materials should reduce it further.

Another risk is that cold temperatures could cause performance issues with the propulsion system. Since AF–M315E does not expand as it undergoes a glass transition at low temperatures, any failures of the thermal system to keep the propellant within acceptable temperature limits should not result in catastrophic hardware damage, rather a lack of thruster operation/availability. Due to this mission's close proximity to the Sun and the lack of any exposed propellant lines in this design, this risk is very minimal. Detailed thermal modeling and testing can further greatly reduce this risk.

4.8.7 Propulsion System Recommendation

The main propulsion system recommendation for this design is to potentially reevaluate the propellant trades once the requirements are further refined. LMP–103S is another low-toxicity monopropellant that could be evaluated in future studies. Although it is becoming popular in Europe, LMP–103S lacks heritage in the United States and has an I_{sp} density

between AF–M315E and hydrazine. Since it currently offers no real advantage relative to AF–M315E, it currently does not buy its way into a propellant trade study for this design. A bipropellant design will yield higher I_{sp} and lower total propellant load, but will increase cost and complexity and will most likely result in a higher total system mass relative to either hydrazine or AF–M315E. If there is sufficient mass margin in the design, it may be worth trading a small solid to perform the Venus orbital insertion or Earth departure maneuver. Although solid motors are denser than monopropellants, this design is both mass and volume limited, and thus the total system mass might be higher for the total system.

4.9 Structures and Mechanisms

4.9.1 Orbiter Structures and Mechanisms Requirements

The V-BOSS Orbiter structures must contain the necessary hardware for science instrumentation, communications, C&DH, and power while fitting within the confines of the launch vehicle fairing. The structural components must be able to withstand applied loads from the launch vehicle and operational maneuvers. In addition, the structures must provide minimum deflections, sufficient stiffness, and vibration damping. The maximum lateral load of 5g is anticipated from the launch vehicle while the Orbiter and Lander are mounted to an ESPA Grande. The goal of the design is to minimize mass of the components that comprise the structure of the Orbiter bus, and must also fit within the physical confines of the launch vehicle. In addition, the structures must survive the environment near Venus.

4.9.2 Orbiter Structures and Mechanisms Assumptions

The bus provides the backbone for the mounted hardware. For this study, the main bus mass is estimated as 15 percent of the Orbiter mass. The 15-percent estimate falls in the range of S/C bus masses as presented by Price (1991) (Ref. 22).

Mechanisms include the active side of a 15-in.-diameter commercial Lightband separation mechanism to the Lander and the passive side of a 24-in.-diameter commercial Lightband separation mechanism to the ESPA. Design changes and/or good thermal protection may be necessary to have the separation mechanisms operate near Venus.

A frustum adapter is necessary for the stack also. The frustum adapter is placed between the Orbiter and Lander.

4.9.3 Orbiter Structures and Mechanisms Design and Master Equipment List (MEL)

Table 28 shows the expanded MEL for the structures subsystem on the Orbiter. This MEL breaks down the structures line elements to the lowest WBS.

4.9.4 Orbiter Structures and Mechanisms Analytical Methods

Ti is specified for the frustum adapter material. Per the Metallic Materials Properties Development and Standardization (MMPDS) (Ref. 23), the Ti-6Al-4V ultimate strength is 579 MPa and the yield strength is 490 MPa at 467 °C. Applying the safety factors of 1.4 on the ultimate strength and 1.25 on the yield strength, as per NASA–STD–5001 (Ref. 24), results in a maximum allowable stress of 393 MPa.

TABLE 28.—ORBITER STRUCTURES MASTER EQUIPMENT LIST

Description	Quantity	Unit mass, kg	Basic mass, kg	Growth, %	Growth, kg	Total mass, kg
Orbiter	-	-----	175.44	8.9	15.70	191.13
Structures and mechanisms	-	-----	29.14	16.4	4.79	33.92
Structures	-	-----	24.60	18.0	4.43	29.03
Primary structures	-	-----	24.60	18.0	4.43	29.03
Miscellaneous 06.3.11.a.a.a	1	24.60	24.60	18.0	4.43	29.03
Mechanisms	-	-----	4.54	7.9	0.36	4.89
Adapters and separation	-	-----	4.54	7.9	0.36	4.89
Lightband active, 15 in.	1	1.96	1.96	3.0	0.06	2.02
Frustum adapter Orbiter to Lander	1	1.47	1.47	18.0	0.27	1.74
Lightband passive, 24 in.	1	1.10	1.10	3.0	0.03	1.13

Hand calculations and a spreadsheet were utilized to determine approximate stress levels in the frustum adapter during launch. The cross-sectional arear by the smaller diameter end is evaluated. Assuming the CG for the Lander is near the center of the structure, the moment arm is taken as half the Orbiter structure height. The launch vehicle acceleration of 5g is applied to the mass of the Orbiter to determine the load and stress in the adapter. The resulting stress is 230 kPa (34 psi). The stress results in a positive margin of 930.

4.9.5 Orbiter Structures and Mechanisms Risk Inputs

Excessive g loads or impact from a foreign object may cause too much deformation, vibrations, or fracture of sections of the support structure. Consequences include lower performance from mounted hardware to loss of mission. The likelihood is 3 of 5. Consequences to cost is 4 of 5, schedule is 4 of 5, performance is 4 of 5, and safety is 1 of 5.

To mitigate risks, the structure is to be designed to NASA standards to withstand expected environment and g loads, a given impact, and to have sufficient stiffness and damping to minimize issues with vibrations. Transport and mission trajectories are to be planned to minimize the probability of excessive loads and impact with foreign objects.

4.9.6 Orbiter Structures and Mechanisms Recommendation

A stress analysis with finite element analysis (FEA) is recommended. Optimum designs may be accomplished with the use of orthogrid or isogrid panels.

4.9.7 Lander Structures and Mechanisms Requirements

The V-BOSS Lander structures must contain the necessary hardware for science instrumentation, communications, C&DH, and power while fitting within the confines of the aeroshell and launch vehicle. The structural components must be able to withstand applied loads from the launch vehicle, operational maneuvers, and landing. In addition, the structures must provide minimum deflections, sufficient stiffness, and vibration damping. The maximum lateral load of 5g is anticipated from the launch vehicle while the Orbiter and Lander are mounted to an ESPA Grande. The Lander is anticipated to encounter a dynamic load with a peak acceleration of 357g upon atmospheric entry. The atmosphere at the surface is at 467 °C (872 °F) and 9.3 MPa (1,330 psi). The Lander surface approach velocity is approximately 5 m/s (197 in./s). The goal of the design is to minimize mass of the components that comprise the structure of the Lander bus and must also fit within the physical confines of the aeroshell and launch vehicle. In addition, the structures must survive the harsh high-temperature environmental conditions.

4.9.8 Lander Structures and Mechanisms Assumptions

The bus provides the backbone for the mounted hardware. The main bus consists of a space frame with angle and plate members, which is assumed to provide the optimum architecture for housing the necessary operational hardware. The material is Ti, Ti-6Al-4V. Titanium angle, tubular, and plate members are utilized. Assembly is by welding and threaded fasteners. A crushable Ti honeycomb pad is used to disperse the energy upon landing.

Mechanisms include a spring lock hinge for the wind sensor mast and a separation mechanism between the Lander and the Orbiter. A commercial 15-in.-diameter Lightband is assumed for the separation mechanism. Design changes and/or good thermal protection may be necessary to have it operate near Venus.

4.9.9 Lander Structures and Mechanisms Design and Materials Equipment List (MEL)

Table 29 shows the expanded MEL for the structures subsystem on the EDL and Lander.

4.9.10 Lander Structures and Mechanisms Trades

Pneumatic pistons were evaluated as a substitute for the honeycomb crush pad. The cylinder would be vented under ambient conditions prior to landing. The piston would quickly compress the gas upon landing. It is assumed that the ideal gas law applies for the carbon dioxide atmosphere. The atmospheric gas density is 67.0 kg/m^3, temperature is 462 °C, and gas constant is 188.9 J-kg^{-1}-K^{-1}. Four pistons are assumed. A 3.5 cm displacement is assumed. The resulting maximum load per cylinder is 1.47 kN upon landing.

Assuming a linear stiffness, 20g mean acceleration results in a cylinder mean gas density of 335 kg/m^3. The mean load per piston is 0.73 kN. The resulting necessary piston area 2.63×10^{-5} m^2. A round piston would be 7.32 mm in diameter. It is assumed cylinder vent sizing provides pressure reduction for a single compression with critical damping.

The landing pad is assumed to provide a maximum 210 kPa on the planet surface. The resulting pad diameter is 20 cm.

The needed minimum dimensions for the cylinders and pads precludes the use of pneumatic pistons for the application. The added hardware exceeds the dimensional constraints of the aeroshell.

TABLE 29.—ENTRY, DESCENT, AND LANDING (EDL) AND LANDER STRUCTURES MECHANISMS MASTER EQUIPMENT LIST

Description	Quantity	Unit mass, kg	Basic mass, kg	Growth, %	Growth, kg	Total mass, kg
EDL	-	----	8.82	18.3	1.62	10.44
Structures and mechanisms	-	----	0.15	18.0	0.03	0.17
Mechanisms	-	----	.15	18.0	0.03	.17
Installations	-	----	.15	18.0	.03	.17
Command and Data Handling (C&DH) installation	1	0.01	.01	18.0	.00	.01
Communications and Tracking installation	1	.02	.02	18.0	.00	.02
Electrical Power (EP) installation	1	.10	.10	18.0	.02	.12
Science installation	1	.02	.02	18.0	.00	.02
Lander	-	----	11.15	21.6	2.41	13.56
Structures and mechanisms	-	----	7.45	16.7	1.24	8.70
Structures	-	----	6.61	18.0	1.19	7.80
Primary structures	-	----	6.61	18.0	1.19	7.80
Main bus	1	.85	4.85	18.0	.87	5.73
Honeycomb crush pad	1	.01	.01	18.0	.00	.01
Drag flap assembly	1	1.75	1.75	18.0	.31	2.06
Mechanisms	-	----	.84	6.1	.05	.90
Science payload	-	----	.03	18.0	.01	.03
Spring lock hinge	1	.03	.03	18.0	.01	.03
Adapters and separation	-	----	.67	3.0	.02	.69
Lightband passive side, 15 in.	1	.67	.67	3.0	.02	.69
Installations	-	----	.15	18.0	.03	.17
C&DH installation	1	.01	.01	18.0	.00	.01
Communications and Tracking installation	1	.02	.02	18.0	.00	.02
EP installation	1	.10	.10	18.0	.02	.12
Science installation	1	.02	.02	18.0	.00	.02

4.9.11 Lander Structures and Mechanisms Analytical Methods

As noted above, Ti is specified for the bus material. Per the MMPDS (Ref. 23), the Ti-6Al-4V ultimate strength is 579 MPa and the yield strength is 490 MPa at 467 °C. Applying the safety factors of 1.4 on the ultimate strength and 1.25 on the yield strength, as per NASA standard NASA–STD–5001 (2016), results in a maximum allowable stress of 393 MPa.

The honeycomb core is assumed to be of Ti-6Al-4V. The architecture of the honeycomb is assumed to match the commercial Hexcel® 3/8-5052-.007 (Hexcel Corporation) Al honeycomb. For this study, the crush strength is derived by scaling the published crush strength for the commercial honeycomb material with the ratio of the yield strengths of Ti and 5052 Al. The resulting assumed crush strength of the Ti honeycomb is 0.42 MPa.

Initially, hand calculations and a spreadsheet were utilized to determine approximate stress levels in key structural members during launch and landing. Upon landing, the vertical frame members are assumed to bear the majority of the load with an assumed 80g peak acceleration and 12.5 kg supported. It is assumed the load is evenly divided among the four components. The result is a peak stress of 15.3 MPa in each vertical member, which provides a positive margin of 24.9. The crush pad is exposed to the same load with a supported mass of 12.6 kg, an 80g peak acceleration, and an approach velocity of 5.0 m/s. The conditions result in a crush pad displacement of 1.6 cm. Assuming 80 percent of the honeycomb is crushed leads to an initial overall height of 2.0 cm, and with the given crush strength of 0.42 MPa, the necessary cross-sectional area of the honeycomb is 2.33×10^{-2} m^2.

The simple geometry of the structure allowed for a quick FEA study of the Lander. The FEA model, illustrated in Figure 41, uses linear plate and beam elements for the bus structure. Solid elements are used for the modeling of the crush pad. Rigid and gluing elements are used to join the various components. Individual concentrated masses are used to represent science, C&DH, and electric power. Constraints are placed at the drag flap perimeter by the four braces to represent the support within the aeroshell. Each constraint fixes all six degrees of freedom.

A modal analysis illustrates a stiff structure with the first modal frequency at 376 Hz. Figure 42 illustrates the model at the first modal frequency. The model is in a free-free condition. Table 30 presents the first 10 modal frequencies of the Lander model. The frequencies range from 376 to 762 Hz.

It was determined that the Lander would be exposed to significant acceleration during atmospheric entry. A dynamic load was determined for the Lander as it decelerates through the atmosphere on its way to an eventual landing. Figure 43 shows the anticipated acceleration relative to time and altitude. A peak acceleration of 357g is anticipated.

A transient dynamic analysis was performed with the FEA with an assumed 20-percent damping coefficient for the structure. The Lander is assumed to be supported at four points around the drag flap as noted above. No isolation from the aeroshell is assumed. A peak stress of 309 MPa in the drag flap area is the result providing a positive margin of 0.27. Figure 44 shows the Lander with its stress contour.

The Lander shows positive margins for the expected loads. The analysis provides a worst-case situation where all the loads are transferred through the aeroshell with no isolation.

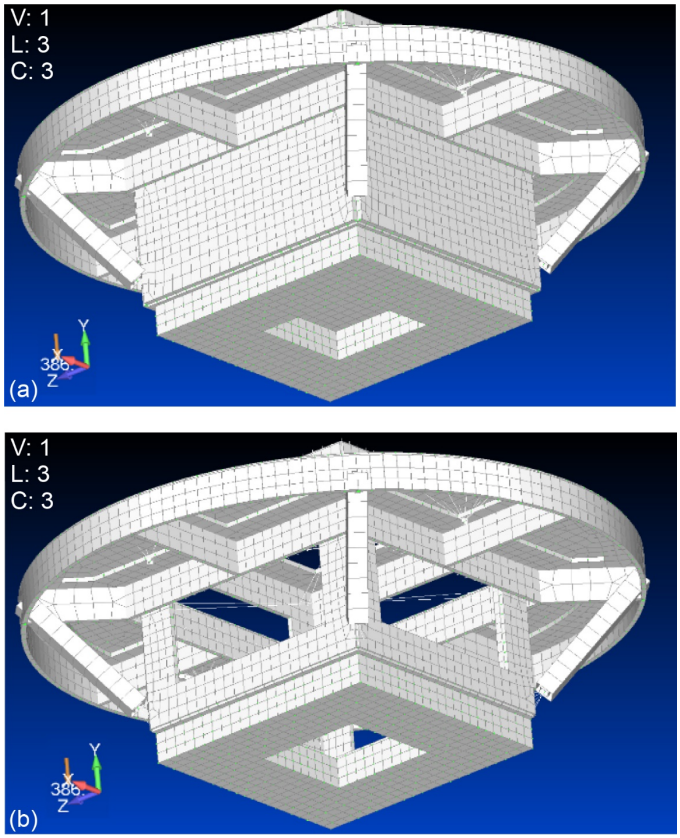

Figure 41.—Finite element analysis (FEA) Lander models. (a) Meshed FEA model. (b) FEA model with panels hidden.

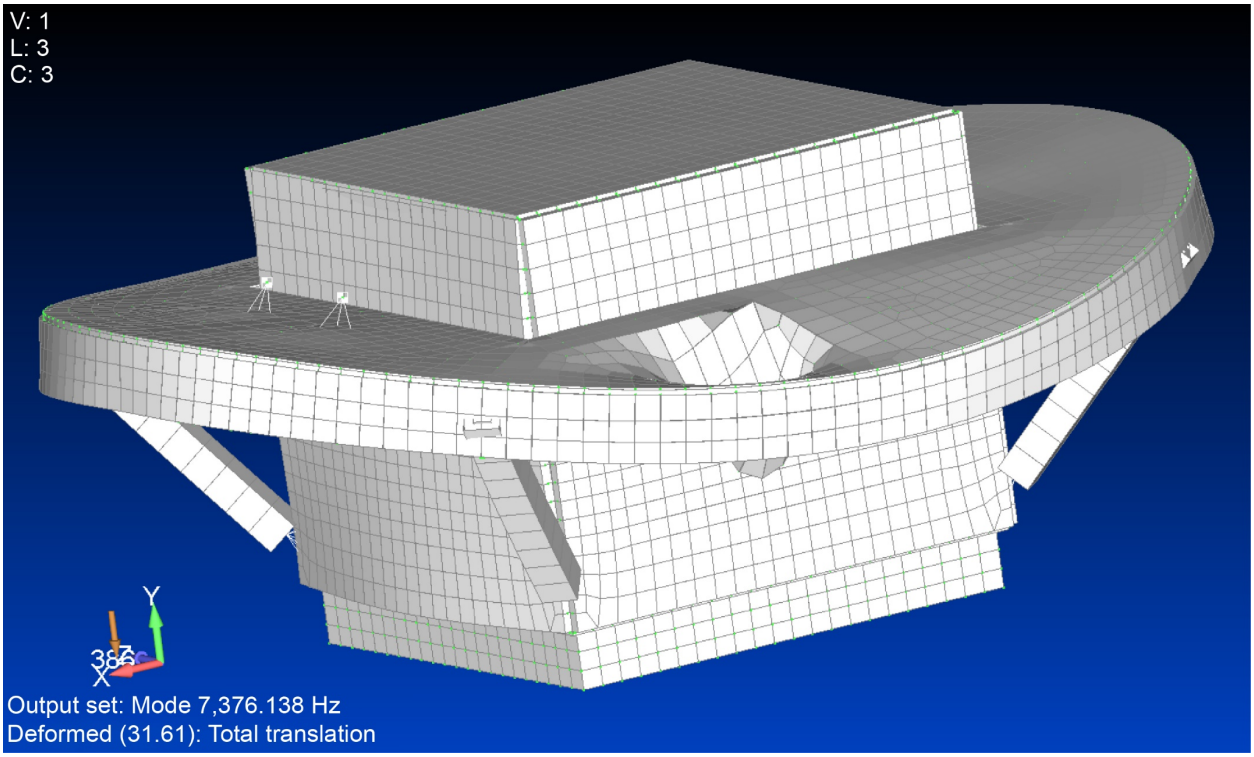

Figure 42.—Lander at first modal frequency of 376 Hz. Section of drag flap is first area to show significant resonance.

TABLE 30.—LANDER MODAL FREQUENCIES

Mode	Frequency, Hz
1	376
2	433
3	454
4	580
5	610
6	653
7	717
8	725
9	757
10	762

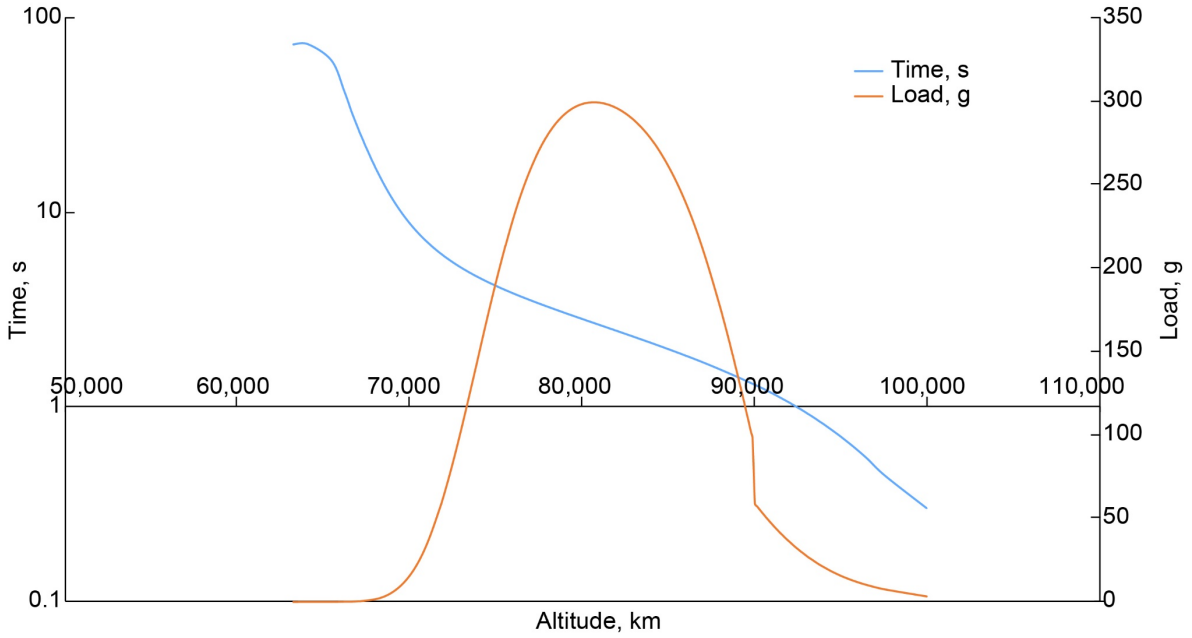

Figure 43.—Acceleration of Lander upon atmospheric entry as function of time and altitude.

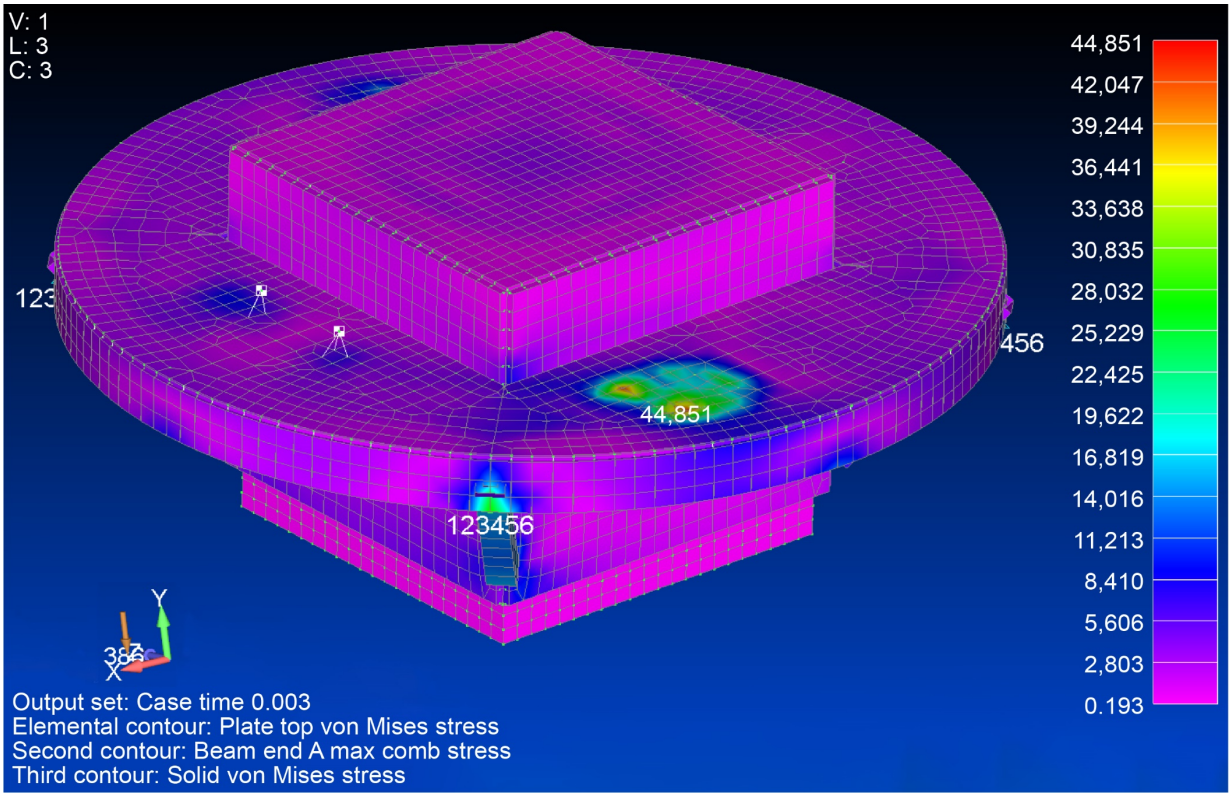

Figure 44.—Lander with stress contour (in psi) resulting from transient dynamic analysis. Maximum stress of 44,851 psi (309 MPa) is shown.

An additional installation mass was added for each subsystem in the mechanisms section of the structures subsystem. These installations were modeled using 4 percent of the CBE dry mass of each of the subsystems. The 4-percent magnitude for an initial estimate compares well with values reported by Heineman (1994) (Ref. 25) for various manned systems. This is to account for attachments, bolts, screws, and other mechanisms necessary to attach the subsystem elements to the bus structure, and not book kept in the individual subsystems. An 18-percent growth margin was applied to the resulting installation mass. These margins are placed onto the subsystem elements.

4.9.12 Lander Structures and Mechanisms Risk Inputs

Excessive g loads or impact from a foreign object or harsh landing may cause too much deformation, vibration, or fracture of sections of the support structure. Consequences include lower performance from mounted hardware to loss of mission. The likelihood is 3 of 5. Consequences to cost is 4 of 5, schedule is 4 of 5, performance is 4 of 5, and safety is 1 of 5.

To mitigate risks, the structure is to be designed to NASA standards to withstand expected environment and g loads, a given impact, and to have sufficient stiffness and damping to minimize issues with vibrations. Transport and mission trajectories are to be planned to minimize the probability of excessive loads and impact with foreign objects.

4.9.13 Lander Structures and Mechanisms Recommendation

A higher fidelity stress analysis with FEA is recommended. Reevaluation and refinement of the assumed damping coefficient is also recommended. Further improvements in stiffness and reduced mass may be accomplished with the use of orthogrid or isogrid panels.

4.10 Thermal Control

The thermal system for the V-BOSS mission involved three different phases and associated vehicles. These included

- The thermal control of the orbiting data relay satellite
- Atmospheric entry aeroshell
- Thermal control of the surface probe with housed science instruments

4.10.1 Orbiting Spacecraft (S/C)

The Venus orbiting relay satellite has a conventional thermal control system consisting of the following components (see MEL in Table 31):

- Radiator panel
- Heat pipes and cold plates for collecting and moving heat to the radiator
- Multilayer insulation (MLI)
- Heaters
- Temperature sensors, controllers, switches, data acquisition
- Thermal paint and coatings

Some of these systems are shown in Figure 45 on the orbiting S/C illustration.

TABLE 31.—ORBITER THERMAL MASTER EQUIPMENT LIST

Description	Quantity	Unit mass, kg	Basic mass, kg	Growth, %	Growth, kg	Total mass, kg
Orbiter	-	----	175.44	8.9	15.70	191.13
Thermal control (nonpropellant)	-	----	10.37	18.0	1.87	12.23
Active thermal control	-	----	0.67	18.0	0.12	0.79
Heaters	2	0.20	0.40	18.0	0.07	0.47
Thermal controller	1	0.20	0.20	18.0	0.04	0.24
Thermocouples	7	0.01	0.07	18.0	0.01	0.08
Passive thermal control	-	----	4.08	18.0	0.73	4.81
Heat sinks	2	0.14	0.28	18.0	0.05	0.33
Heat pipes	2	0.43	0.85	18.0	0.15	1.01
Spacecraft multilayer insulation	1	2.95	2.95	18.0	0.53	3.48
Semipassive thermal control (cruise deck and internal)	-	----	5.62	18.0	1.01	6.63
Thermal switches	2	0.10	0.20	18.0	0.04	0.24
Radiator	1	5.42	5.42	18.0	0.98	6.40

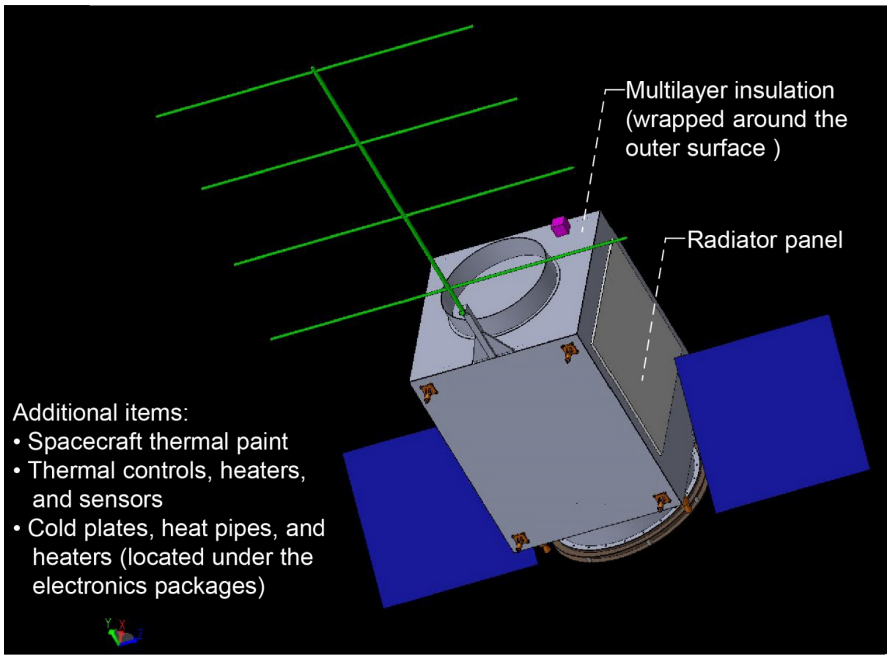

Figure 45.—Orbiting spacecraft thermal components.

TABLE 32.—ORBITING SPACECRAFT (S/C)
RADIATOR SPECIFICATIONS

Radiator characteristic	Value
Radiator solar absorptivity	0.14
Radiator emissivity	0.84
Maximum radiator angle to the Sun	30°
Average view factor to Earth when in LEO[a] operation	0.27
Average view factor to S/C SAs[b]	0.20
Nominal operating temperature	300 K
Power dissipated	120 W
Radiator area	0.65 m^2

[a]Low Earth orbit.
[b]Solar arrays.

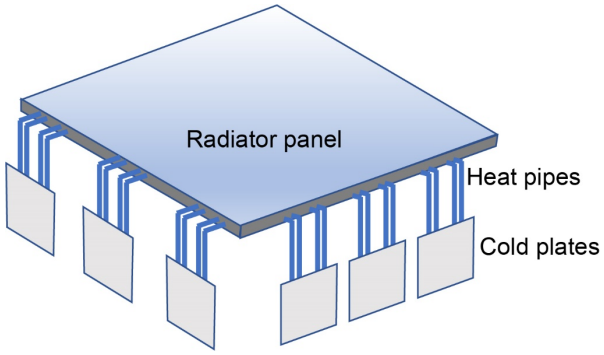

Figure 46.—Radiator panel with integral heat pipes and cold plates.

The radiator on the orbiting S/C is body mounted, as shown in Figure 45. There is MLI between the radiator and S/C body to help prevent heat leak back into the S/C. The radiator is connected to the cold plates with heat pipes to move heat from the interior to the radiator. The radiator sizing was based on an energy balance analysis of the area needed to reject the identified heat load to space. From the area, a series of scaling equations were used to determine the mass of the radiator. The radiator was sized to remove the waste heat from the S/C during worst-case (warm) operational conditions that occur in Venus orbit. The specifications for the radiator are given in Table 32.

Since the shadow periods were limited and the S/C is operating in a warm environment less than 1 AU, louvers were not utilized as part of the radiator design.

To move the heat from the electronics to the radiator, a series of cold plates and heat pipes are utilized. An example of this arrangement is shown in Figure 46.

This example, in Figure 46, shows the integration of a body-mounted radiator with heat pipes and cold plates. The electronics packages or other heat-generating devices are mounted to the cold plates and heat pipes transfer the heat generated to the backside of the radiator. The exposed radiator side rejects the heat to space. The glossy surface of the radiator is due to coatings that are applied to reflect sunlight from the radiator. This reduces the heat load on the S/C from direct sunlight as well as Venus's albedo.

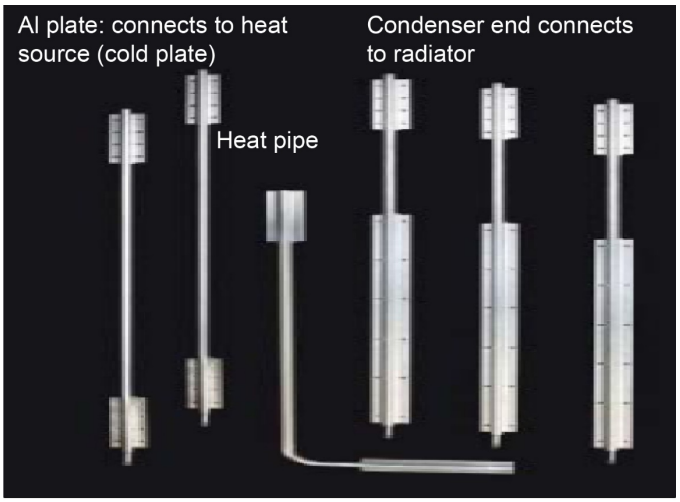

Figure 47.—Example of cold plates with integral heat pipes (Ref. 26).

The cold plates are constructed from Al and have the heat pipes integrally connected to the radiator. For this design, two 0.1-m by 0.1-m by 5-mm-thick electronics cold plates were used. An example of these is shown in Figure 47. The cold plates also incorporated heaters in order to maintain the desired electronics temperature throughout the mission.

To insulate the S/C to maintain thermal control, MLI was used to cover the exterior exposed portion of the S/C. The insulation was analyzed to determine the required number of layers and the corresponding mass and heat loss needed to maintain the average 300 K interior S/C temperature. A tradeoff was performed between the insulation mass and the required heater power. The insulation model was based on radiation heat transfer analysis of the heat transfer from the S/C through the insulation to space. A mission worst-case 1-AU thermal environment was used to size the insulation and determine the heat loss. A 5-percent passthrough area was assumed for the insulation heat loss.

MLI is constructed of a number of layers of metalized material with a nonconductive spacer between the layers, as illustrated in Figure 48. The metalized material has a low absorptivity, which resists radiation heat transfer between the layers. The low-conductivity spacers keep the layers from touching limiting conduction through the layers.

For this S/C design, 25 layers of MLI were utilized. The layers consisted of metalized Mylar® film (DuPont Teijin Films) and silica mesh spacers. In addition to the insulation, heat is also lost from the S/C through items that pass through the insulation such as wires or structural components. Also, heat can be lost out of the radiator at times when the radiator is not needed to reject excess heat. A summary of the total heat loss from the S/C for operation in shadow at LEO is given in Table 33.

TABLE 33.—SPACECRAFT HEAT LOSS SUMMARY

Heat loss source	Value
Insulation (multilayer insulation)	1.0 W
Passthrough and insulation seams	6.1 W
Radiator	17.8 W
Total	24.9 W

To maintain the internal temperature, waste heat from the internal components or electric heaters are used to provide heat to the S/C interior if needed. Strip heaters were used to provide heat to the components within the payload package. Flat plate heaters were used on the cold plates to provide heat to the electronics if necessary. Heaters are located on each cold plate.

Thermal control is accomplished through the use of a network of thermocouples whose output is used to control the power to the various heaters. A data acquisition and control computer is used to operate the thermal system. Under normal operating conditions, and for the S/C location throughout most of the mission, no heater power should be required. At times where there is very little internal heat being generated, heater power on the order of less than 10 W may be required. At shadow conditions at the beginning of the mission, heater power of 25 W will be required to compensate for the heat loss listed in Table 33.

4.10.2 Aeroshell

The initial mission phase is the transition from Earth to Venus. During this phase, the satellite has a controlled thermal system, whereas the aeroshell with the surface Lander does not. The orbiting S/C's, or satellite's, thermal system was designed to maintain the internal components of the Orbiter within their desired temperature range of 260 to 310 K throughout the mission. Since the surface probe and aeroshell were not thermally controlled, their temperature had a larger variation during the transit between Earth and Venus. This transition and corresponding equalization temperatures during the transfer are shown in Figure 49.

Thermal paint on the aeroshell was used to set the emissivity (0.65) and absorptivity (0.30) of the aeroshell to help minimize the temperature swing during transit.

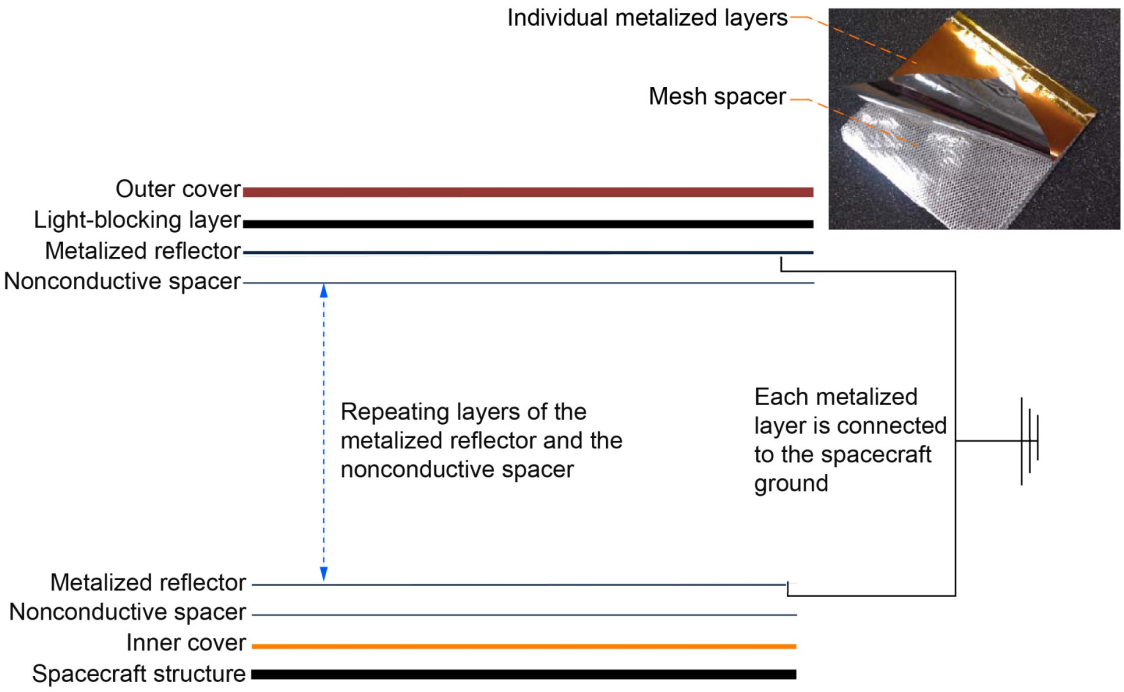

Figure 48.—Multilayer insulation layup (Ref. 27) illustration.

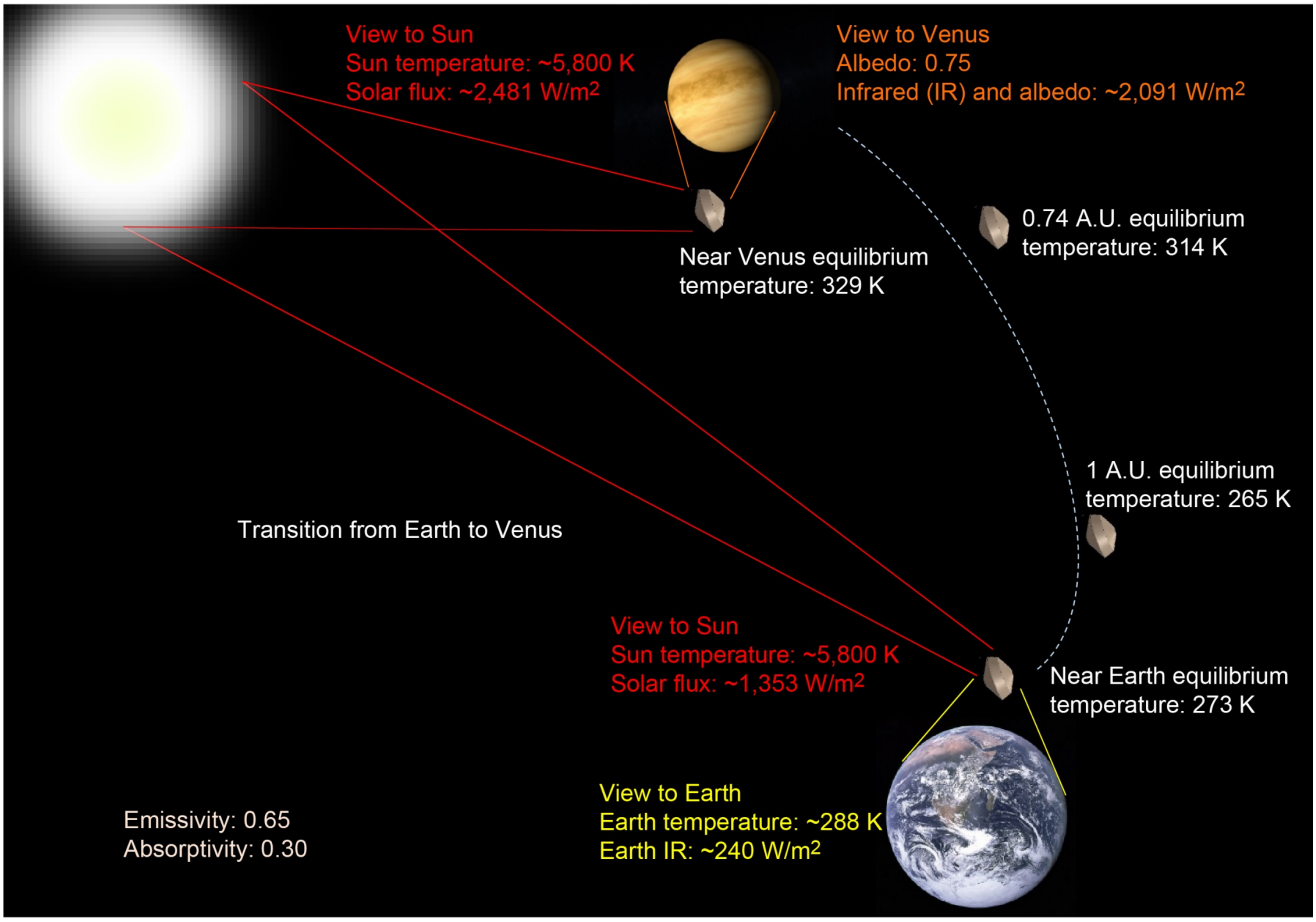

Figure 49.—Aeroshell temperature in transit from Earth to Venus.

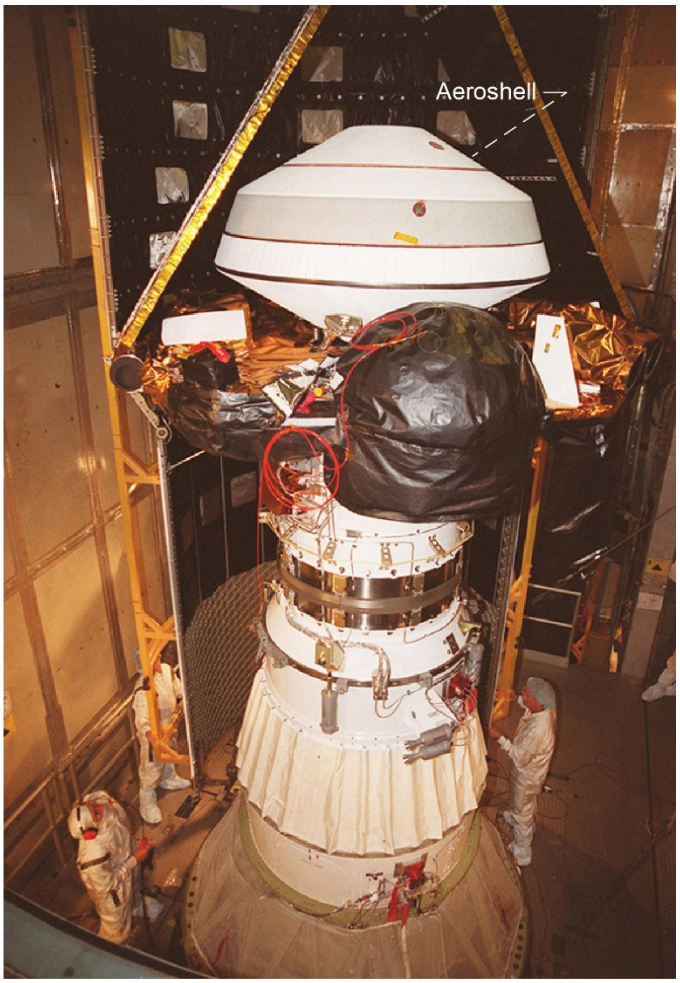

Figure 50.—Genesis aeroshell (Ref. 28).

Prior to entering orbit around Venus, the surface probe is released and enters the Venus atmosphere at the interplanetary orbital velocity of 11 km/s. The aeroshell, consisting of the heat shield and the back shell, was used to slow down the probe upon entry and absorb the heat dissipated during the atmospheric entry. Once within the atmosphere, the backshell is used to help slow the descent of the probe. The probe is released and impacts the surface upon landing.

The aeroshell utilized for entry into the Venus atmosphere was based on the Genesis aeroshell design, shown in Figure 50. The aeroshell was scaled from the 1.52 m diameter used by the Genesis mission to 0.5 m diameter. The aeroshell dimensions are shown in Figure 15.

The heat shield is constructed of 1.5 cm of phenolic impregnated carbon ablator (PICA) ablative insulation material with a 2.5-cm-thick Ti honeycomb backing. The ablation thickness of the heat shield was calculated to be 0.8 mm. This was consistent with the ablation levels experienced with the Pioneer Venus probes. The backshell of the aeroshell was constructed of 1.5-mm-thick Ti.

To determine the descent time, the drag on the aeroshell was estimated based on the atmospheric properties as it descended through the atmosphere. The initial entry of the aeroshell is given by Figure 51. This figure shows the time and velocity versus altitude. The entry begins at a 100-km altitude. The entry probe takes approximately 20 s to reach subsonic speed at an altitude of 67 km. Any time after this point, the drag flaps can be released and the heat shield can be dropped.

The subsequent entry and descent to the surface of Venus is illustrated in Figure 52.

The aeroshell remains intact during the initial part of the descent. Its drag coefficient is estimated to be 0.8 and it has a cross-sectional area of approximately 0.2 m^2. After 25 min 20 s at an altitude of 25 km, the drag flaps are deployed on the backshell and the heat shield is dropped. The drag coefficient with the flaps deployed and the heat shield removed increases to 1.2 with a total cross-sectional area of 0.33 m^2. After another 12 min and descent to 20 km, the Lander is released from the backshell. The drag coefficient of the Lander remains at 1.2 with a cross-sectional area of 0.13 m^2. The descent of the Lander from 20 km to the surface takes 48 min 48 s. The total descent time from entry to the surface is 85 min 8 s.

Based on the estimated wind speeds during descent, the total potential drift of the Lander during descent is 112.5 km.

4.10.3 Lander Thermal Control

The battery, electronics, and other heat-generating devices will operate at the ambient surface conditions. Therefore, no active cooling will be utilized. Any excess heat generated will be dissipated to the atmosphere through the use of finned heat sinks on the Lander surface. The convective heat transfer coefficient on the surface is estimated to vary between 17 and 65 W/m·K, depending on the wind speed of 0.1 to 0.5 m/s.

Once on the surface, the probe does not have an active thermal control system. The components on the probe are designed to operate within the ambient Venus environment. Natural convection is used to remove any excess heat that is generated during operation on the surface.

The thermal control components were sized for the different phases of the mission. The mass breakdown of the thermal system for the EDL system is shown in Table 34.

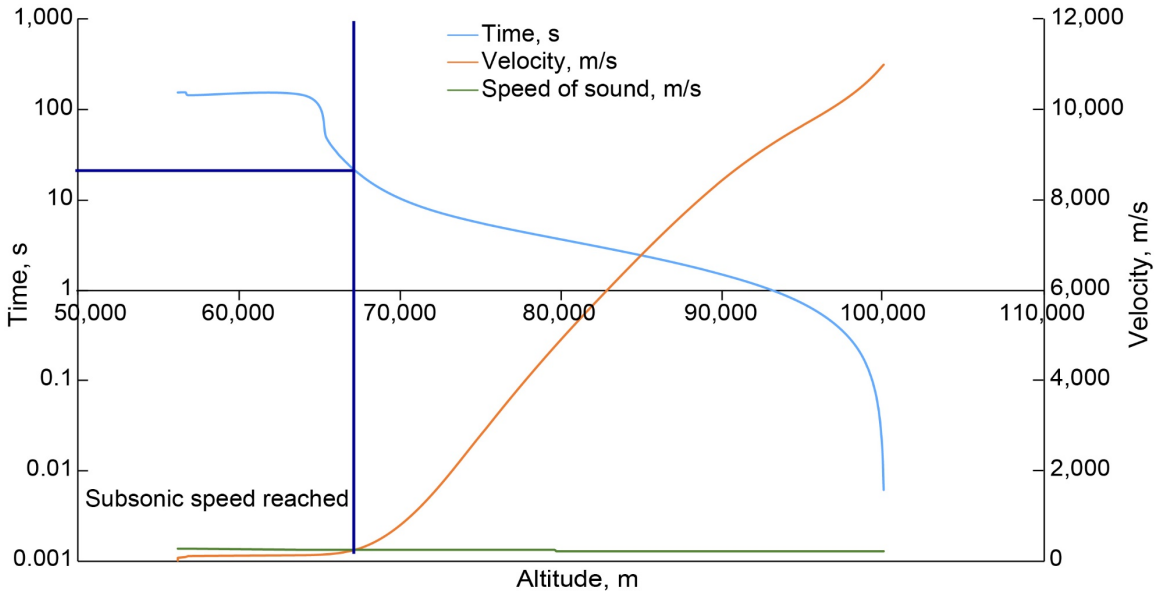

Figure 51.—Initial Venus entry profile for Bridge Lander.

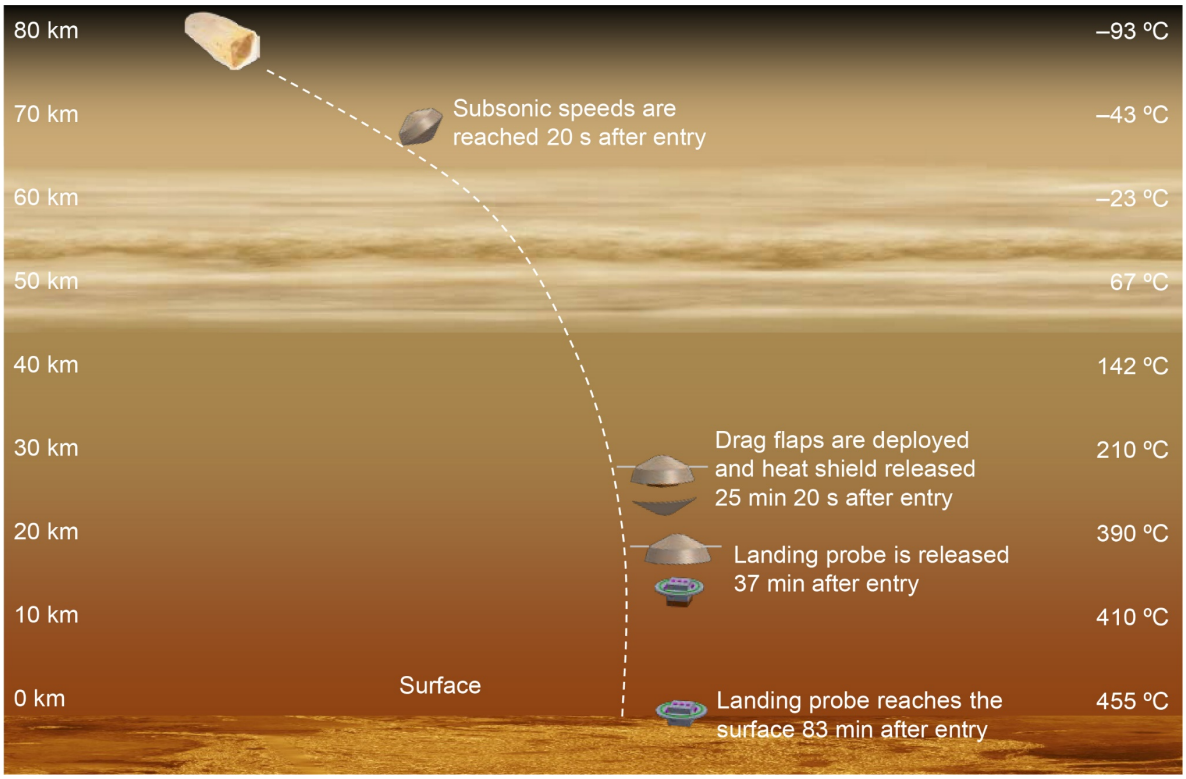

Figure 52.—Entry and descent to Venus's surface illustration.

TABLE 34.—ENTRY, DESCENT, AND LANDING (EDL) THERMAL MASTER EQUIPMENT LIST

Description	Quantity	Unit mass, kg	Basic mass, kg	Growth, %	Growth, kg	Total mass, kg
EDL	-	-----	8.82	18.3	1.62	10.44
Thermal control (nonpropellant)	-	-----	8.47	18.0	1.52	10.00
Passive thermal control	-	-----	8.47	18.0	1.52	10.00
Backshell timing computer	1	0.07	0.07	18.0	0.01	0.08
Thermal coatings/paint	1	.09	.09	18.0	.02	.11
Aeroshell support structure	1	.25	.25	18.0	.04	.29
Heat shield	1	4.53	4.53	18.0	.81	5.34
Backshell	1	1.67	1.67	18.0	.30	1.97
Backshell drag flaps	1	1.25	1.25	18.0	.23	1.48
Backshell separation system	1	.17	.17	18.0	.03	.20
Heat shield separation system	1	.45	.45	18.0	.08	.53

5.0 Cost and Risk

Cost estimates for the V-BOSS mission were created under the following ground rules and assumptions. The scope of the mission estimate is Phases A to D, including the Lander, EDL, Orbiter, and payload and all associate mission costs with the following exceptions. The estimates do not include technology development up to TRL 6, Iris communication components, Phase E, Education and Public Outreach (WBS 11), and fuel. This mission is assumed to use protoflight development and all Orbiter thrusters are assumed to be TRL 9 by the time this mission is being developed (all other TRL assumptions match those listed in the subsystem designs). Reserves are carried at 25 percent and launch vehicle/services (WBS 8) are assumed to be provided at no cost to the mission. The Lander, EDL, and Orbiter are assumed to be contracted to a major aerospace firm; a 10-percent fee is included. All hardware is assumed to be the responsibility of the contractor, with the exception of the Iris communication components.

The estimates were developed using a combination of in-house cost estimating relationships (CERs), mainly developed using minimum unbiased percentage error (MUPE) regression, and an off-the-shelf cost estimation package, PRICE True Planning. Quantitative risk analysis was performed using Monte Carlo simulation driven by the input parameter uncertainties and error statistics of the CERs. Costs are presented in fiscal year 2018 dollars (in millions) and the point estimate shown is the mode (most likely) of the resulting lognormal distribution, approximately the 35th percentile. Coefficient of variance (standard deviation/mean) of the estimate is approximately 44 percent.

The point estimate of the total mission, including 25 percent reserves, is $201M. Of that total, the science payloads on both the Obiter and Lander make up $10M and the flight system (including Orbiter, Lander, and EDL) make up $86M. Further details of the costs can be seen in Table 35. Additionally, the results of the quantitative risk analysis can be found in Figure 53 This figure shows an additional $36M would need to be added to the point estimate to reach the 70th percentile.

TABLE 35.—MISSION COST SUMMARY

Mission cost summary	Fiscal year 2018, $M
Phase A	4
Phase B/C/D	157
1 Program Management	10
2 Systems Engineering	13
3 Safety and Mission Assurance	5
4 Science	6
5 Payload	10
5.1 Lander Payload	4
5.2 Orbiter Payload	6
6 Flight System	86
6.1 Lander	19
6.2 Entry, Descent, and Landing	8
6.3 Orbiter	59
7 Mission Operations	13
9 Ground System	6
10 Systems Integration and Testing	8
Phases A to D mission cost	161
Reserves (25 percent)	40
Total cost with reserves	201

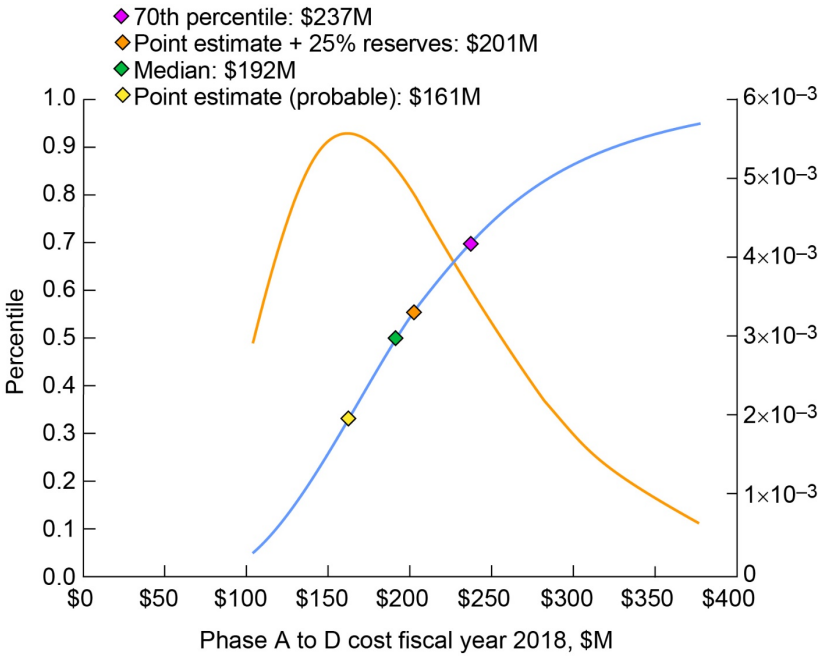

Figure 53.—Mission cost summary and cost curve (constant fiscal year 2018 in millions of dollars).

Appendix A.—Nomenclature

ACS	Attitude Control System
AD	analog-to-digital
AD&C	Attitude Determination and Control
AFRL	Air Force Research Laboratory
AIAA	American Institute of Aeronautics and Astronautics
ADN	ammonium dinitramine
AOP	argument of periapsis
APXS	alpha particle x-ray spectrometer
ARU	Array Regulator Unit
BCDU	Battery Charge-Discharge Unit
BOL	beginning of life
C_3	characteristic energy
C&DH	Command and Data Handling
CAD	computer-aided design
CBE	current best estimate
CER	cost estimating relationship
CG	center of gravity
CONOPS	concept of operations
COTS	commercial off-the-shelf
cPCI	compact peripheral component interconnect
DA	digital-to-analog
DC	direct current
DOD	depth of discharge
DSN	Deep Space Network
ECC	eccentricity
ECLSS	Environmental Control and Life Support System
EDL	entry, descent, and landing
EELV	Evolved Expendable Launch Vehicle
EGA	Earth gravity assist
EOL	end of life
EP	Electrical Power
ESA	European Space Agency
ESPA	Evolved Expendable Launch Vehicle Secondary Payload Adapter
FEA	finite element analysis
fO_2	oxygen fugacity
GEER	Glenn Extreme Environments Rig
GN&C	Guidance, Navigation and Control
GPIM	Green Propellant Infusion Mission
GPIO	general-purpose input/output
GW	gravity wave
HAN	hydroxyl ammonium nitrate
HOTTech	Hot Operating Temperature Technology
I2C	Inter-Integrated Circuit
IMAP	Interstellar Mapping and Acceleration Probe
IMU	inertial measurement unit
INC	inclination
IR	infrared
I_{sp}	specific impulse
LGA	lunar gravity assist
LLISSE	Long-Lived In-Situ Solar System Explorer
MatISSE	Maturation of Instruments for Solar System Exploration
MEL	master equipment list
MET	mission event time
MGA	mass growth allowance
MIREM	Multispectral Infrared Emissivity Mapper
MLI	multilayer insulation
MMPDS	Metallic Materials Properties Development and Standardization
MOI	moment of inertia
MUPE	minimum unbiased percentage error
N	Brunt-Vaisala frequency
NIR	near infrared
O	ongoing
P	potential
P&ID	piping and instrumentation diagram
PDU	Power Distribution Unit
PEL	power equipment list
PI	Principal Investigator
PICA	phenolic impregnated carbon ablator
PMAD	Power Management and Distribution
RAAN	right ascension of ascending node
RCS	Reaction Control System
RF	radiofrequency
Rx	receive
S/C	spacecraft
SA	solar array

SADA	solar array drive assembly
SAW	solar array wing
SDI	serial digital interface
SDRAM	synchronous dynamic random access memory
SEP	solar electric propulsion
SMA	semi-major axis
SMD	Science Mission Directorate
SPI	Serial Peripheral Interface
STP–5	Solar Terrestrial Probe-5
TBD	to be determined
TLI	trans-lunar injection
TRL	technology readiness level
Tx	transmit
U	zonal wind velocity
UHF	ultrahigh frequency
USAF	United States Air Force
UTC	Coordinated Universal Time
ΔV	change in velocity
UV	ultraviolet
V-BOSS	Venus Bridge Orbiter and Surface Study
VEXAG	Venus Exploration Analysis Group
VHF	very high frequency
VISE	Venus In Situ Explorer
VOI	Venus orbit insertion
WBS	work breakdown structure
XRD	x-ray diffraction

Appendix B.—Terms and Definitions

Mass: The measure of the quantity of matter in a body.

Basic mass (a.k.a. CBE mass): Mass data based on the most recent baseline design. This is the bottoms-up estimate of component mass, as determined by the subsystem leads.

Note 1: This design assessment includes the estimated, calculated, or measured (actual) mass, and includes an estimate for undefined design details like cables, multilayer insulation (MLI), and adhesives.

Note 2: The mass growth allowances (MGA) and uncertainties are not included in the basic mass.

Note 3: Compass has referred to this as current best estimate (CBE) in past mission designs.

Note 4: During the course of the design study, the Compass team carries the propellant as line items in the propulsion system in the master equipment list (MEL). Therefore, propellant is carried in the basic mass listing, but MGA is not applied to the propellant. Margins on propellant are handled differently than they are on dry masses.

CBE mass: See basic mass.

Dry mass: The dry mass is the total mass of the system or spacecraft (S/C) when no propellant is added.

Wet mass: The wet mass is the total mass of the system, including the dry mass and all of the propellant (used, predicted boiloff, residuals, reserves, etc.). It should be noted that in human S/C designs, the wet masses would include more than propellant. In these cases, instead of propellant, the design uses consumables and will include the liquids necessary for human life support.

Inert mass: In simplest terms, the inert mass is what the trajectory analyst plugs into the rocket equation in order to size the amount of propellant necessary to perform the mission delta-velocities (ΔVs). Inert mass is the sum of the dry mass, along with any unused, and therefore trapped, wet materials, such as residuals. When the propellant being modeled has a time variation along the trajectory, such as is the case with a boiloff rate, the inert mass can be a variable function with respect to time.

Basic dry mass: This is basic mass (a.k.a. CBE mass) minus the propellant or wet portion of the mass. Mass data is based on the most recent baseline design. This is the bottoms-up estimate of component mass, as determined by the subsystem leads. This does not include the wet mass (e.g., propellant, pressurant, cryogenic fluids boiloff, etc.).

CBE dry mass: See basic dry mass.

Mass growth allowance (MGA): MGA is defined as the predicted change to the basic mass of an item based on an assessment of its design maturity, fabrication status, and any in-scope design changes that may still occur.

Predicted mass: This is the basic mass plus the MGA for each line item, as defined by the subsystem engineers.

Note: When creating the MEL, the Compass team uses predicted mass as a column header, and includes the propellant mass as a line item of this section. Again, propellant is carried in the basic mass listing, but MGA is not applied to the propellant. Margins on propellant are handled differently than they are handled on dry masses. Therefore, the predicted mass as listed in the MEL is a wet mass, with no growth applied on the propellant line items.

Predicted dry mass: This is the predicted mass minus the propellant or wet portion of the mass. The predicted mass is the basic dry mass plus the MGA as the subsystem engineers apply it to each line item. This does not include the wet mass (e.g., propellant, pressurant, cryogenic fluids boiloff, etc.).

Mass margin (a.k.a. margin): This is the difference between the allowable mass for the space system and its total mass. Compass does not set a mass margin; it is arrived at by subtracting the total mass of the design from the design requirement established at the start of the design study such as allowable mass. The goal is to have a margin greater than or equal to zero in order to arrive at a feasible design case. A negative mass margin would indicate that the design has not yet been closed and cannot be considered feasible. More work would need to be completed.

System-level growth: The extra allowance carried at the system level needed to reach the 30-percent aggregate MGA applied growth requirement.

For the Compass design process, an additional growth is carried and applied at the system level in order to maintain a total growth on the dry mass of 30 percent. This is an internally agreed upon requirement.

Note 1: For the Compass process, the total growth percentage on the basic dry mass (i.e., not wet) is

Total growth = System-level growth + MGA * basic dry mass

Total growth = 30 percent * basic dry mass

Total mass = 30 percent * basic dry mass + basic dry mass + propellants

Note 2: For the Compass process, the system-level growth is the difference between the goal of 30 percent and the aggregate of the MGA applied to the basic dry mass.

MGA aggregate percent = (total MGA mass / total basic dry mass) * 100

Where total MGA mass = sum of (MGA percent * basic mass) of the individual components

System-level growth = 30 percent * basic dry mass – MGA * basic dry mass = (30 percent – MGA aggregate percent) * basic dry mass

Note 3: Since CBE is the same as basic mass for the Compass process, the total percentage on the CBE dry mass is

Dry mass total growth + dry basic mass = 30 percent * CBE dry mass + CBE dry mass.

Therefore, dry mass growth is carried as a percentage of dry mass rather than as a requirement for launch vehicle performance, and so on. These studies are before phase A and considered conceptual, so 30 percent is standard Compass operating procedure, unless the customer has other requirements for this total growth on the system.

Total mass: The summation of basic mass, applied MGA, and the system-level growth.

Allowable mass: The limits against which margins are calculated.

Note: Derived from or given as a requirement early in the design, the allowable mass is intended to remain constant for its duration.

Appendix C.—Additional Design Images

Figure C.1 to Figure C.19 show different design images from the V-BOSS.

C.1 Venus Bridge Orbiter and Surface Study (V-BOSS) Launch Stack

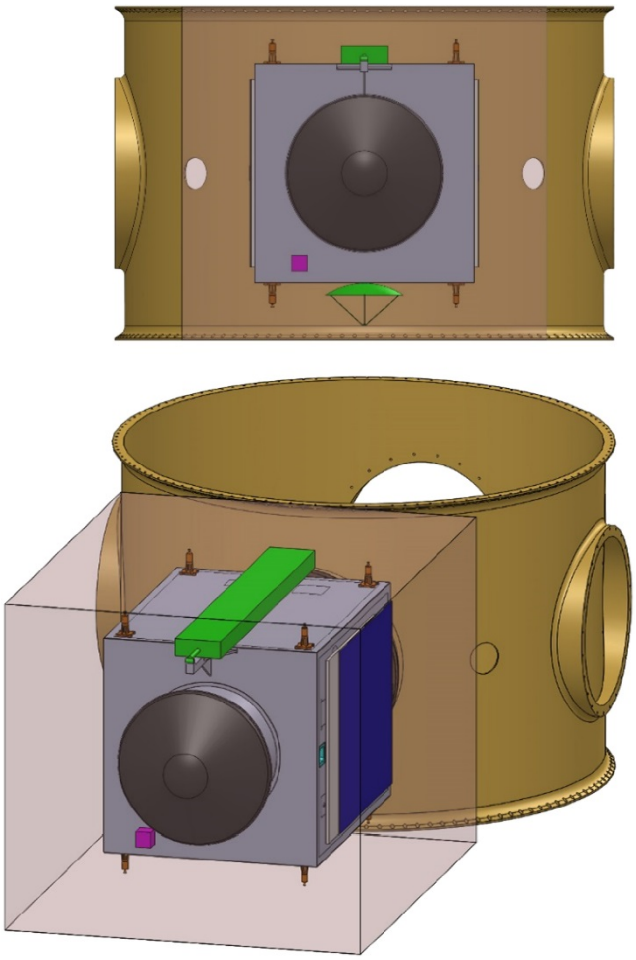

Figure C.1.—Views of V-BOSS launch stack stowed on Evolved Expendable Launch Vehicle Secondary Payload Adapter Grande.

C.2 V-BOSS Orbiter

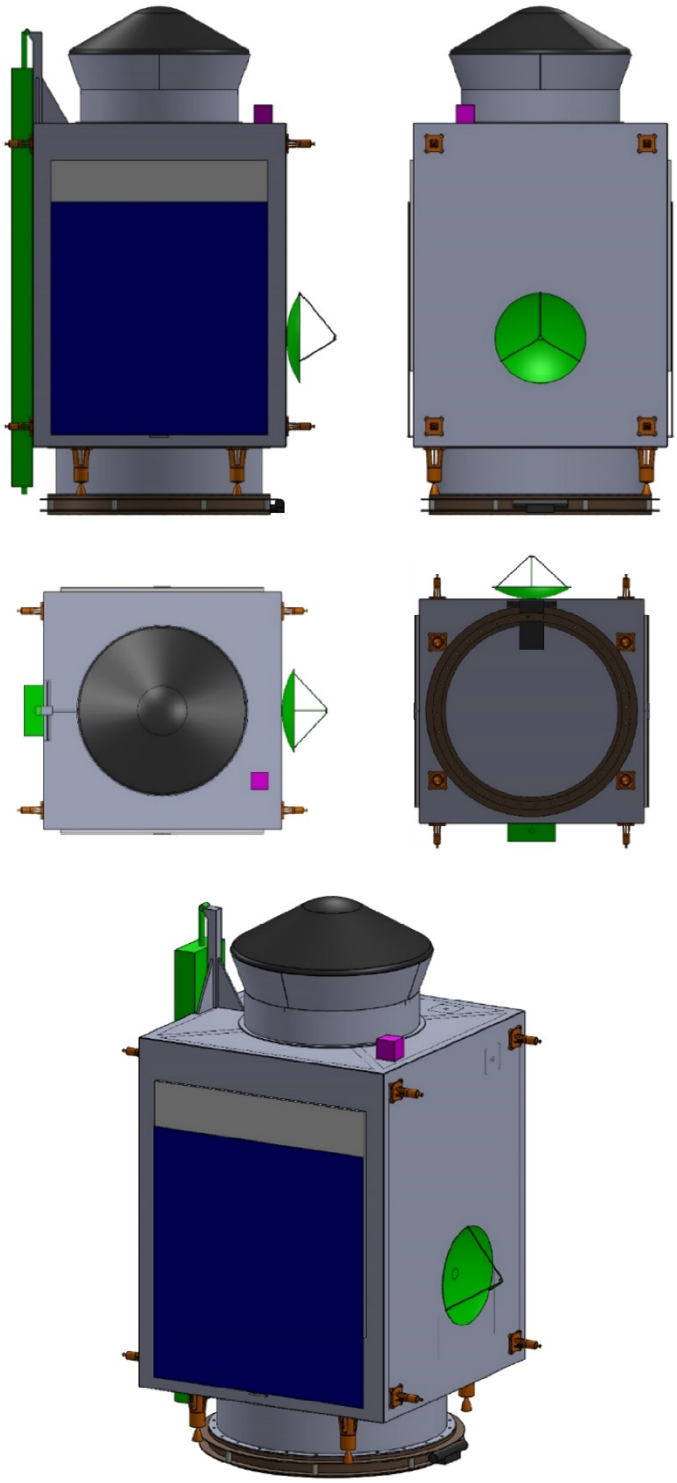

Figure C.2.—Views of Orbiter in stowed configuration.

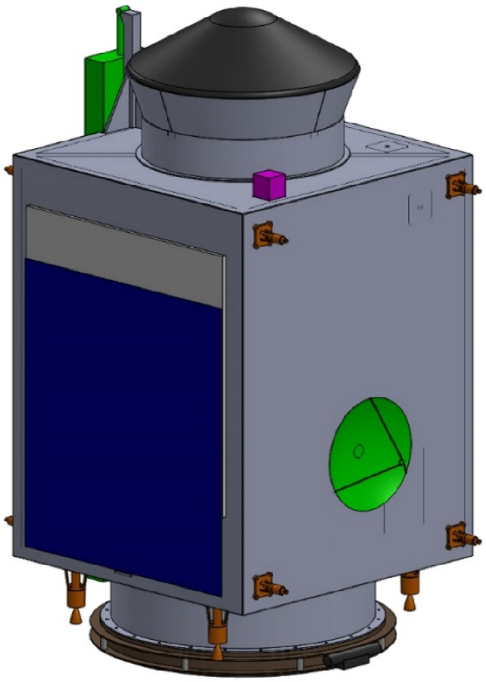

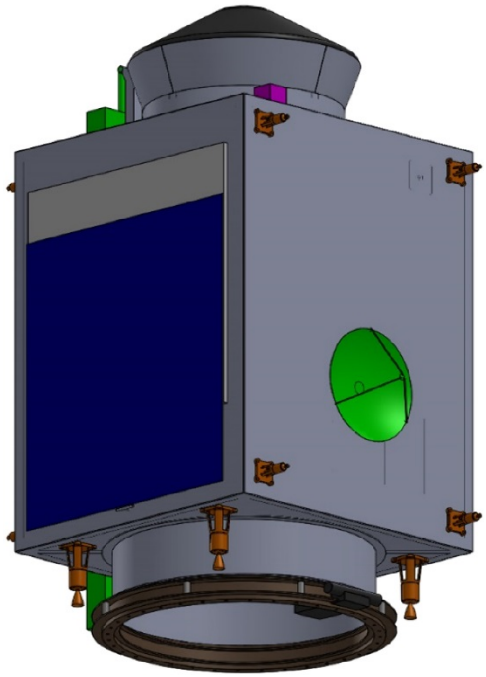

Figure C.3.—Views of stowed Orbiter.

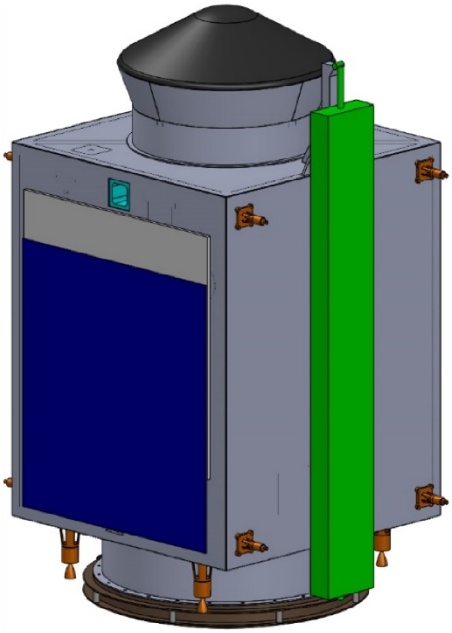

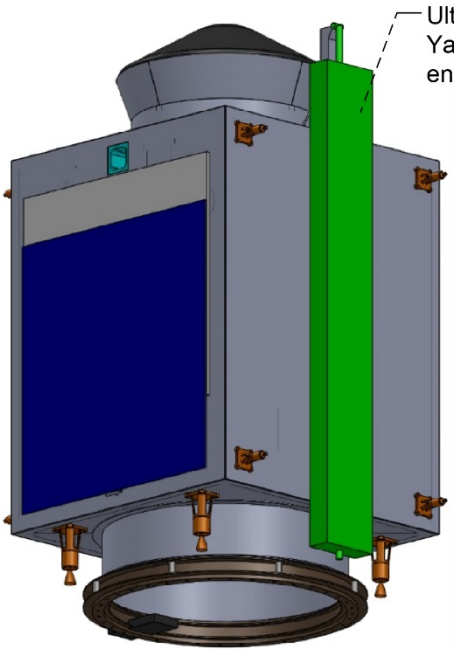

Figure C.4.—Additional views of stowed Orbiter.

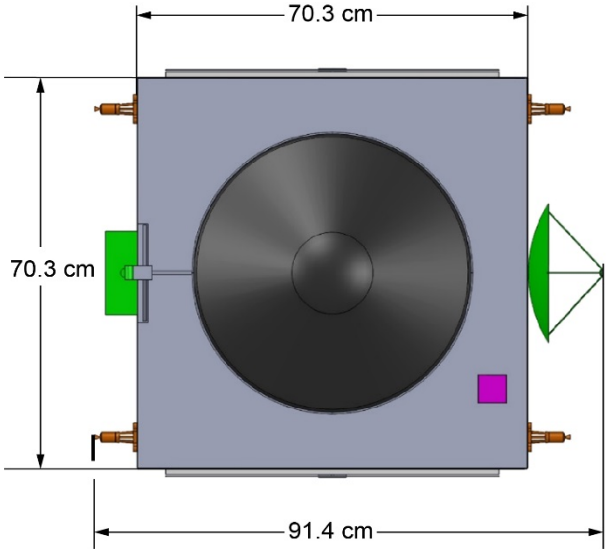

Figure C.5.—Dimensions of stowed Orbiter (top view).

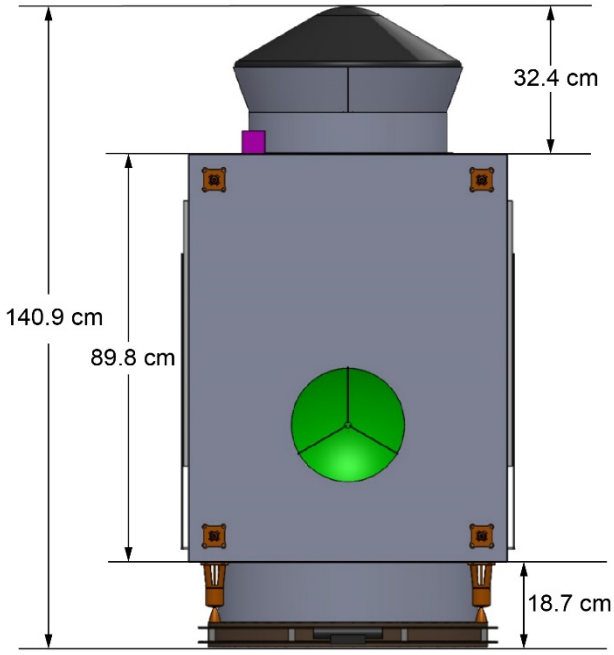

Figure C.6.—Dimensions of stowed Orbiter (side view).

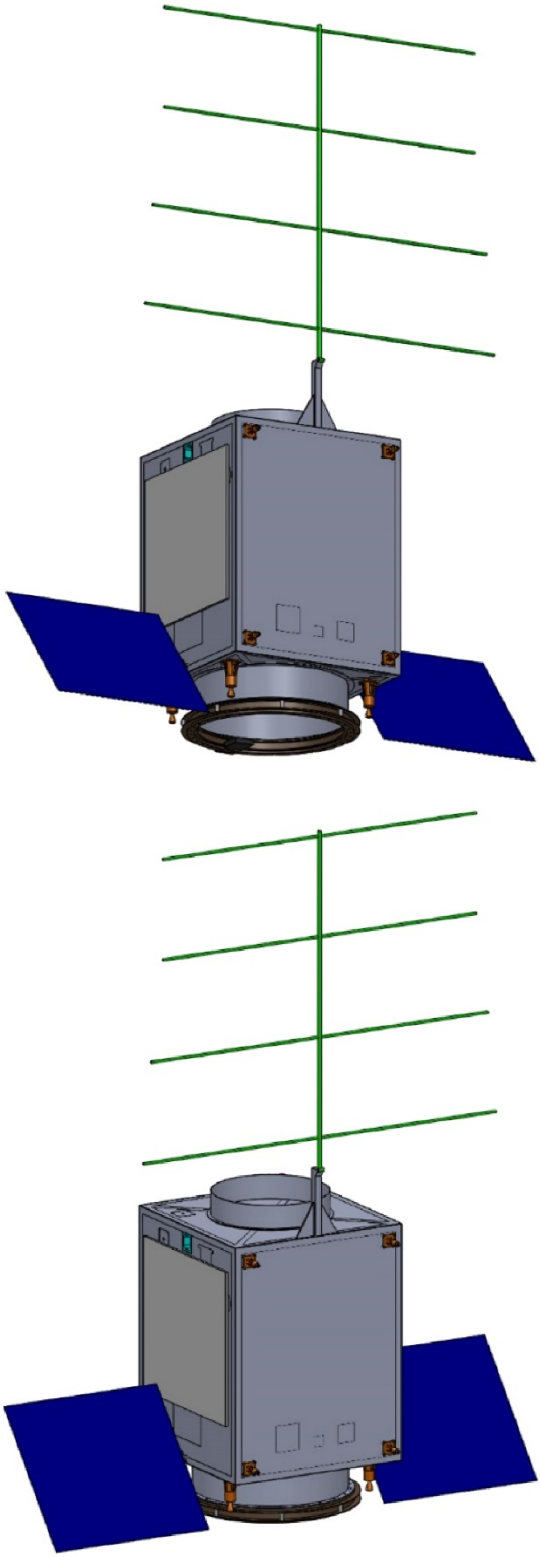

Figure C.7.—Views of deployed Orbiter.

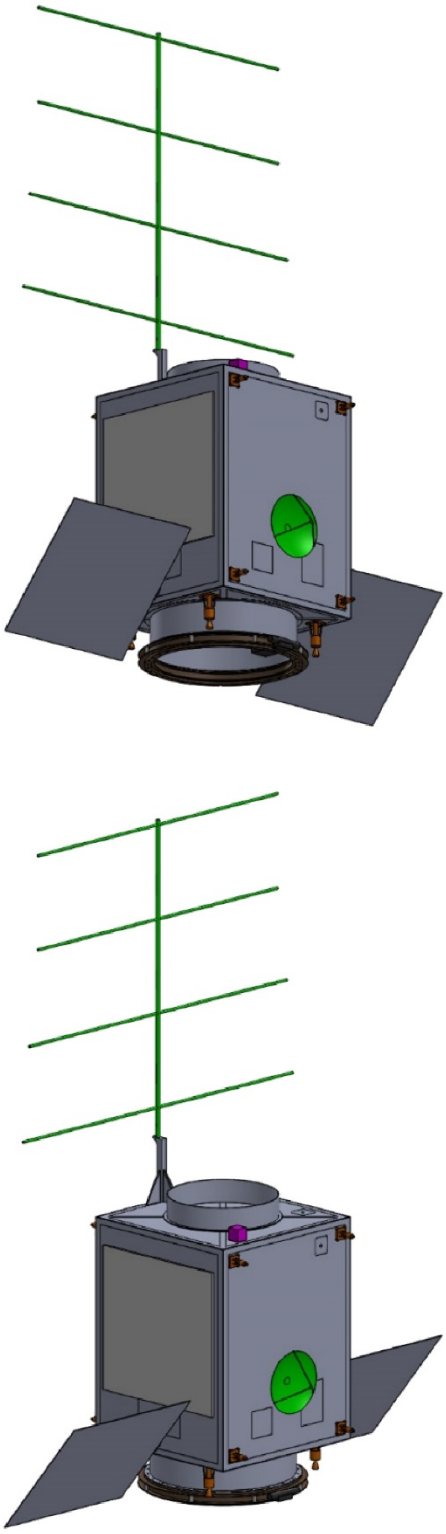

Figure C.8.—Additional views of deployed Orbiter.

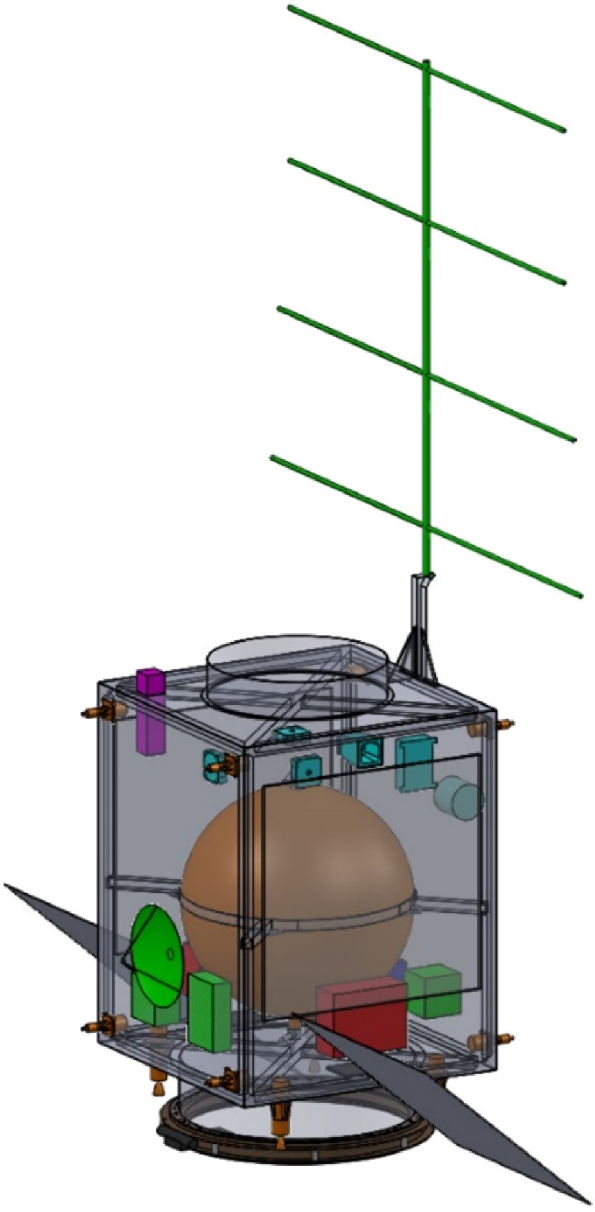

Figure C.9.—Transparent view of deployed Orbiter.

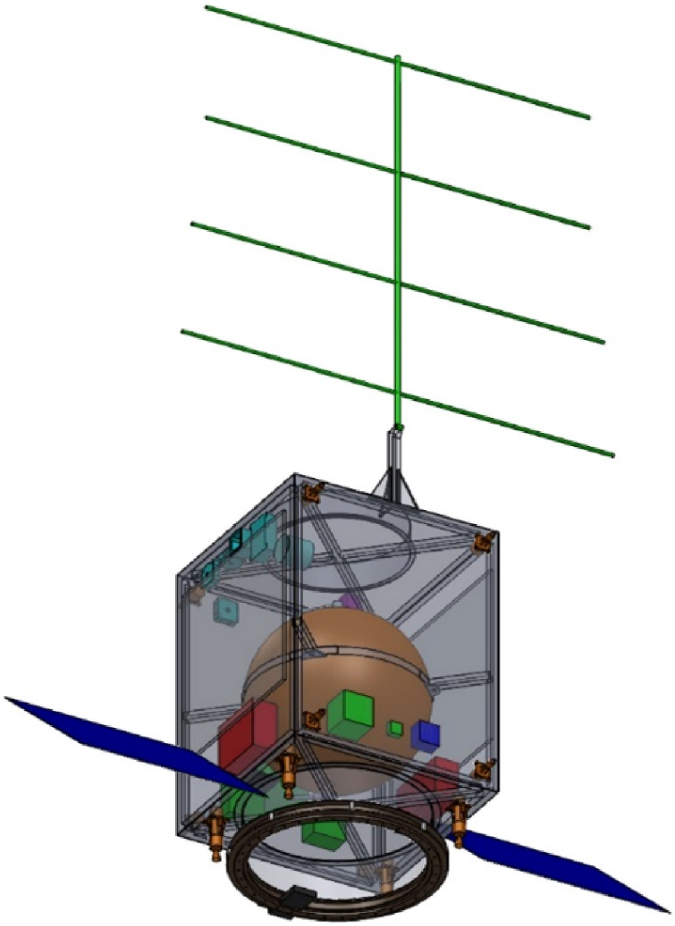

Figure C.10.—Additional transparent view of deployed Orbiter.

C.3 V-BOSS Entry, Descent, and Landing (EDL) System

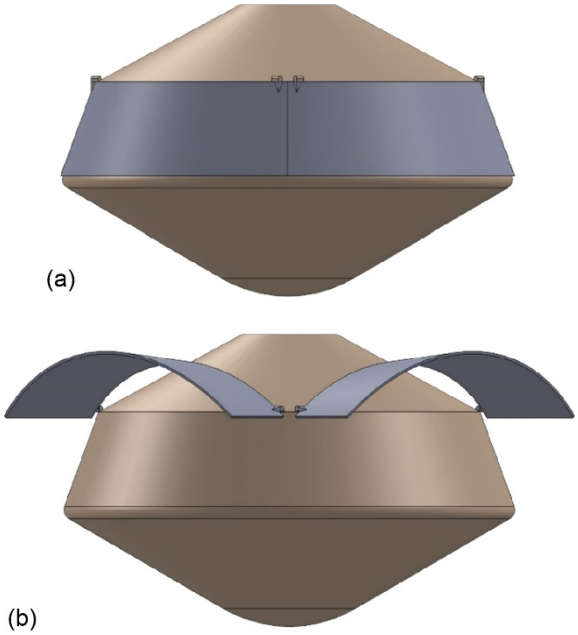

Figure C.11.—Side view of entry, descent, and landing system. (a) Stowed. (b) Deployed.

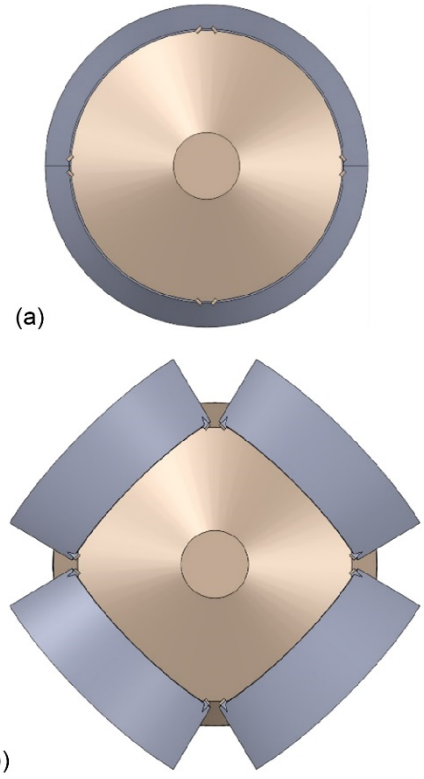

Figure C.12.—Top view of stowed and deployed entry, descent, and landing system. (a) Stowed. (b) Deployed.

C.4 V-BOSS Lander

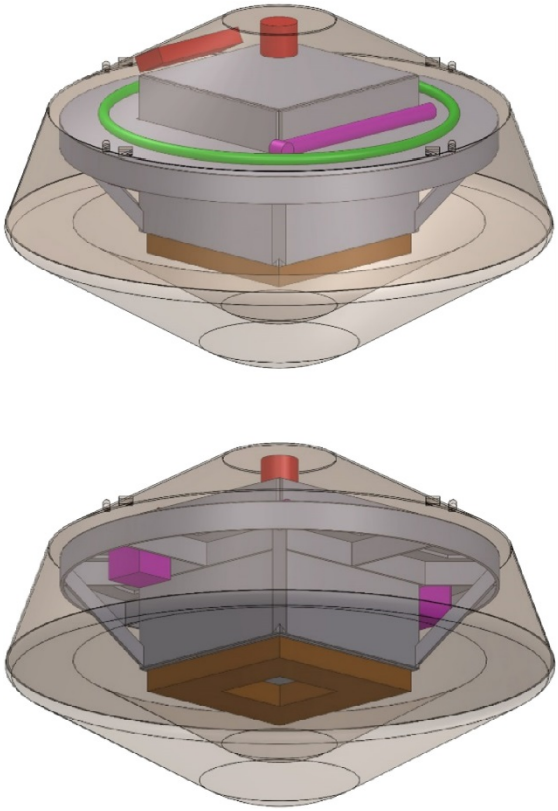

Figure C.13.—Views of Lander inside aeroshell.

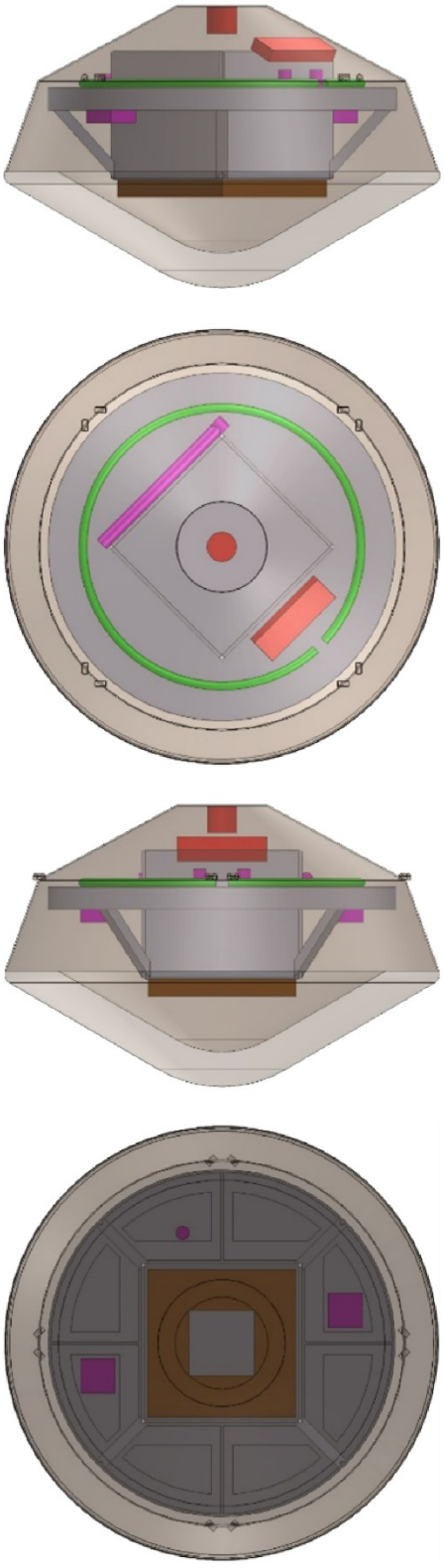

Figure C.14.—Additional views of Lander inside aeroshell.

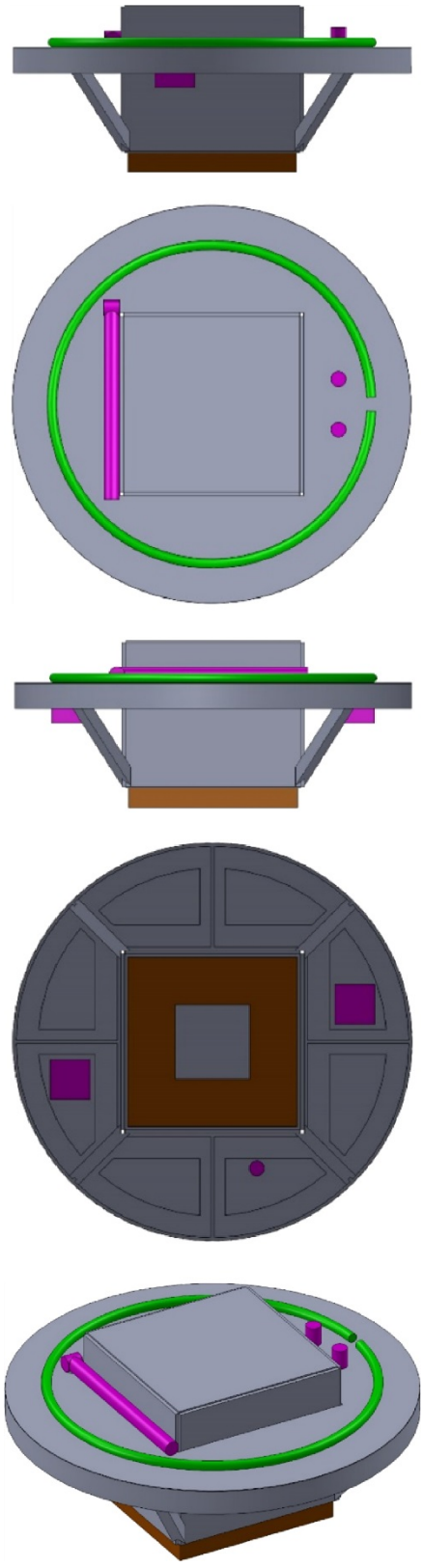

Figure C.15.—Views of stowed Lander.

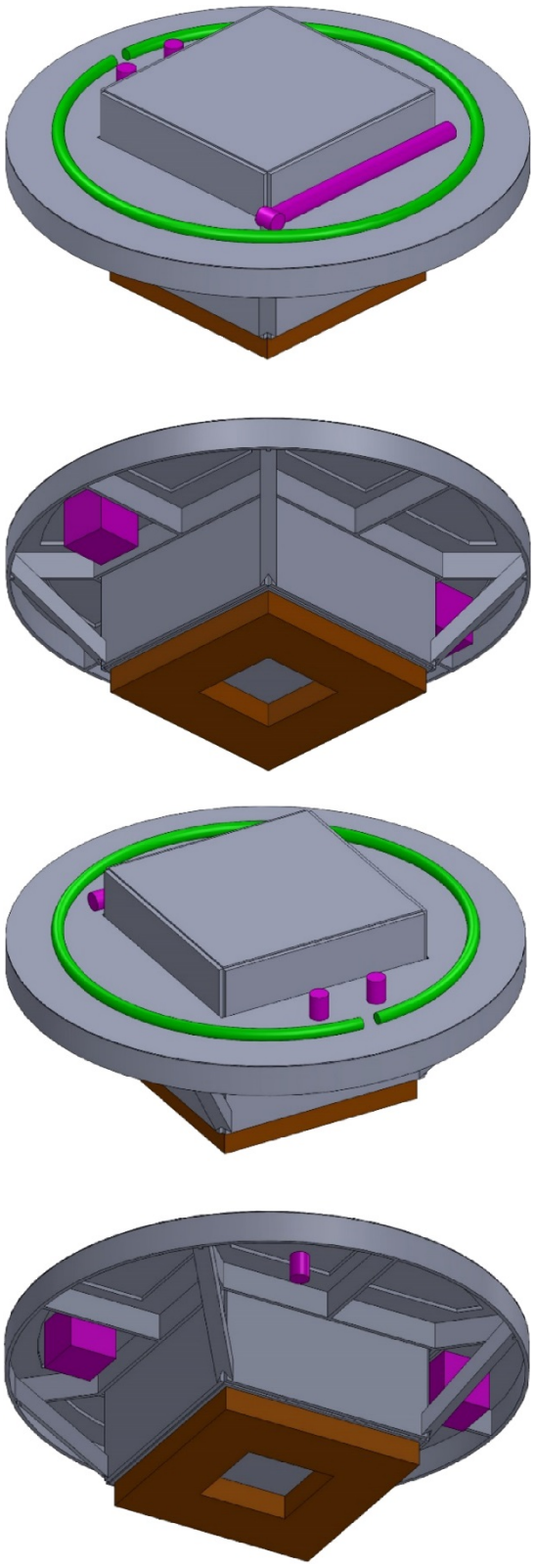

Figure C.16.—Additional views of stowed Lander.

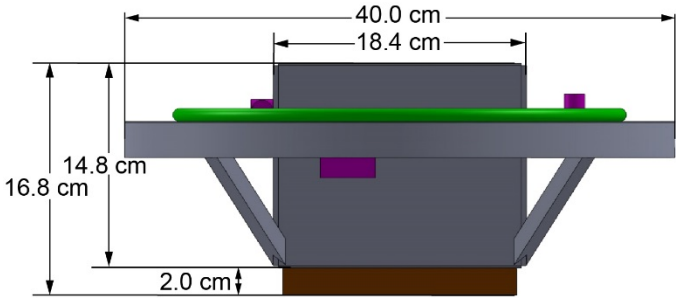

Figure C.17.—Dimensions of stowed Lander.

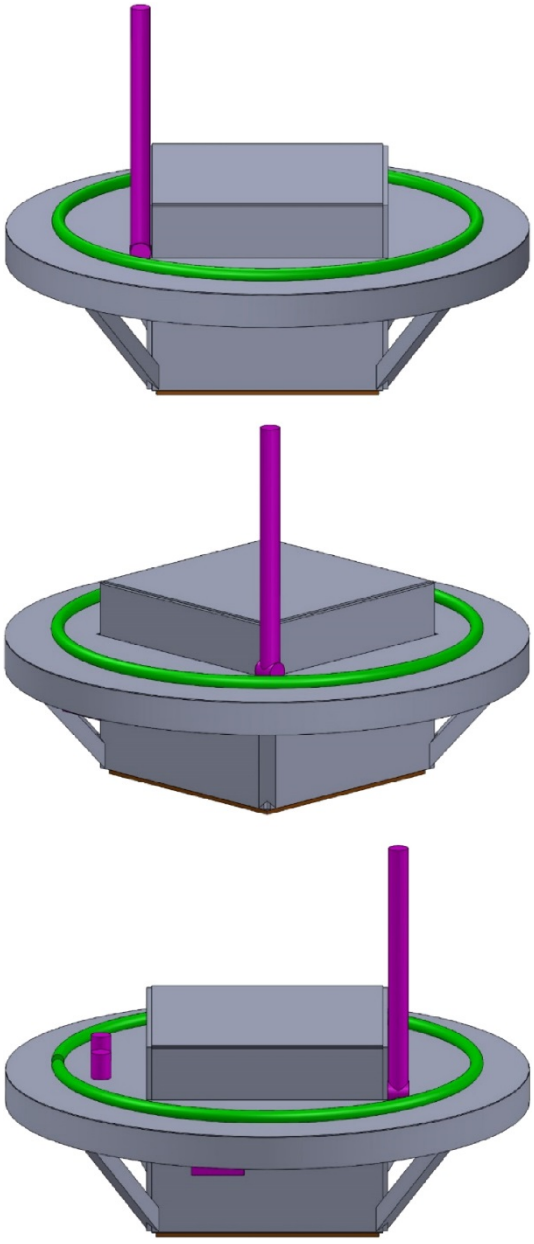

Figure C.18.—Views of deployed Lander.

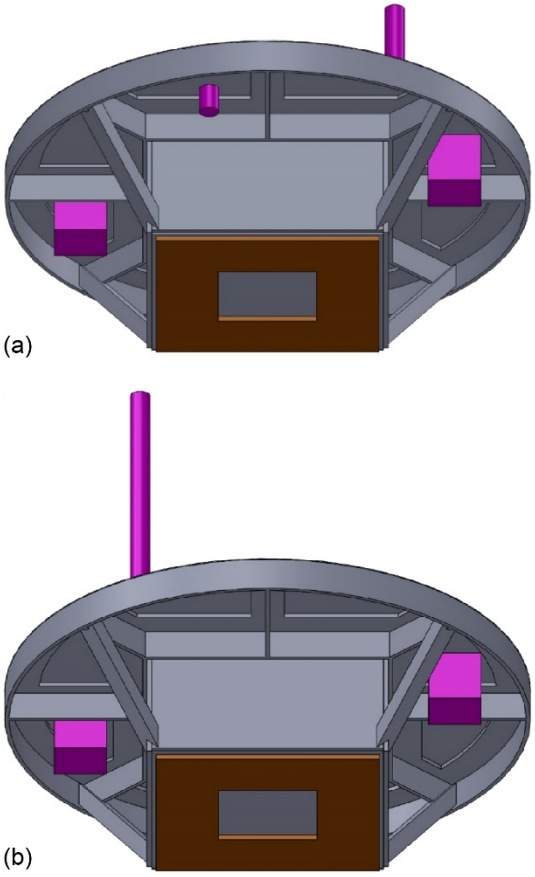

Figure C.19.—Additional views of deployed Lander.

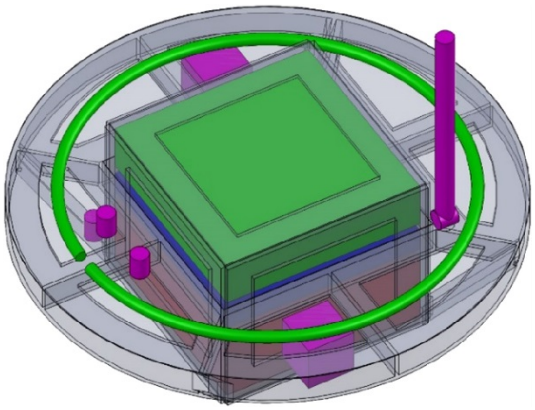

Figure C.19.—Transparent view of deployed Lander.

Appendix D.—Study Participants

Venus Bridge Orbiter and Surface Study (V-BOSS) design session			
Subsystem	Name	Center	Email
Study Principal Investigator (PI)	Gary Hunter	NASA Glenn Research Center (Glenn)	gary.w.hunter@nasa.gov
Science PI	Noam Izenberg	JHU Applied Physics Laboratory	noam.izenberg@jhuapl.edu
Science PI	Martha Gilmore	Wesleyan University	mgilmore@wesleyan.edu
Science PI	Kandis Lea Jessup	Southwest Research Institute, Boulder	jessup@boulder.swri.edu
Science PI	Robert Herrick	University of Alaska, Fairbanks	rrherrick@alaska.edu
Science PI	Jeffrey Balcerski	Glenn	jeffrey.balcerski@nasa.gov
Compass team			
Lead	Steve Oleson	Glenn	Steven.R.Oleson@nasa.gov
Lead systems engineer	J.Michael Newman	Glenn	j.m.newman@nasa.gov
Science	Geoffrey Landis	Glenn	geoffrey.landis@nasa.gov
Mission	Steven McCarty	Glenn	steven.mccarty@nasa.gov
Mission	David Smith	Glenn	david.a.smith-1@nasa.gov
Guidance, Navigation and Control	Brent Faller	Glenn	brent.f.faller@nasa.gov
Guidance, Navigation and Control	Michael Martini	Glenn	michael.c.martini@nasa.gov
Propulsion	James Fittje	Glenn	james.e.fittje@nasa.gov
Structures and mechanisms	John Gyekenyesi	Glenn	John.Z.Gyekenyesi@nasa.gov
Thermal	Anthony Colozza	Glenn	Anthony.J.Colozza@nasa.gov
Power	James Fincannon	Glenn	james.fincannon@nasa.gov
Power	Brandon Klefman	Glenn	brandon.klefman@nasa.gov
Orbiter Command and Data Handling	Anthony Colozza	Glenn	anthony.j.colozza@nasa.gov
Communications	Robert Jones	Glenn	rejones@nasa.gov
Configuration	Thomas Packard	Glenn	Thomas.W.Packard@nasa.gov
Cost	Elizabeth Turnbull	Glenn	elizabeth.r.turnbull@nasa.gov

References

1. Peralta, J., et al.: Stationary Waves and Slowly Moving Features in the Night Upper Clouds of Venus. Nat. Astron., vol. 1, Article number 0187, 2017.
2. Marcq, Emmanuel: Venus: Tickling the Clouds. Nat. Astron., vol. 1, Article number 0198, 2017. https://www.nature.com/search?title=tickling%20the%20clouds&order=relevance Accessed July 18, 2019.
3. Fukuhara, Tetsuya, et al.: Large Stationary Gravity Wave in the Atmosphere of Venus. Nat. Geosci., vol. 10, 2017, pp. 85–88.
4. National Research Council: Vision and Voyages for Planetary Science in the Decade 2013–2012. The National Academies Press, Washington, DC, 2011, p. 127.
5. National Research Council: Vision and Voyages for Planetary Science in the Decade 2013–2012. The National Academies Press, Washington, DC, 2011, p. 118.
6. Esposito, L.W.: Sulfur Dioxide: Episodic Injection Shows Evidence for Active Venus Volcanism. Sci., vol. 223, 1984, pp. 1072–1074.
7. Krasnopolsky, V.A.: Lightning and Nitric Oxide on Venus. Planet. Space Sci., vol. 31, no. 11, 1983, pp. 1363–1369.
8. Krasnopolsky, V.A.: A Sensitive Search for Nitric Oxide in the Lower Atmospheres of Venus and Mars: Detection on Venus and Upper Limit for Mars. Icarus, vol. 182, no. 1, 2006, pp. 80–91.
9. National Research Council: Vision and Voyages for Planetary Science in the Decade 2013–2012. The National Academies Press, Washington, DC, 2011, p. 129.
10. National Research Council: Vision and Voyages for Planetary Science in the Decade 2013–2012. The National Academies Press, Washington, DC, 2011, p. 133.
11. VEXAG Goals, Objectives, and Investigations for Venus Exploration. 2014, p. 5. http://www.lpi.usra.edu/vexag/reports/GOI-140625.pdf Accessed July 11, 2019.
12. Kounaves, S.P., et al.: Wet Chemistry Experiments on the 2007 Phoenix Mars Scout Lander Mission: Data Analysis and Results. J. Geophys. Res., vol. 115, no. E00E10, 2010.
13. Laghzizi, A.: Comparison of Electrical Properties Between Fluoroapatite and Hydroxyapatite Materials. J. Solid State Chem., vol. 156, no. 1, 2001, pp. 57–60.
14. Neudeck, Philip G., et al.: Prolonged Silicon Carbide Integrated Circuit Operation in Venus Surface Atmospheric Conditions. AIP Adv., vol. 6, no. 125119, 2016.
15. Spry, D.J., et al.: Prolonged 500 °C Operation of 100+ Transistor Silicon Carbide Integrated Circuits. Mat. Sci. Forum, vol. 924, 2018, pp. 949–952.
16. Kremic, Tibor; and Hunter, Gary; and Rock, Jennifer: Long-Lived In-Situ Solar System Explorer. VEXAG presentation, 2017. https://www.lpi.usra.edu/vexag/meetings/archive/vexag_15/presentations/8-Kremic-LLISSE.pdf Accessed July 11, 2019.
17. Voosen, Paul: Armed With Tough Computer Chips, Scientists Are Ready To Return to the Hell of Venus. 2017. http://www.sciencemag.org/news/2017/11/armed-tough-computer-chips-scientists-are-ready-return-hell-venus Accessed July 11, 2019
18. Landis, Geoffrey A.; and Harrison, Rachel: Batteries for Venus Surface Operation. J. Propul. Power, vol. 26, no. 4, 2010.
19. High-Temperature Tolerant Batteries (HTTBs) for Long-Life In-Situ Solar System Explorer (LLISSE). Request for Proposals, 2017. https://govtribe.com/project/nasa-next-generation-space-relay-architecture-concept-study Accessed July 11, 2019.
20. Mewaldt, R.A., et al.: The Cosmic Ray Radiation Dose in Interplanetary Space—Present Day and Worst-Case Evaluations. 29th International Cosmic Ray Conference Pune, 2005, pp. 101–104.
21. Jet Propulsion Laboratory: Energy Storage Technology for Future Space Science Missions. JPL D–30268, 2004.
22. Price, Kent M.; Pidgeon, David; and Tsao, Alex: Mass and Power Modeling of Communication Satellites. NASA CR–189186 (LORAL Technical Report No. SS/L–TR00821), 1991. http://ntrs.nasa.gov
23. Metallic Materials Properties Development and Standardization (MMPDS) Handbook. Federal Aviation Administration, Battelle Memorial Institute, Columbus, OH, 2016.
24. Structural Design and Test Factors of Safety for Spaceflight Hardware. NASA–STD–5001, 2016.
25. Heineman W., Jr.: Design Mass Properties II: Mass Estimating and Forecasting for Aerospace Vehicles Based on Historical Data. NASA JSC–26098, 1994.
26. Ku, Jentung: Introduction to Heat Pipes. NASA Goddard Space Flight Center, TFAWS, 2015.
27. NASA Technology Transfer Program: Temperature-Resistant Materials Enable Space-Like Cold on Earth. NASA Spinoff, 2016. https://spinoff.nasa.gov/Spinoff2016/ip_3.html Accessed July 11, 2019.
28. National Aeronautics and Space Administration: Genesis Mission. https://www.nasa.gov/mission_pages/genesis/main/index.html Accessed July 11, 2019.

Bibliography

System

Mass Properties Control for Space Systems. AIAA Standard S–120–2006, 2006.

Recommended Practice for Mass Properties Control for Satellites, Missiles, and Launch Vehicles. ANSI/AIAA R–020, Rev. A, 1999.

Larson, Wiley J.; and Wertz, James R., eds., Space Mission Analysis and Design, Third ed., Space Technology Library, Microcosm Press, El Segundo, CA, 1999.

Mission

Anderson, David J., et al.: The NASA In-Space Propulsion Technology Project's Current Products and Future Directions. AIAA 2010–6648, 2010.

Desai, P.N., et al.: Mars Ascent Vehicle Flight Analysis. AIAA 98–2850, 1998.

Dillman, Robert; and Corliss, James: Overview of the Mars Sample Return Earth Entry Vehicle. Presented at the Sixth International Planetary Probe Workshop, Atlanta, GA, 2008.

Dux, Ian J., et al.: Mars Ascent Vehicle Gross Lift-Off Mass Sensitivities for Robotic Mars Sample Return. NASA/TM—2010-216968, 2010. http://ntrs.nasa.gov

ESA Aurora Program. http://www.esa.int/esaMI/Aurora/SEMCWB1A6BD_0.html Accessed July 12, 2019.

Holmberg, Neil A.; Faust, Robert P.; and Holt, H. Milton: Viking '75 Spacecraft Design and Test Summary Volume III–Engineering Test Summary. NASA Reference Publication 1027, 1980. http://ntrs.nasa.gov

Johnston, M.D., et al.: Mars Global Surveyor Aerobraking at Mars. AAS 98–112, 1998. http://Mars.jpl.nasa.gov/mgs/sci/aerobrake/SFMech.html Accessed July 15, 2019.

Matousek, Steve, et al.: A Few Good Rocks: The Mars Sample Return Mission Architecture. AIAA 98–4282, 1998.

Palaszewski, B.; and Frisbee, R.: Advanced Propulsion for the Mars Rover Sample Return Mission. AIAA 88–2900, 1988.

Preliminary Planning for an International Mars Sample Return Mission: Report of the International Mars Architecture for the Return of Samples (iMARS) Working Group. 2008. https://mepag.jpl.nasa.gov/reports/iMARS_FinalReport.pdf Accessed July 15, 2019.

Rose, J.: Conceptual Design of the Mars Rover Sample Return System. AIAA–89–0418, 1989.

Spencer, D.A.; and Tolson, R.: Aerobraking Cost and Design Considerations. J. Spacecraft Rockets, vol. 44, no. 6, 2007.

Stephenson, David: Mars Ascent Vehicle—Concept Development. AIAA 2002–4318, 2002.

Whitehead, John C.: Mars Ascent Propulsion Options for Small Sample Return Vehicles. AIAA 97–2950, 1997.

Williams, R., et al.: Interplanetary Sample Return Missions Using Radioisotope Electric Propulsion. AIAA–2005–4273, 2005.

Zubrin, Robert: A Comparison of Approaches for the Mars Sample Return Mission. AIAA Paper 96–0489, 1996.

Power

Arde, Inc.: Propellant Storage Tank Specifications. http://www.ardeinc.com Accessed July 15, 2019.

Northrop Grumman: Propellant Storage Tank Specifications. http://www.psi-pci.com Accessed July 15, 2019.

Masse, Robert, et al.: GPIM AF–M315E Propulsion System. AIAA 2015–3753, 2015.

MOOG, Inc.: Spacecraft Component Specifications. http://www.moog.com Accessed July 15, 2019.

National Institute of Standards and Technology: Thermophysical Properties of Fluid Systems. 2018. http://webbook.nist.gov/chemistry/fluid/ Accessed July 15, 2019.

Spores, Ronald A., et al.: GPIM AF–M315E Propulsion System Development. AIAA 2014–3482, 2014.

Vacco, Inc.: Spacecraft Component Specifications http://www.vacco.com Accessed July 15, 2019.

United States Air Force: Military Specification: Rubber, Ethylene-Propylene, Hydrazine Resistant. MIL–R–83412A (SAE–AMS–R–8412), 1977.

GN&C

Norris, Lee, et al.: Analysis of Ares I Ascent Navigation Options. AIAA 2008–6290, 2008.

Structures

Persons, D.; Mosher, L.; and Hartka, T.: The NEAR and MESSENGER Spacecraft: Two Approaches to Structure and Propulsion Design. AIAA–00–I406 (A00–24531), 2000.

Zibdeh, Hazim S.; and Heller, Robert A.: Rocket Motor Service Life Calculations Based on the First-Passage Method. J. Spacecraft Rockets, vol. 26, no. 4, 1989, pp. 279–284.

Thermal

Wikipedia contributors: Aerodynamic Heating. Wikipedia, The Free Encyclopedia, 2019. http://en.wikipedia.org/wiki/Aerodynamic_heating Accessed July 15, 2019.

Alexander, M., ed.: Mars Transportation Environment Definition Document. NASA/TM—2001-210935, 2001. http://ntrs.nasa.gov

Bejan, Adrian; and Kraus, Allen D.: Heat Transfer Handbook. John Wiley & Sons, New York, NY, 2003.

Chapman, Alan J.: Heat Transfer. Third ed., Macmillan Publishing Company, New York, NY, 1974.

Gilmore, David G., ed.: Spacecraft Thermal Control Handbook: Volume 1: Fundamental Technologies. American Institute of Aeronautics and Astronautics, Reston, VA, 2002.

Hyder, A.K., et al.: Spacecraft Power Technologies. Imperial College Press, London, England, 2000.

Incropera, Frank P.; and DeWitt, David P.: Fundamentals of Heat and Mass Transfer. John Wiley & Sons, New York, NY, 1990.

Larson, Wiley J.; and Wertz, James R., eds.: Space Mission Analysis and Design. Third ed., Space Technology Library, Microcosm Press, El Segundo, CA, 1999.

Olds, J.; and Walberg, G.: Multidisciplinary Design of a Rocket-Based Combined Cycle SSTO Launch Vehicle Using Taguchi Methods. AIAA 93–1096, 1993.

Penuela, David, et al.: Investigation of Possible Heliocentric Orbiter Applications for Crewed Mars Missions. NIA/Georgia Institute of Technology, Project 1004, 2006.

Smith, Trent M., et al.: Ice Mitigation Approaches for Space Shuttle External Tank. Final Report, NESC 05–019, 2007.

Sutton, Kenneth; and Graves, Randolph A., Jr.: A General Stagnation-Point Convective-Heating Equation for Arbitrary Gas Mixtures. NASA TR R–376, 1971. http://ntrs.nasa.gov